

Article

Novel Benzohydroxamate-based Potent and Selective Histone Deacetylase 6 (HDAC6) Inhibitors Bearing a Pentaheterocyclic Scaffold: Design, Synthesis and Biological Evaluation

Barbara Vergani, Giovanni Sandrone, Mattia Marchini, Chiara Ripamonti, Edoardo Cellupica, Elisabetta Galbiati, Gianluca Caprini, Gianfranco Pavich, Giulia Porro, Ilaria Rocchio, Maria Lattanzio, Marcello Pezzuto, Malgorzata Skorupska, Paola Cordella, Paolo Pagani, Pietro Pozzi, Roberta Pomarico, Daniela Modena, Flavio Leoni, Raffaella Perego, Gianluca Fossati, Christian Steinkühler, and Andrea Stevenazzi

J. Med. Chem., **Just Accepted Manuscript** • DOI: 10.1021/acs.jmedchem.9b01194 • Publication Date (Web): 11 Nov 2019

Downloaded from pubs.acs.org on November 14, 2019

Just Accepted

"Just Accepted" manuscripts have been peer-reviewed and accepted for publication. They are posted online prior to technical editing, formatting for publication and author proofing. The American Chemical Society provides "Just Accepted" as a service to the research community to expedite the dissemination of scientific material as soon as possible after acceptance. "Just Accepted" manuscripts appear in full in PDF format accompanied by an HTML abstract. "Just Accepted" manuscripts have been fully peer reviewed, but should not be considered the official version of record. They are citable by the Digital Object Identifier (DOI®). "Just Accepted" is an optional service offered to authors. Therefore, the "Just Accepted" Web site may not include all articles that will be published in the journal. After a manuscript is technically edited and formatted, it will be removed from the "Just Accepted" Web site and published as an ASAP article. Note that technical editing may introduce minor changes to the manuscript text and/or graphics which could affect content, and all legal disclaimers and ethical guidelines that apply to the journal pertain. ACS cannot be held responsible for errors or consequences arising from the use of information contained in these "Just Accepted" manuscripts.

1
2
3
4
5
6
7
8
9
10
11
12
13
14
15
16
17
18
19
20
21
22
23
24
25
26
27
28
29
30
31
32
33
34
35
36
37
38
39
40
41
42
43
44
45
46
47
48
49
50
51
52
53
54
55
56
57
58
59
60

	Preclinical R&D Fossati, Gianluca; Italfarmaco SpA Head Office and Research Centre, Preclinical R&D Steinkühler, Christian; Italfarmaco SpA Head Office and Research Centre, Preclinical R&D Stevenazzi, Andrea; Italfarmaco SpA Head Office and Research Centre, Preclinical R&D

SCHOLARONE™
Manuscripts

Novel Benzohydroxamate-based Potent and Selective Histone Deacetylase 6 (HDAC6) Inhibitors Bearing a Pentaheterocyclic Scaffold: Design, Synthesis and Biological Evaluation

*Barbara Vergani, † Giovanni Sandrone, † Mattia Marchini, † Chiara Ripamonti, Edoardo Cellupica, Elisabetta Galbiati, Gianluca Caprini, Gianfranco Pavich, Giulia Porro, Ilaria Rocchio, Maria Lattanzio, Marcello Pezzuto, Malgorzata Skorupska, Paola Cordella, Paolo Pagani, Pietro Pozzi, Roberta Pomarico, Daniela Modena, Flavio Leoni, Raffaella Perego, Gianluca Fossati, Christian Steinkühler and Andrea Stevenazzi**

Preclinical R&D, Italfarmaco Group, Via dei Laboratori 54, I-20092 Cinisello Balsamo, Milan, Italy

KEYWORDS: HDAC6 inhibitors, ITF3756, ITF3791, Treg suppression

ABSTRACT:

Histone deacetylase 6 (HDAC6) is a peculiar HDAC isoform whose expression and functional alterations have been correlated with a variety of pathologies such as autoimmune disorders,

neurodegenerative diseases, and cancer. It is primarily a cytoplasmic protein, and its deacetylase activity is focused mainly on non-histone substrates such as tubulin, heat shock protein (HSP)90, Foxp3 and cortactin, to name a few. Selective inhibition of HDAC6 does not show cytotoxic effects in healthy cells, normally associated with the inhibition of Class I HDAC isoforms. Here we describe the design and synthesis of a new class of potent and selective HDAC6 inhibitors that bear a pentaheterocyclic central core. These compounds show a remarkably low toxicity both in vitro and in vivo and are able to increase the function of regulatory T cells (Tregs) at well tolerated concentrations, suggesting a potential clinical use for the treatment of degenerative, auto-immune diseases and organ transplantation.

INTRODUCTION

Histones, together with DNA, are the main components of the nucleosome, the primary chromatin unit. In eukaryotic cells, post-translational modifications of the core histones' N-termini are involved in regulation of gene expression by modulating chromatin accessibility and by providing anchoring points for "reader" proteins that help guiding the transcription machinery to gene promoters. Reversible acetylation of histones is regulated by the interplay of 'writer' histone acetyltransferases (HATs) and 'eraser' histone deacetylases (HDACs).¹

There are 18 known human HDACs divided into two groups: zinc-dependent HDACs and nicotinamide adenine dinucleotide (NAD)-dependent HDACs, also known as sirtuins (Class III). Zinc-dependent HDACs are further grouped into four classes depending on their sequence homology and on their catalytic activity: (1) Class I includes HDAC1, 2, 3, and 8, ubiquitary isoenzymes primarily localized in nucleus; (2) Class IIa includes HDAC4, 5, 7, and 9,

1
2
3 isoenzymes localized both in nucleus and in cytoplasm; (3) Class IIb, includes HDAC6 and 10,
4
5 mainly localized in cytoplasm; and (4) Class IV, which includes only HDAC11.²
6

7
8 Proteomic studies have shown that in addition to histones, post-translational acetylation
9
10 regulates the function and stability of a growing number of proteins with diverse biological
11
12 activities, from transcription factors to metabolic and contractile proteins.³ Indeed, protein lysine
13
14 acetylation has long been recognized to have a comparable role to protein phosphorylation⁴ and
15
16 the widespread activity of these enzymes has led to the proposal to rename the family as “lysine
17
18 deacetylases” or KDACs.
19

20
21 Numerous HDAC inhibitors have been synthesized. Most of them are characterized by the
22
23 presence of a hydroxamate group, able to bind the zinc in the active site of the enzyme.⁵ There
24
25 are also several examples of non-hydroxamate HDAC inhibitors, among them the most
26
27 important are the 2-aminophenylbenzamide-derivatives, like Entinostat and Mocetinostat,⁶
28
29 currently in clinical phase III and II, respectively. Some HDAC inhibitors have been approved by
30
31 Food and Drug Administration (FDA) for the treatment of cancer: Vorinostat and Romidepsin
32
33 for cutaneous T-cell lymphoma (CTCL), Belinostat for peripheral T-cell lymphoma and
34
35 Panobinostat for multiple myeloma (MM). These compounds are relatively non-selective
36
37 inhibitors of all or most of the zinc-dependent HDACs and have a modest therapeutic window. In
38
39 clinical trials, side effects such as decreased platelet levels, fatigue, or gastrointestinal toxicity
40
41 are dose-limiting.⁷ The scientific community is, therefore, actively trying to develop novel
42
43 inhibitors that are highly selective for individual HDAC subtypes with the goal of identifying
44
45 more active and better tolerated compounds. In addition, selective inhibitors may also allow
46
47 specific biological functions of individual HDAC subtypes to be addressed.
48
49
50
51
52
53
54
55
56
57
58
59
60

In this context, HDAC6 is an interesting, emerging target, since its expression and functional alterations have been correlated to a variety of pathologies such as autoimmune disorders, neurodegenerative diseases and cancer.⁸

HDAC6 is the only isoform with two catalytic domains and a C-terminal zinc finger domain, which can bind ubiquitinated proteins. Even though it can be localized in the nucleus under certain conditions,⁹ HDAC6 is primarily a cytoplasmic protein and its main deacetylase activity is toward a number of non-histone substrates including α -tubulin, heat shock protein 90 (Hsp90), β -catenin, forkhead box 3 (Foxp3), p53 and cortactin. In contrast to many other HDACs, whose ablation is lethal in mice or leads to severe functional impairment, HDAC6 KO mice are viable, suggesting that the selective inhibition of this isoenzyme is likely to be well-tolerated.^{9a, 10}

Among different functions, HDAC6 has an important role in immune response regulation. HDAC6, as well as other isoforms, deacetylates the Foxp3 transcription factor,^{9a, 10} a master regulator of Treg cell development and activity. Selective inhibition of HDAC6 leads to the acetylation of Foxp3 which in turn results in an increased Treg suppressor function.¹¹ Tregs play an important role in maintaining immune system homeostasis,¹² and their alteration is involved in the development of auto-immune pathologies such as rheumatoid arthritis, psoriasis, lupus, myasthenia gravis, as well as graft versus host disease (GVHD) and organ rejection. In these pathologic conditions, pharmacologic increase of Treg suppression function is an active field of investigation.¹³ Increased Treg activity exerted by selective HDAC6 inhibitors appears a promising approach for the treatment of these disorders and, in particular, in organ transplantation.¹⁴

Many selective HDAC6 inhibitors are described in the literature,^{5, 8a, 15} and a new generation of candidates have recently appeared.¹⁶ Tubastatin A (see Table 1 and Figure 1), a compound

obtained through rational design combined with homology modeling was a milestone in the discovery of this class of compounds.¹⁷ The tricyclic molecule is highly selective for HDAC6 and is largely used as a research tool. In order to improve the druglike properties of this kind of structure, Kozikowski et al. later generated a range of analogues with a bicyclic-capped scaffold¹⁸ and identified HDAC6 inhibitors with improved pharmacokinetics and *in vitro* selectivity. The same group developed Nexturastat A (see Table 1 and Figure 1), an urea derivative compound, that shows *in vitro* antiproliferative activity on B16 murine melanoma cells.¹⁹ Another worth mentioning compound is HPOB (see Table 1 and Figure 1), which shows good selectivity for HDAC6 and seems to enhance the anticancer activity of some known drugs such as doxorubicin and etoposide.²⁰ ACY-738 (see Table 1 and Figure 1) and ACY-775 are two pyrimidine-derivatives that inhibit HDAC6 with high selectivity and potency. These compounds rapidly distribute to the brain and show antidepressant properties in animal models.²¹ To the best of our knowledge, however, none of these selective inhibitors are under active development, probably due to stability issues or non-optimal druglike properties (as an example, compare stability data of the above mentioned compounds with the ones of Ricolinostat, Table 1).

Two selective HDAC6 inhibitors, namely Ricolinostat (see Table 1 and Figure 1) and Citarinostat, are currently under clinical phase I/II investigation, in combination with various agents such as dexamethasone and bortezomib for the treatment of multiple myeloma²² and immune checkpoint inhibitor nivolumab in non-small cell lung cancer, respectively. These two molecules, however, exhibit very low selectivity over HDAC Class I isoforms (see Table 1) and may have a suboptimal therapeutic index.

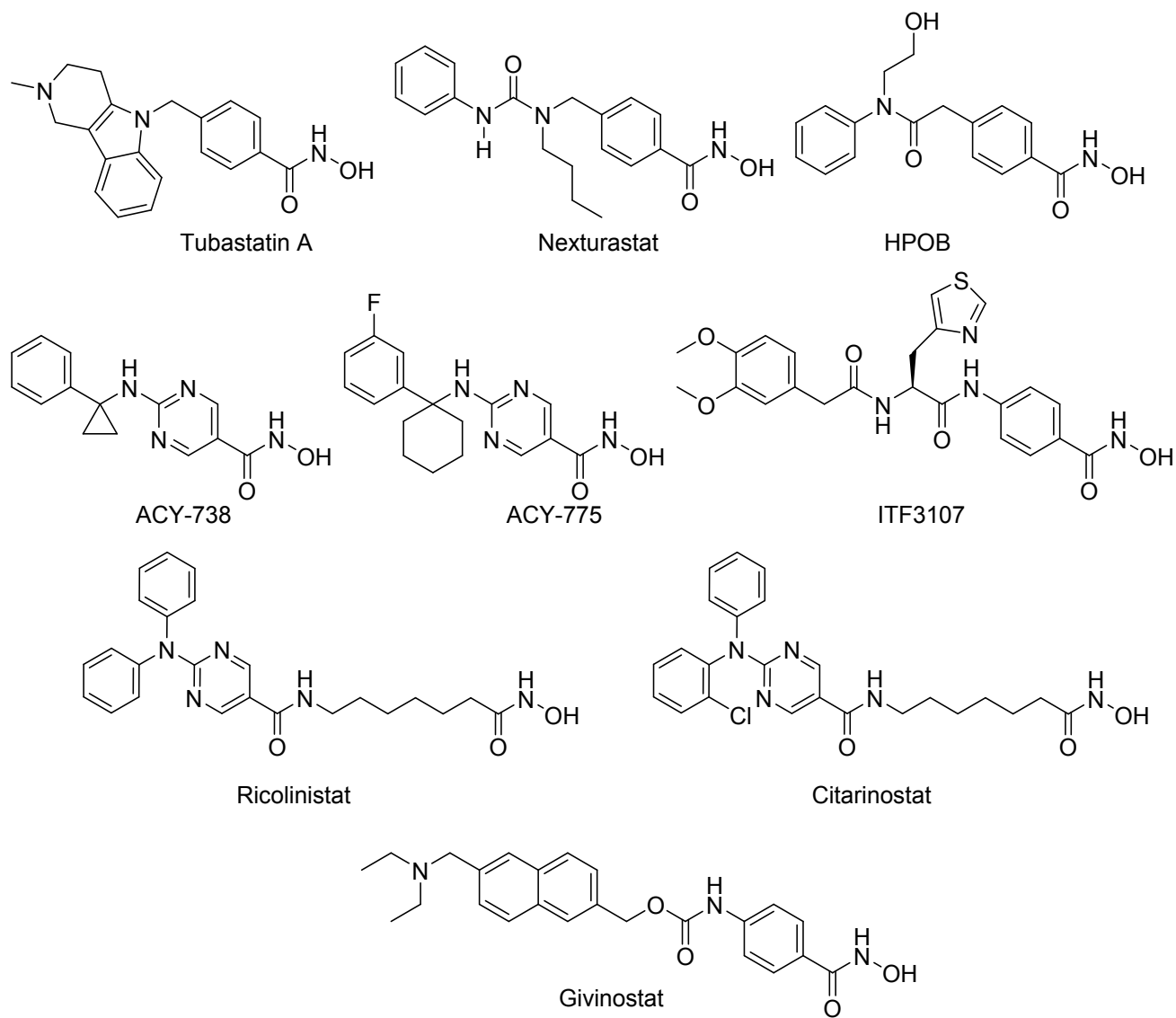


Figure 1. Representative examples of selective histone deacetylase 6 (HDAC6) inhibitors along with the pan-inhibitor Givinostat and an internally developed HDAC6 inhibitor, i.e. ITF3107.

Table 1. In-house biological evaluation of the most representative selective HDAC6 inhibitors along with the pan-inhibitor Givinostat and an internally developed HDAC6 inhibitor, i.e. ITF3107.

Compd	HDAC6 IC ₅₀ ^a	Sel. vs HDAC1 ^b	Sel. vs HDAC2 ^b	Sel. vs HDAC3 ^b	Rat plasma ^c	Human plasma ^c	697 toxicity ^d
Tubastatin A	21±6	218	942	246	38±3	98±2	2006±327
Nexturastat	25±1	84	172	64	40±1	100±1	401±34
HPOB	121±2	38	146	53	45±1	79±22	8330±464
ACY-738	2±1	156	1176	200	12±1	100±1	3390±246
Ricolinostat	12±1	28	101	16	91±1	100±1	201±29
ITF3107	5±1	120	547	73	18±1	100±1	>10000
Givinostat	44±5	2	9	1	72±1	97±2	100±15

a – Enzymatic data (IC₅₀) in nM unit were obtained from curve-fitting of a 5-point enzymatic assay starting from 100, 30 or 10 μM with 10-fold serial dilution. Experiments were done in triplicate. Single experiment, except for ITF3107 and Givinostat (n=4). In-house data are in accordance with the literature.¹⁹⁻²²

b - Selectivity indicator, expressed in terms of ratio between IC₅₀ values ($\frac{HDACn IC50}{HDAC6 IC50}$). See the SI spreadsheet for the original data and the statistical evaluation.

c – Residual percentage of compounds after 4 h. Experiments were done in duplicate. SDs were calculated on technical replicates

d - IC₅₀ values in nM unit are the mean of at least two experiments obtained from the curve fitting of a 4-points viability assay starting from 10 μM with 10-fold serial dilution.

ITF3107,²³ a benzohydroxamate-based molecule bearing an amino acid scaffold (see Figure 1), shares the same selectivity, but also the same stability issues of the other selective HDAC6 inhibitors (see Table 1), probably due to the presence of an amide bond. The compound is, indeed, a substrate of chymotrypsin (data not shown).

Here we report how our rational drug design approach led to: (1) the modification of the structure of ITF3107 in order to generate a new class of stable and selective hydroxamate-based HDAC6 inhibitors, and (2) the identification of potential preclinical candidates.

RESULTS AND DISCUSSION

Structure–Activity Relationship (SAR): The design strategy adopted in the discovery of the new class of compounds was essentially ligand-based, although several docking calculations were performed in order to cast light on protein motif involved in the binding with the inhibitors. All new molecular entities were conceived to satisfy simultaneously two conditions: to be highly potent versus HDAC6 (IC_{50} in the low nM range) and extremely selective (two or three orders of magnitude) over HDAC3, the latter being selected as representative of Class I HDAC isoforms. HDAC3 was preferred to HDAC1 as during the early stage of our screening campaign the selectivity over HDAC3 was the most demanding to achieve. Activity on both isoforms (HDAC6 and HDAC3) was evaluated in terms of IC_{50} (nM), whereas the simple potency ratio $IC_{50}(\text{HDAC3})/IC_{50}(\text{HDAC6})$ was used to monitor the selectivity.

The extensive literature on HDAC inhibitors helped us to define a paradigm for an efficient inhibitor, partitioning the structure²⁴ (Figure 2) in four distinct domains: (1) the zinc binding group (ZBG); (2) a spacer (usually hydrophobic) filling the dip between the catalytic metal ion and the outermost surface; (3) a junction capable of addressing (4) the last inhibitor component (namely the cap term) toward the flexible rim of enzyme.

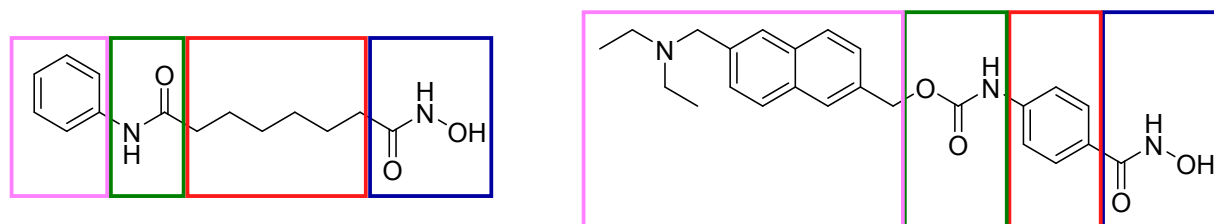
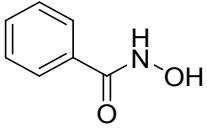
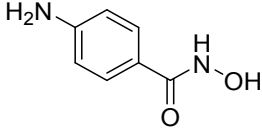


Figure 2. Qualitative partition of Vorinostat (Zolinza) and Givinostat, two HDAC pan-inhibitors. It is possible to distinguish in both molecules the zinc binding group (ZBG) in blue, the spacer region in red, the “junction” in green, and the cap term, in pink.

The hydroxamic acid moiety is a well-known and highly efficient ZBG²⁵ that has been widely adopted in the development of reversible inhibitors of zinc-based hydrolases such as matrix metalloproteinases (MMPs)²⁶ or tumor necrosis factor- α converting enzymes (TACE),²⁷ enzymes in which the closed shell transition metal ion acts as a Lewis acid and triggers the substrate hydrolysis. The relatively high zinc affinity of this functional group favors both flexible (Vorinostat,²⁸ Ricolinostat²⁹) and rigid aromatic²⁹⁻³⁰ (Givinostat) spacers in the dip between the zinc cation and the enzyme rim. The *N*-hydroxybenzamide itself (Table 2, compound **1**) exhibits an inhibitory activity close to 2 μ M and a moderate selectivity versus HDAC6 (in terms of IC₅₀).²⁴ Substitution in the para position with an amino group (compound **2**) improves the potency with a mild reduction in the selectivity, whereas acetylation of this amino group leads to sub-micromolar activity versus HDAC6 (compound **3**). The resulting molecular entity still exhibits some selectivity and can be considered as a promising starting point for a new class of HDAC6 selective inhibitors, provided that stability of the amide bond is being monitored.

Table 2. Potency and selectivity trend in small similar moieties.

	Compd	HDAC6 ^a	HDAC3 ^a	Selectivity 6 vs 3 ^b
	1	2370 \pm 255	71572 \pm 10438	30
	2	1395 \pm 59	18402 \pm 1092	13

	3	270±21	1671±110	6
	4	695±7	5000±469	7

a – Enzymatic data (IC_{50}) in nM unit were obtained from curve-fitting of a 5-point enzymatic assay starting from 100, 30 or 10 μ M with 10-fold serial dilution. Experiments were done in triplicate (single experiment). SDs were calculated on technical replicates.

b - Selectivity indicator, expressed in terms of ratio between IC_{50} values $\left(\frac{HDAC3\ IC_{50}}{HDAC6\ IC_{50}}\right)$.

On the other hand, the amide bond can be replaced with a substructure having similar behavior and compatible geometry but higher resistance versus the activity of the metabolic enzymes.³¹ Substitution can be particularly convenient when the replacement not only mimics all or part of interactions of the amide group with the binding site residues, but it also adds new ones. The five-membered heterocycles reported in Figure 3 can potentially mimic the lone pairs localized on the amide oxygen thanks to the two adjacent nitrogen atoms,³² but only the 1,2,4-triazole (A) and the 1,2,3-triazole (F) have a hydrogen bond donor (HBD) similar to the amide, whereas the other pentaheterocycles are apparently closer to the ester functional group (B-E).

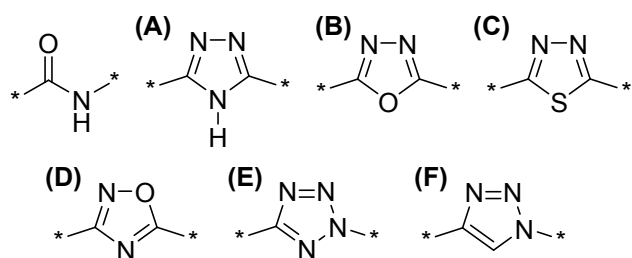
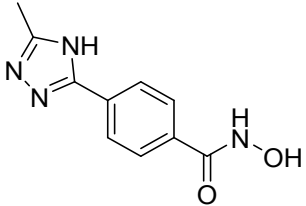
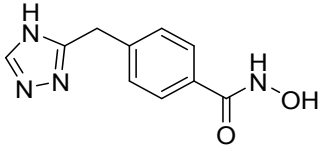


Figure 3. Five-membered rings acting as non-classical bioisosteres of the amide/ester bond.

Direct replacement of the amide of compound **3** with a 1,2,4-triazole results in better selectivity (compound **5**, Table 3) that is retained also when a methylene group is introduced between the phenyl and the triazole rings (compound **6**, Table 3). In the literature there are examples of azole-containing benzohydroxamate-based HDAC6 inhibitors.¹⁸

Table 3. Effects on enzymatic inhibitory activity of para substitution on the benzoic hydroxamate with 1,2,4 triazole, directly bound to phenyl substructure (compound **5**) or bearing a methylene spacer (compound **6**).

	Compd	HDAC6 ^a	HDAC3 ^a	Sel 6 vs 3 ^b
	5	353±36	3563±203	10
	6	198±9	2896±135	15

a – Enzymatic data (IC₅₀) in nM unit were obtained from curve-fitting of a 5-point enzymatic assay starting from 100, 30 or 10 μM with 10-fold serial dilution. Experiments were done in triplicate (single experiment). SDs were calculated on technical replicates.

b - Selectivity indicator, expressed in terms of ratio between IC₅₀ values $\left(\frac{HDAC3\ IC_{50}}{HDAC6\ IC_{50}}\right)$.

In the early stage of the investigation a crude homology model was prepared using HDACs or homologue HDACs structures available at the time. Despite its low quality (especially if compared with the recently published complex),³³ the model was able to capture several features

of the enzyme and address the design of cap term region of the inhibitors. It is of note that the hypothetical binding conformer was derived from docking calculations where the large amount of high ranking poses of the training compounds (selective inhibitors) were similar to the Trichostatin A binding conformer available in h-HDAC8 (pdb code 1T64):³⁰ the cap term of the ligand is pointing toward loop L1, although able to engage an intramolecular bond with Asp101, a conserved residue in Class I isoforms and part of loop L2.

The structures of hydroxamates co-crystallized with HDAC6 show relevant details in the inner catalytic core, not previously detected in complexes involving other HDAC isoforms.^{30, 34} The denticity (i.e. the number of donor groups in a single ligand that bind to a central atom in a coordination compound)³⁵ of the hydroxamate in Class I enzymes is usually bidentate, with oxygen atoms both involved in the Zn-O bond, allowing a distorted trigonal bipyramid coordination for the cation. A common feature of several hydroxamate-based inhibitors co-crystallized with HDAC6^{29, 36} indicates that only the hydroxyl oxygen atom is directly bound to the metal, whereas the carbonyl oxygen is engaged in a hydrogen bond with the catalytic tyrosine (Y745 for z-CD2, PDB code:5G0I/ Y782 for h-CD2, PDB Code 5EDU). This particular binding mode likely allows the presence of one catalytic water molecule in the inner zinc coordination sphere, a feature that can play a possible role for the selectivity. It must be said, though, that the bidentate mode is also detected in several HDAC6 - complexes^{29, 37} as the energy barrier between these two binding conformers is quite low. As a consequence, the delicate balance between the two different denticities, combined with the interaction between the cap-term of the inhibitor and the rim residues of the enzyme could be the key for the selectivity.

Moving from the catalytic core to the outermost region of the enzyme both zebra fish and human CD2 domains exhibit a dyadic motif that involves F620 and F680 in h-CD2 (F583 and

F643 in z-CD2), two highly conserved residues among HDAC isoforms (see Figure 4). The facing aryl side chains define a crevice where the phenyl moiety of benzylhydroxamate can fit in, stabilized by π - π interactions, as shown, as illustrative examples, for compounds **42** in Figure 4 and **13** in Figure 5. Comparison of available HDAC6 complexes with both pan and selective hydroxamic-based inhibitors^{29, 33, 38} along with recent docking studies³⁹ indicate the relevance of residues in loops L1 (H500/H463, P501/P464, h-CD2/z-CD2) and L2 (S568/S531), where binding can be related to a direct contact with enzyme residues or mediated by water molecules, respectively. Although the loop L1 is shared between class I isoforms and the CD2 of HDAC6, recent docking results and related structural analysis³⁹ suggest that the selectivity for HDAC6 can be explained in terms of narrow (HDAC1) or different shape of the binding pocket (HDAC8, where loop L1 is shorter). Rim details do not justify, however, the selectivity of compounds shown in tables 2 and 3, due to the lack of the cap-term, but recent biophysical investigations indicate that the larger affinity toward HDAC6 exhibited by the benzohydroxamic acid itself (compound **1**) is probably entropy driven.⁴⁰

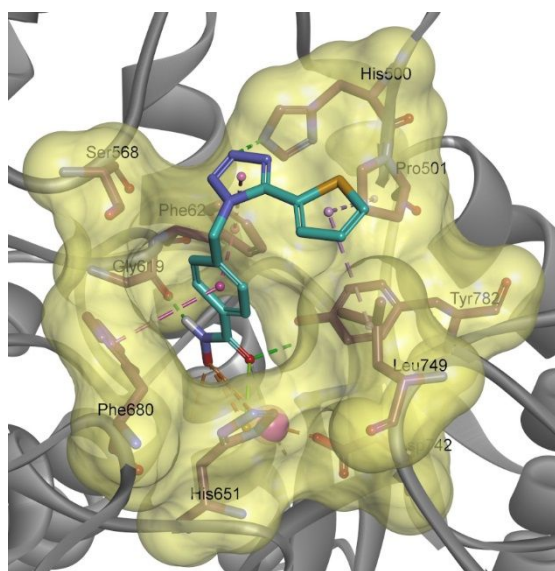


Figure 4. The docking pose of compound **42** having the highest Dreiding score (the best ranking function detected in the preliminary docking of the training set compounds). The aryl cap term is pointing toward loop L1, interacting with a hydrophobic pocket defined by Pro501, His500, His499 and Leu749 (h-CD2, PDB code 5EDU). H-bond, electrostatic and π - π interactions are represented as green, orange and purple dashed lines, respectively; Zn ion as a magenta sphere. The surface of the binding site was generated and rendered in transparent solid yellow.

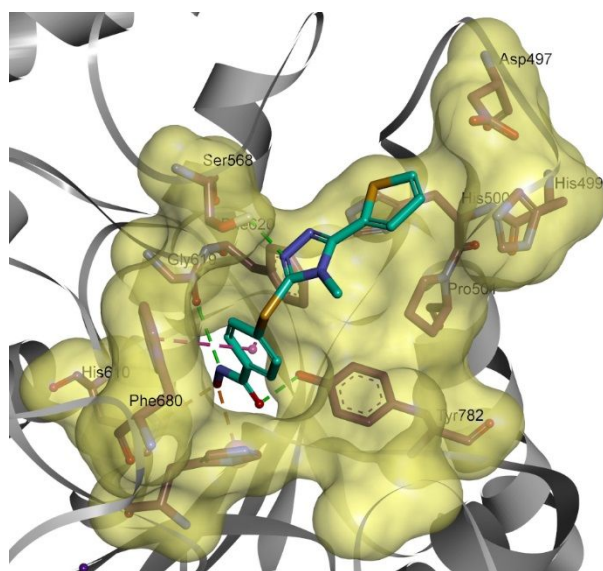


Figure 5. The docking pose of compound **13** having the highest Dreiding score (the best ranking function detected in the preliminary docking of the training set compounds). The aryl cap term is pointing toward loop L1, interacting with a hydrophobic pocket defined by Pro501, His500 and His499 (h-CD2, PDB code 5EDU). H-bond, electrostatic and π - π interactions are represented as green, orange and purple dashed lines, respectively; Zn ion as a magenta sphere. The surface of the binding site was generated and rendered in transparent solid yellow.

Docking calculations were performed using the libdock protocol of the Discovery Studio (DS) Suite (see Supporting Information for details) and the conformational search of candidates was focused in a sphere centered in the center of mass of aligned inhibitors available in the crystal structures (radius equal to 8.0 Å). The sphere volume includes both L1 and L2 loops, the catalytic core, the zinc cation and the residues directly bound to the metal ion.

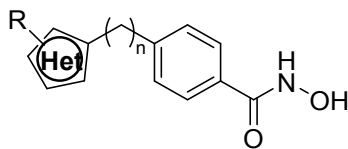
The best score function for the ranking of the poses was the “Dreiding scores”,⁴¹ identified by analyzing the Receiving Operator Curves (ROCs) evaluated in a preliminary calculation where a training set of HDAC6 selective and pan inhibitors were mixed with compounds exhibiting low HDAC6 inhibition potency (at least 10 fold less).

The results emerging from the qualitative docking calculations led us to synthesize a collection of compounds having several five-membered ring heteroaromatic cycles, bearing the *p*-methylbenzohydroxamic acid and an aromatic group. Among them, 1,2,4-triazole, tetrazole (both 1,5- and 2,5-disubstituted), 1,3,4-oxadiazole, 1,2,4-oxadiazole, and 1,3,4-thiadiazole (Table 4, compounds **7a–c**; **7e–g**) generated molecules exhibiting good activity on isoform 6 (4 nM) and selectivity (105 fold) over HDAC3, a robust proof that i) five-membered rings can be interchanged without relevant loss of potency and selectivity and that ii) the small aromatic cap-term is a relevant pharmacophoric feature for both potency and selectivity.

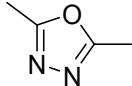
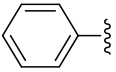
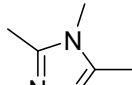
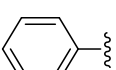
The key role played by the methylene group between the benzohydroxamate moiety and the five-membered ring is clearly evident when comparing compounds **7b** and **8** (Table 4), where the lack of an sp^3 carbon atom of the latter induces a significant decrease in both potency and selectivity. A comparable effect has already been described for other HDAC6 selective inhibitors that bear a phenothiazine-based benzhydroxamic acid.³⁹ An sp^3 atom acting as a bridge between

the two aromatic rings seems beneficial for the HDAC6 inhibitory activity,^{17, 19-20} as it allows a tilted conformation of the molecule which, in turn, maximizes the interaction with the enzyme's binding site.

Table 4. Confirmatory analysis of aromatic heterocycle equivalence and relevance of methylene spacer between the five-membered ring and the benzohydroxamate moiety.



Compd	Het	n	R	HDAC6 ^a	Sel 6 vs 3 ^b
7a		1		5±1	21
7b		1		4±1	32
7c		1		3±1	72
7d		1		52±1	26
7e		1		6±1	50
7f		1		16±1	105
7g		1		9±1	83

8		0		660±9	3
9		1		17±1	129

a – Enzymatic data (IC_{50}) in nM unit were obtained from curve-fitting of a 5-point enzymatic assay starting from 100, 30 or 10 μ M with 10-fold serial dilution. Experiments were done in triplicate (single experiment). SDs were calculated on technical replicates.

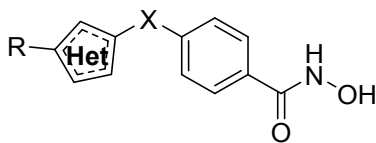
b - Selectivity indicator, expressed in terms of ratio between IC_{50} values $\left(\frac{HDAC3\ IC_{50}}{HDAC6\ IC_{50}}\right)$. See the SI spreadsheet for the original data and the statistical evaluation.

The shape and the extension of the hydrophobic pocket in the outer portion of the binding site was then evaluated by adding a methylene spacer between the apical phenyl group and the 2,5-disubstituted tetrazole (compound **7d**, table 4); although the selectivity is still acceptable, the potency decreases (compare compounds **7c** and **d**), suggesting a commensurable misfit on both HDAC isoforms tested.

The next step was the exploration of a possible (bioisosteric) replacement of the $-CH_2-$ group. The sulfur atom, despite the larger volume of the atomic orbitals in the valence shell, leads to potent analogues (Table 5, compounds **10a** and **b**) although reduced selectivity is detected when combined with 1,2,4-oxadiazole. On the contrary, the $-NH-$ moiety fails in both exploratory compounds synthesized (compounds **11a** and **b**). The different behavior of these analogues can apparently be explained in terms of the different orbital hybridization in which the sp^3 valence orbitals on the sulfur atom allow for a higher degree of freedom with a small energetic barrier between inactive and active (bent) conformers. The setup is not perfectly compatible with the nitrogen atom in which the sp^2 component is more prominent and the related lone pair in the residual p atomic orbital can be delocalized between the phenyl group and the five-membered

ring. The resulting structures (**11a** and **b**) are then flat, linear and rigid and unable to efficiently fit into the external portion of the binding site.

Table 5. Possible replacement of methylene group (-S- and -NH-) between the aromatic substructures.



Compd	Het	X	R	HDAC6 ^a	Sel 6 vs 3 ^b
10a		S		6±1	17
10b		S		6±1	62
11a		NH		66±10	19
11b		NH		136±1	10

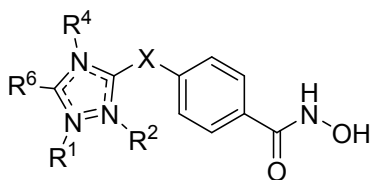
a – Enzymatic data (IC₅₀) in nM unit were obtained from curve-fitting of a 5-point enzymatic assay starting from 100, 30 or 10 μM with 10-fold serial dilution. Experiments were done in triplicate (single experiment). SDs were calculated on technical replicates.

b - Selectivity indicator, expressed in terms of ratio between IC₅₀ values $\left(\frac{HDAC3\ IC_{50}}{HDAC6\ IC_{50}}\right)$. See the SI spreadsheet for the original data and the statistical evaluation.

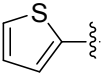
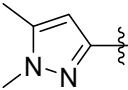
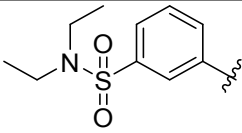
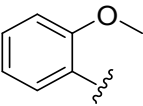
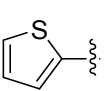
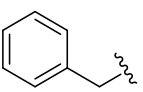
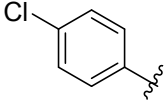
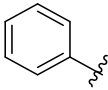
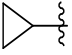
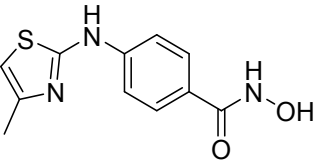
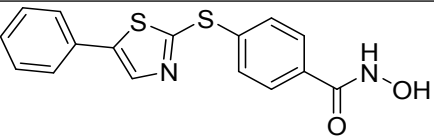
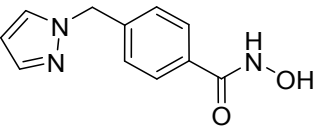
Methylation in position 4 of the 1,2,4-triazole ring (compound **9**, Table 4) confirms the hypothesis of the low relevance of a hydrogen bond donor in that position and the experimentally detected efficiency of oxadiazoles, tetrazoles, and thiadiazoles as isosteres of the amide group. Although the lack of a polar hydrogen slightly decreases potency on HDAC6 of compound **9**,

selectivity is substantially improved, suggesting a different local environment in the two isoforms. These considerations are true if the substituent group is small, as a methyl or an amine (compound **13**, **14** and **15**, Table 6), while both selectivity and especially potency on HDAC6 are negatively affected by a bulkier substituent, as e.g. a phenyl group (compound **12**, Table 6). On the other hand, the importance of the lone pairs on adjacent nitrogen atoms of the pentacycles has been verified by the introduction of substituents in positions 1 and 2 of the 1,2,4-triazole core. The analysis of the data collected in Table 6 shows that all of these types of substitutions have a small influence on the selectivity profile, but they deeply affect the potency of the HDAC6 inhibitory activity. Substitutions in these positions, especially in position 1, in fact, involve a drastic drop in potency (see compounds **16–18**, Table 6). Alkylation of the nitrogen in position 1 means somehow silencing it by preventing hydrogen bond formation or other types of interactions with the protein residues. These results are in accordance with the ones exhibited by compounds **19**, **20** and **21**¹⁸ (Table 6): these molecules, where the nitrogen in position 1 has been replaced by a carbon atom, show indeed lower inhibitory activities.

Table 6. Effects of triazole nitrogen atoms substitution on the enzymatic activity.



Compd	R ⁴	R ¹	R ²	R ⁶	X	HDAC6 ^a	Sel 6 vs 3 ^b
12		abs	abs		S	56±1	25

13 ^c	CH ₃	abs	abs		S	8±1	61
14	CH ₃	abs	abs		S	5±1	71
15	NH ₂	abs	abs		S	9±1	55
16	abs	abs			CH ₂	333±24	16
17	abs	abs			CH ₂	368±20	24
18	abs		abs		S	162±16	12
19						137±12	4
20						62±12	27
21						102±6	49

a – Enzymatic data (IC₅₀) in nM unit were obtained from curve-fitting of a 5-point enzymatic assay starting from 100, 30 or 10 μM with 10-fold serial dilution. Experiments were done in triplicate (single experiment). SDs were calculated on technical replicates.

b - Selectivity indicator, expressed in terms of ratio between IC₅₀ values $\left(\frac{HDAC3\ IC_{50}}{HDAC6\ IC_{50}}\right)$. See the SI spreadsheet for the original data and the statistical evaluation.

c - HDAC6 IC₅₀ value is the mean of three experiments and SD was calculated on these independent experiments.

abs = not present.

A careful analysis of the poses generated by the highly potent compounds of the training set revealed two possible (average) “active” conformations, shown in Figure 6 for compound **42**. The first geometry, light blue in the figure, is in agreement with the results observed in the crystal structures of HDAC6-inhibitor complexes,^{29, 33, 36-39} where the aryl moiety of the cap term lies close to L1 and L2 loops and interacts with the hydrophobic pocket generated by H500 and P501 (hCD2). The second conformation (in yellow) can be obtained from the former geometry by a 180° rotation of a C-C bond (see Figure 6). These results are consistent with the literature.⁴²

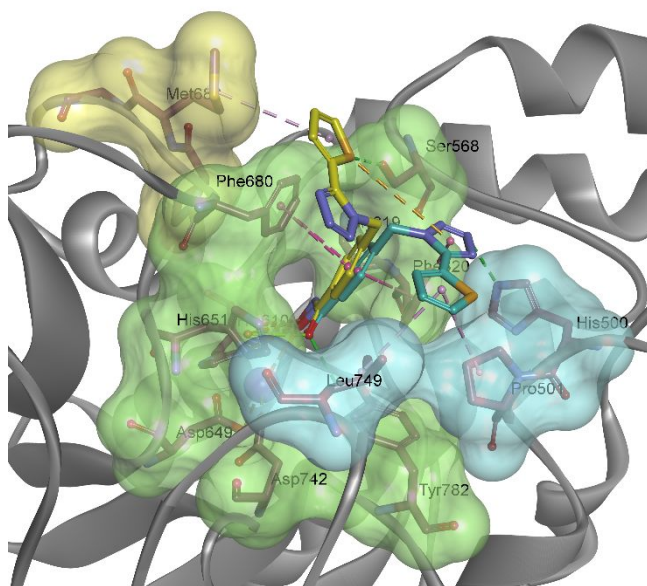


Figure 6. Binding conformers of compound **42** detected in docking experiment (hHDAC6 CD2, PDB code 5EDU): conformer A in light blue and conformer B in yellow. The green surface shows residues which interact with both conformers; light blue and yellow surfaces show specific interactions with conformer A and B respectively. H-bond, electrostatic and π - π interactions are represented as green, orange and purple dashed lines, respectively; the Zn ion as a magenta sphere.

The aryl moiety of the cap term is pointing toward the loop (L5) where T678 (A641 in zCD2) was recently indicated as a key residue involved in a hydrogen bond network triggered by the peptidoid moiety of several HDAC6 selective inhibitors and the water molecules.³⁷ It should be noticed that the aryl moiety of the cap-term lies too far from threonine and the conserved F679 (F642 in zCD2), whereas the tetrazole moiety is still close to S658.

To further study the variability on the apical portion (R^6 substituent, Figure 5) we investigated the SAR of some tetrazole-core compounds with a couple of R^6 aryl substructures with high similarity (such as the phenyl and the pyridyl groups).

Both (average) identified conformations show an interesting feature: a residue with an acidic functionality can be detected in the direction of an ideal vector exiting from para position of the phenyl terminal substructure: D497 (D460 in zCD2) and D675 (E638 in zCD2) for the first and second pose, respectively.

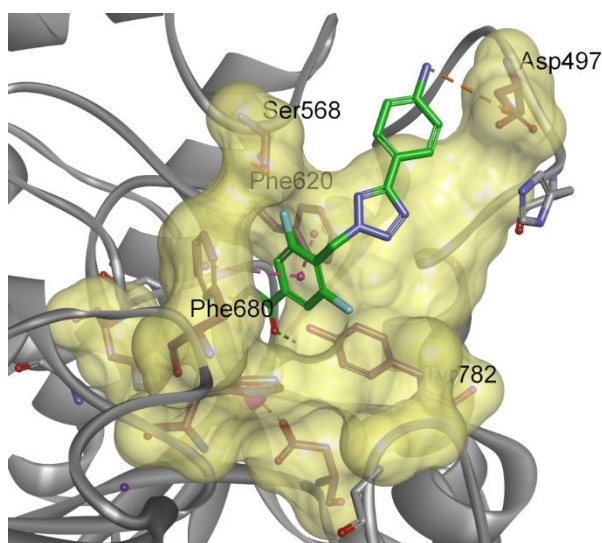
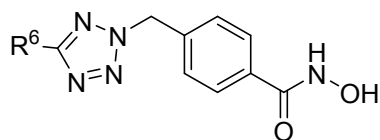


Figure 7. Binding conformers of compound **35** (in green) detected in docking experiment (hHDAC6 CD2 PDB code 5EDU). The interaction between the aniline cap term and Asp497 contributes to stabilization of the inhibitor into the enzyme binding pocket (yellow surface).

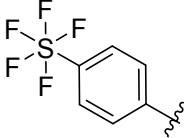
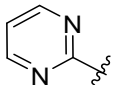
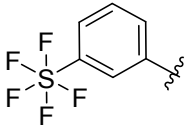
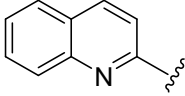
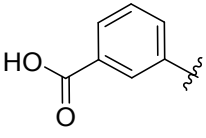
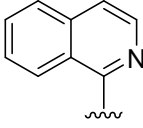
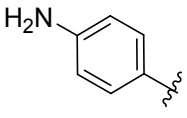
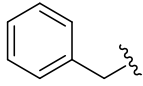
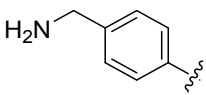
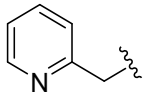
The presence of a local positive charge attractors (loops L1 and L2) suggests the introduction of an ionizable group in the para position of aryl moiety, as shown, by way of example, in Figure 7 for compound **35** (first pose). This hypothesis was confirmed by data related to all compounds bearing a positively ionizable group in that position, as evident in table 7.

Substituents in para- or meta- position with high electron density ($-\text{CF}_3$, $-\text{SF}_5$, $-\text{COOH}$) tend to slightly reduce potency and selectivity (compare compounds **22–25**, Table 7 with compound **7c**, Table 4). On the contrary, amino groups seem to slightly increase activity on HDAC6 down to one-digit nanomolar (compounds **26** and **27**) although selectivity decreases when the nitrogen atom is not directly bound to the aryl substructure.

Table 7. Tetrazole-based inhibitors bearing a range of phenyl and pyridinyl substituents.



Compd	R6	HDAC6 ^a	Sel 6 vs 3 ^b	Compd	R6	HDAC6 ^a	Sel 6 vs 3 ^b
22		11±2	51	28		9±1	189

23		25±2	50	29^c		7±2	126
24		26±3	35	30		20±1	7
25		12±1	43	31		20±1	132
26		1±1	75	7d		52±1	26
27		2±1	30	32		25±4	157

a – Enzymatic data (IC_{50}) in nM unit were obtained from curve-fitting of a 5-point enzymatic assay starting from 100, 30 or 10 μ M with 10-fold serial dilution. Experiments were done in triplicate (single experiment). SDs were calculated on technical replicates.

b - Selectivity indicator, expressed in terms of ratio between IC_{50} values $\left(\frac{HDAC3\ IC_{50}}{HDAC6\ IC_{50}}\right)$. See the SI spreadsheet for the original data and the statistical evaluation.

c - HDAC6 IC_{50} value is the mean of three independent experiments. SD was calculated on the independent experiments.

If the phenyl ring is then replaced by a pyridyl moiety (compound **28** vs compound **7c**), selectivity increases up to a factor of 189 with a small loss in the potency. The pyrimidinyl substituent (compound **29**) shows a similar behavior, whereas the inclusion of a methylene group between the tetrazole and pyridinyl substructure causes a decrease in potency and an increase in selectivity (compare compound **32** and compound **7d**). The remarkable selectivity exhibited by pyridyl and pyrimidinyl analogues could be related to new interactions in the HDAC6 isoform

1
2
3 triggered by the nitrogen atom of the ring (extra hydrogen bond) or by an enhancement of a π - π ,
4
5 or cation- π non-local bond already available for phenyl-based inhibitors. Unfortunately, docking
6
7 results did not confirm this hypothesis. If the pyridinyl group is replaced by a larger moiety, as a
8
9 quinoline or an iso-quinoline (compounds **30** and **31**, respectively), a moderate decrease in
10
11 potency is observed.
12
13
14
15
16

17 Data in Table 2 clearly show that the benzohydroxamic substructure has a role in the
18
19 selectivity for HDAC6.²⁴ This observation suggests that modifications of the aromatic ring could
20
21 improve the selectivity for this isoform. The excellent potency and selectivity of ACY-738⁴³
22
23 (Figure 1), where a pyrimidine is adopted instead of a benzene ring, confirm this hypothesis.
24
25 Fluorine atoms, due to their small volume and high electronegativity, are able to generate, when
26
27 introduced in 1,3-position, an electrostatic field equivalent to that generated by the pyrimidine
28
29 nitrogens.⁴⁴
30
31
32

33 The hydrogen to fluorine substitution is extensively adopted in drug discovery and almost 20%
34
35 of drugs actually available on the market exhibit at least one fluorine atom,⁴⁵ despite the lack of a
36
37 clear rationale. Several investigations pointed out that fluorine can hardly act as hydrogen bond
38
39 acceptor⁴⁶ or trigger a halogen bond, whereas computational studies at high level of theory drew
40
41 opposite conclusions.⁴⁷
42
43
44

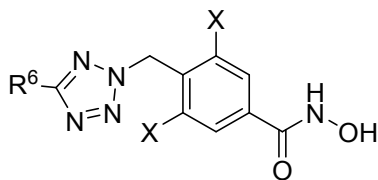
45 The superimposition (see the Supporting Information) of the complex obtained by the best
46
47 pose of compound **35** in h-CD2 (Figure 7) and the experimental active conformer detected for
48
49 Bavarostat and ACY-1083 (PDB codes 6DVO and 5WGM, respectively – see the Supporting
50
51 Information) indicate that fluorinated phenyl and pyrimidine moieties adopt a very similar
52
53
54
55
56
57
58
59
60

position, with fluorinated substrate exhibiting the F atom pointing toward Ser568, a convenient orientation at a favorable distance for both hydrogen and halogen bonds.

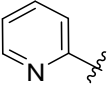
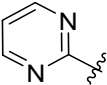
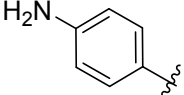
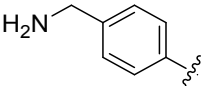
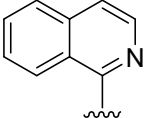
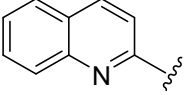
Moreover, compound **35** shows the other fluorine atom close to Leu749 (2.54 Å), that might be stabilized by a possible weak interaction between the halogen and the non-polar hydrogens of leucine, a feature detected for the Carbonic Anhydrase II and 2,3,4,5,6 Pentafluoro-SBB complex using QM/MM methods.⁴⁸ If h-CD2 HDAC6 and hHDAC1 (5ICN) are superimposed, the conserved leucine in isoform 1 (Leu271) appears too close to the cleft where the difluorophenyl substructure lies, suggesting a shape of HDAC1 binding site unfavorable for the weak bond C-F...H.

The first group of difluorine-substituted analogues took into consideration only the 2,5-disubstituted tetrazole scaffold. The results summarized in Table 8 show a systematic relevant increase in selectivity for all reported fluorinated compounds compared to the non-fluorinated analogues, whereas the potency on HDAC6 is substantially unaltered (compare, for example, the quinoline analogues **30** and **38**, Table 8).

Table 8. Effects of 3,5-fluoro substitution of benzohydroxamate moiety, when a tetrazole ring is adopted as a scaffold.



R6	Compd	X	HDAC6 ^a	Sel 6 vs 3 ^b	Compd	X	HDAC6 ^a	Sel 6 vs 3 ^b
----	-------	---	--------------------	----------------------------	-------	---	--------------------	----------------------------

	28	H	9±1	189	33^c	F	7±1	921
	29^c	H	7±2	126	34^c	F	5±1	967
	26	H	1±1	75	35^c	F	3±2	210
	27	H	2±1	30	36	F	4±2	96
	31	H	20±1	132	37	F	22±1	676
	30	H	20±1	7	38	F	10±1	58

a – Enzymatic data (IC_{50}) in nM unit were obtained from curve-fitting of a 5-point enzymatic assay starting from 100, 30 or 10 μ M with 10-fold serial dilution. Experiments were done in triplicate (single experiment). SDs were calculated on technical replicates.

b - Selectivity indicator, expressed in terms of ratio between IC_{50} values $\left(\frac{HDAC3\ IC_{50}}{HDAC6\ IC_{50}}\right)$. See the SI spreadsheet for the original data and the statistical evaluation.

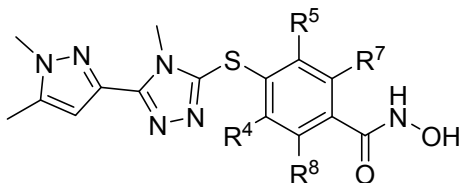
c - HDAC6 IC_{50} value is the mean of three independent experiments. SD was calculated on the independent experiments.

The same difluorine motif was then assembled on the other heteropentacyclic scaffolds (such as triazoles, oxadiazoles, and thiadiazoles) and a similar behavior was observed regardless of the scaffold used (data not shown).

The effects of fluorine atoms on the other positions of the phenyl ring were also investigated (Table 9). Both the tetrafluoro-substituted analogue (compound **40**, Table 9) and the monofluoro

in the *ortho* position to the hydroxamate moiety (compound **41**) exhibited a heavy drop in potency and in selectivity, as already observed in other examples in the literature.¹⁸

Table 9. Effects of fluorine substitution on benzohydroxamate.



Compd	R4	R5	R7	R8	HDAC6 ^a	Sel 6 vs 3 ^a
14	H	H	H	H	5±1	71
39^c	F	F	H	H	6±2	413
40	F	F	F	F	2527±21	58
41	H	H	H	F	2238±19	7

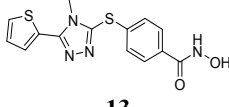
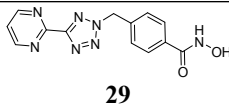
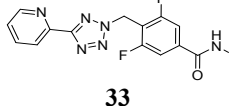
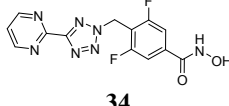
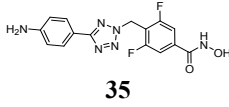
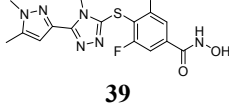
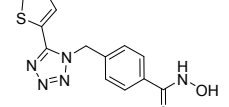
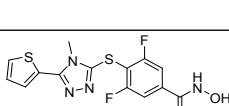
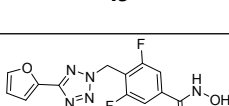
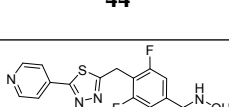
a – Enzymatic data (IC₅₀) in nM unit were obtained from curve-fitting of a 5-point enzymatic assay starting from 100, 30 or 10 μM with 10-fold serial dilution. Experiments were done in triplicate (single experiment). SDs were calculated on technical replicates.

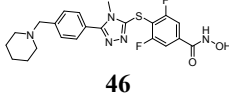
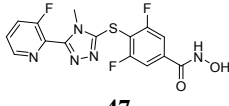
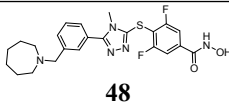
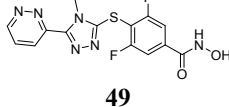
b - Selectivity indicator, expressed in terms of ratio between IC₅₀ values $\left(\frac{HDAC3\ IC_{50}}{HDAC6\ IC_{50}}\right)$. See the SI spreadsheet for the original data and the statistical evaluation.

c - HDAC6 IC₅₀ value is the mean of three independent experiments and SD was calculated on the independent experiments.

On the basis of the results and the considerations discussed above, a large number of compounds were finally synthesized and tested (data not shown).⁴⁹ Compounds with the best profiles, in terms of potency, selectivity and stability, are shown in Table 10.

Table 10. The most promising HDAC6 inhibitors.

Compound	Compnd code	HDAC6 ^a	Sel vs HDAC1 ^b	Sel vs HDAC2 ^b	Sel vs HDAC3 ^b	Rat plasma ^c	Human plasma ^c	Rat S9 ^d	HumanS9 ^d
 13	ITF3791	8±1	123	541	61	86±1	100±1	82±1	95±1
 29	ITF3983	7±2	134	435	126	99±1	76±5	99±1	83±10
 33	ITF3925	7±1	960	3699	921	87±2	96±1	97±3	86±4
 34	ITF3985	5±1	739	3109	967	78±1	93±10	96±1	89±3
 35	ITF4075	3±2	333	1138	210	77±1	88±6	48±6	74±8
 39	ITF3933	6±2	428	1910	413	80±3	92±1	30±2	76±10
 42	ITF3756	17±8	54	236	51	62±5	91±1	82±2	100±1
 43	ITF3886	9±1	460	1780	233	87±1	99±1	71±2	83±2
 44	ITF3921	3±2	751	3078	786	100±7	100±1	68±8	94±2
 45	ITF4209	4±2	733	2672	445	84±4	93±14	32±2	68±8

 46	ITF3978	5±1	803	2530	464	75±6	90±12	74±15	69±1
 47	ITF4084	6±1	584	2116	489	100±5	97±2	70±5	80±7
 48	ITF4070	10±4	522	1995	354	85±13	91±6	55±3	78±3
 49	ITF4083	13±3	624	2428	840	98±3	100±1	58±8	79±7
Givinostat		44±5	2	9	1	72±1	97±1	6±1	83±7

a – Enzymatic data (IC_{50}) in nM units are the mean of at least 3 experiments (see also the SI, Table S5) obtained from curve-fitting of a 5-point enzymatic assay starting from 100, 30 or 10 μ M with 10-fold serial dilution (technical triplicate).

b – Selectivity indicator, expressed in terms of ratio between IC_{50} values $\left(\frac{HDACn\ IC_{50}}{HDAC6\ IC_{50}}\right)$. HDAC2 inhibition assay was carried out in single experiment (technical triplicate) and the SD was calculated on technical replicates (see the SI spreadsheet).

c – Residual percentage of compounds after 4 h compared to t0 (chromatographic area). Experiments were carried out in duplicate.

d – Residual percentage of compounds after 90 minutes compared to t0 (chromatographic area). Experiments were carried out in duplicate.

As expected, the replacement of an amide bond with a more metabolically resistant substructure generated stable compounds both in plasma and in the S9 fraction (both murine and human), regardless of the nature of the heterocyclic scaffold (see Table 1 for reference standard compounds containing amide bonds, like Nexturastat, HOPB and the internally developed ITF3107).

BIOLOGICAL EVALUATION. The HDAC6 inhibitors described above have been tested on all of the remaining HDAC isoforms (see Table 11). All molecules were selective of at least one order of magnitude for HDAC6 even if some of them displayed significant activity versus HDAC8 and HDAC Class IIa isoforms (namely HDAC4, 5, 7, and 9).

Table 11. Complete profiles of the most promising HDAC6 inhibitors.

Compd	Compd code	HDAC6 ^a	Sel vs HDAC4 ^b	Sel vs HDAC5 ^b	Sel vs HDAC7 ^b	Sel vs HDAC8 ^b	Sel vs HDAC9 ^b	Sel vs HDAC10 ^b	Sel vs HDAC11 ^b
13	ITF3791	8±1	304	326	99	62	132	343	119
29	ITF3983	7±2	665	721	146	46	246	111	103
33	ITF3925	7±1	139	141	119	138	102	1463	696
34	ITF3985	5±1	105	521	157	73	89	1753	531
35	ITF4075	3±2	162	144	325	230	118	138	86
39	ITF3933	6±2	48	42	48	19	24	497	294
42	ITF3756	17±8	176	158	87	80	102	118	81
43	ITF3886	9±1	155	171	61	21	55	763	254
44	ITF3921	3±2	219	194	330	210	192	876	259
45	ITF4209	4±2	101	67	77	139	44	507	291
46	ITF3978	5±1	126	101	83	32	36	814	342
47	ITF4084	6±1	53	54	38	64	24	432	250
48	ITF4070	10±4	86	82	79	41	23	310	169
49	ITF4083	13±3	33	34	15	34	16	372	278
	Givinostat	44±5	16	13	20	5	10	4	6

a – Enzymatic data (IC₅₀) in nM units are the mean of at least 3 experiments (see also the SI, Table S5) obtained from curve-fitting of a 5-point enzymatic assay starting from 100, 30 or 10 μM with 10-fold serial dilution (technical triplicate).

b – Selectivity indicator, expressed in terms of ratio between IC₅₀ values $\left(\frac{HDACn\ IC_{50}}{HDAC6\ IC_{50}}\right)$. HDAC inhibition assays were carried out in single experiment (technical triplicate) and the SDs were calculated on technical replicates (see the SI spreadsheet).

High HDAC6 inhibitory activity and selectivity were then confirmed also in a more physiological environment. For this purpose, *in vitro* determination of α -tubulin and histone H3 acetylation was evaluated in the human 697 B-precursor acute lymphoblastic leukemia (B-Pre-ALL) cell line (see Figure 8).

Givinostat, a pan-HDAC inhibitor, was used as a reference compound for both α -tubulin and histone H3 acetylation. As expected, the reference compound showed a good acetylation of both α -tubulin and histone H3. On the contrary, the selective HDAC6 inhibitors caused α -tubulin, but not histone H3 acetylation: a small increase in H3 acetylation was detectable only at the highest concentration (see also the Supporting Information)

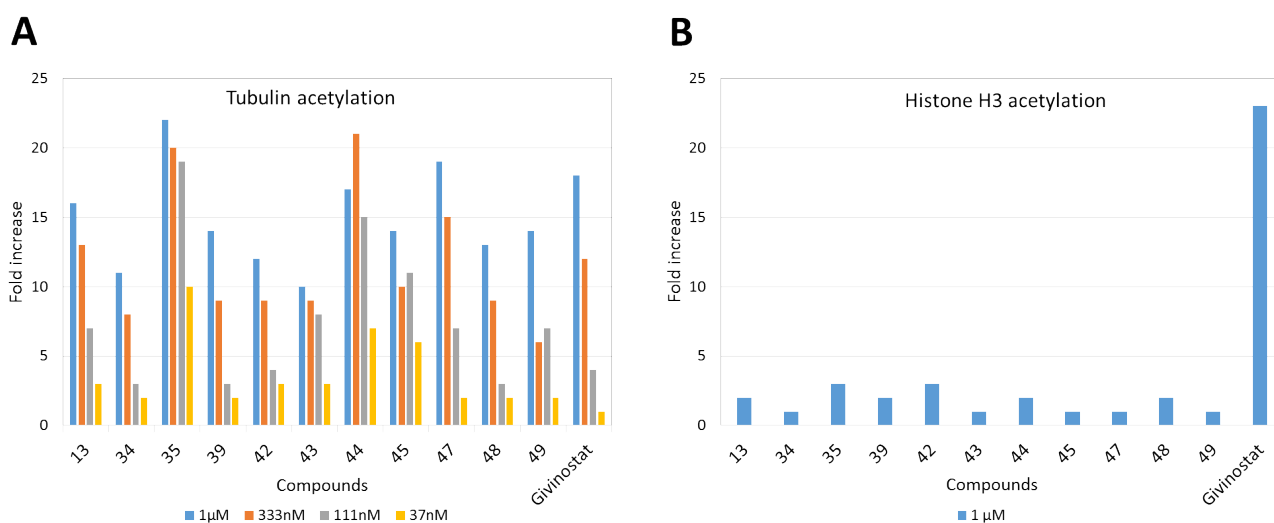


Figure 8. Acetylation after *in vitro* treatment of human 697 B-precursor acute lymphoblastic leukemia (B-Pre-ALL) cell line with selective HDAC6 inhibitors of A) Tubulin: fold increase versus control of the acetylated α -tubulin/total α -tubulin ratio at four different concentrations (37,

1
2
3 111, 333, and 1000 nM) and B) histone H3: fold increase versus control of the acetylated H3/total
4 H3 ratio, at 1000 nM. All compounds induced tubulin acetylation at all tested doses. On the
5
6 H3 ratio, at 1000 nM. All compounds induced tubulin acetylation at all tested doses. On the
7
8 contrary, histone H3 acetylation was detectable only at the highest concentration used (1 μ M),
9
10 except for the pan-inhibitor Givinostat, for which a dose-response effect was observed (data not
11
12 shown). The test has been performed in dose/response (4-points, in triplicate) starting from 1 μ M
13
14 with 3-fold serial dilution for tubulin and at single point, 1 μ M, for histone H3 (see the SI for the
15
16 original data and the statistical evaluation).
17
18
19
20
21
22
23
24
25

26 The potent and specific HDAC6 inhibitory activities were also determined *in vivo* on two
27
28 examples of the “first generation” compounds, i.e. the non-fluorinated compounds **13** and **42**,
29
30 using the degree of tubulin acetylation as a pharmacodynamic marker (data on the second
31
32 generation of compounds are in progress). C57BL/6 mice were treated intraperitoneally (ip) with
33
34 compounds **13** and **42** at 30 mg/Kg, and the amounts of tubulin and acetylated-tubulin in addition
35
36 to histone H3 and acetylated-histone H3 were determined by a specific enzyme-linked
37
38 immunosorbent assay (ELISA) in the animals’ spleens and plasma at 60 min and 4 and 24 h after
39
40 drug administration.
41
42
43

44 The results obtained are shown in Figure 9.
45
46
47
48
49
50
51
52
53
54
55
56
57
58
59
60

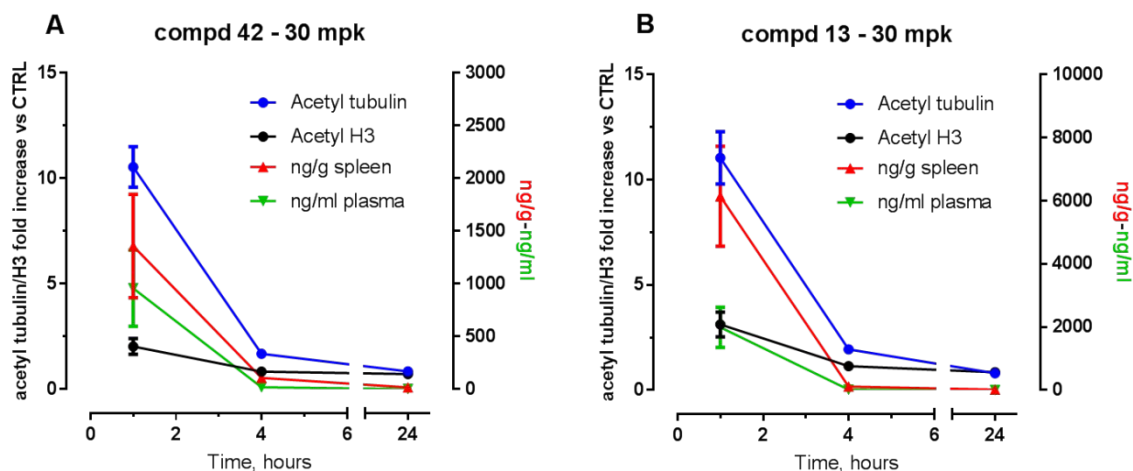


Figure 9. Levels of tubulin and histone H3 acetylation (left Y axis) and concentrations (right Y axis) of compound **42** (A) and **13** (B) in the spleen and in plasma of mice at different time points (X axis) following ip administration of inhibitors.

Both compounds were potent in inducing tubulin acetylation proportionally to their concentrations in the spleen. In fact, the maximal effect was exerted 60 min after administration (about 11-fold increase versus the vehicle-treated group) corresponding to the T_{max} of both compounds. Moreover, both compounds resulted in specific HDAC6 inhibition as detected by elevated tubulin acetylation (about 10-fold increase after 60 min) and low histone H3 acetylation (about 3-fold increase after 60 min). In particular, compound **42** resulted in more specific inhibitory activity than compound **13** as indicated by the higher Ac-tubulin/Ac-histone H3 ratio (5.2 versus 3.5) (for relative data, see the Supporting Information). In this experiment a single high dose was administered in order to determine plasma and spleen concentrations up to 24 hours after administration. It must be noted that plasma levels of both compounds at 24 hours were below the limit of detection. The pharmacodynamic effect was determined by monitoring tubulin acetylation that was constantly higher than histone H3 acetylation and detectable even

after 24 hours. These results provide evidence for *in vivo* selectivity of both compounds, however, dose response experiments and the determination of an *in vivo* EC₅₀ will be needed in the future to derive quantitative data.

A wealth of literature data suggests that toxicity at the cellular level is mainly linked to Class I inhibition, HDAC6 selective inhibitors are expected to be less cytotoxic. Hence, we evaluated the cytotoxicity of all synthesized compounds in a tumor cell line (697 B-precursor acute lymphoblastic leukemia (B-Pre-ALL)) and, for a limited number of compounds, on human peripheral blood mononuclear cells (PBMCs). Unlike Givinostat, whose IC₅₀s were far below 500 nM in both tests (100 nM and 313 nM for 697 B-precursor acute lymphoblastic leukemia and PBMC respectively), all HDAC6 selective inhibitors displayed values above 1 μM (see the Supporting Information).

Since the identified HDAC6 inhibitors are minimally cytotoxic *in vitro*, it is reasonable to expect a well-tolerated profile *in vivo*. To this aim, we determined the maximum tolerated dose (MTD) of the “first generation” compounds **13** and **42**.

The study was conducted in mice, and the compounds were administered in three *ip* doses (10, 30, and 50 mg/Kg) for two cycles of five consecutive days separated by two wash-out days. During the treatment period, the body weights and the clinical signs were monitored, and the levels of circulating white blood cells (WBC) and of platelets (PLTs) were determined 1 h after the last treatment.

The results are reported in Table 12.

Table 12. MTD evaluation of compound **13** and **42** after repeated treatment in the mouse.

Cmpd	Treatment	Body weight ^a	PLTs ^{a,b}	WBC ^{a,c}
42	10 mg/Kg	2.2	-5	-4
	30 mg/Kg	3.5	-7	-11
	50 mg/Kg	1.4	-1	-15
13	10 mg/Kg	2.8	-11	1
	30 mg/Kg	3.9	-2	-34
	50 mg/Kg	3.5	-8	-30

a - % vs control

b - PLTs = level of platelets

c - WBC = level of white blood cells

The overall results indicate that neither one of the two HDAC6 inhibitors, up to the dose of 50 mg/Kg, caused any biologically significant effects on body weight, indicating that they did not show any over toxicity. In addition, no clinical signs (postural changes, inactivity/hyperactivity, kyphosis, piloerection, spasms, cold-to-touch, soft stools, diarrheha, etc) or behavioural changes (grooming, social behaviour etc) were noticed.

On the other hand, a leucopenic effect was evident for compound **13**, whereas compound **42** was well-tolerated. The MTD of the latter molecule, in fact, was higher than 50 mg/Kg, and at this dose none of the three different monitored parameters was significantly modified (body weight <5%, PLTs, and WBC <30%).

Compound **13** showed an MTD of <30 mg/Kg (WBC -34%)

As the MTD for both compounds tested (**13** and **42**) produced overall good results, it was necessary to understand their pharmacokinetic profiles. For this purpose, plasma levels and the

main pharmacokinetic parameters were evaluated after single intravenous and oral administrations in mice (see table 13).

After intravenous administration of 2.6 mg/kg, compound **42** led to a concentration of 685 ng/mL 5 minutes after injection. The terminal half-life was 1.0 hour and the total clearance was 10.3 L/h*kg and apparent volume of distribution at steady state was 4.8 L/kg. Oral administration of 5.2 mg/kg, gave a C_{max} of 237.5 ng/mL at the first sampling point and an AUC of 93.6 ng*h/mL, corresponding to an absolute bioavailability of 18.5%.

Compound **13** gave a maximum concentration of 540 ng/mL 5 minutes after intravenous injection of 2.6 mg/kg, a total AUC of 238.6 ng*h/mL and a terminal half-life of 1.3 hours. The total clearance was 10.9 L/h*kg, whereas the apparent volume of distribution at steady state was 5.4 L/kg. After oral dosing this compound showed a C_{max} of 144.4 ng/mL 15 minutes after the administration. AUC_{tot} was 123.1 ng*h/mL, accounting for an absolute bioavailability of 25.8%. In conclusion, the pharmacokinetic profile of the two compounds are similar and both molecules show acceptable oral bioavailability.

Table 13. Pharmacokinetic parameters in mice.

	42		13	
	i.v.	oral	i.v.	oral
Dose (mg/kg)	2.6	5.2	2.6	5.2
C _{max} (ng/mL)	-	238	-	144

Tmax (h)	-	0.08	-	0.25
AUCtot (ng*h/mL)	253	94	239	123
C0 (ng/mL)	1287	-	949	-
CL (L/h*kg)	10.3	-	10.9	-
Vd (L/kg)	15.3	-	20.5	-
Vss (L/kg)	4.8		5.4	
T1/2 (h)	1	-	1.3	-
F %	19		26	

Compounds **13** and **42** were tested as possible inhibitors of the cytochrome P450 3A4 (CYP3A4) using testosterone as substrate. Ketoconazole, a strong CYP3A4 inhibitor, was used as positive control. The inhibitory potential was evaluated monitoring the activity of CYP3A4 in the metabolism of the marker substrate testosterone at its Km concentration, in human liver microsomes (HLM), in the presence of different concentrations of the potential inhibitors. IC₅₀ values for the two compounds were determined.

The results indicate that both compounds have a weak inhibitory effect on CYP3A4 since their IC₅₀ values are in the micromolar range, (IC₅₀ = 47.4 μM for compound **42** and IC₅₀ = 26.6 μM for compound **13**).

Further investigations were performed on compound **42**. The pharmacokinetic profile was evaluated in rats and dogs confirming a short half-life, a high systemic clearance and a low to moderate Vss in both species (data not shown). The oral bioavailability was 16% and 25% in dogs and rats, respectively. Ascending doses of compound **42** were also orally administered to mice resulting in a linear pharmacokinetics when administered in the range 5-50 mg/kg (data not shown).

We also explored the biological activities of our HDAC6 inhibitors. HDAC6 was shown to be involved in regulating immune response¹⁰ and specifically Treg function. Foxp3 is a Forkhead family transcription factor that is crucial for the development and inhibitory functions of regulatory T-cells. Its stable expression is a prerequisite to maintain physiologic Treg suppressive activity,⁵⁰ which is central for immune homeostasis. Mice and patients that lack Foxp3, in fact, develop a profound autoimmune-like lymphoproliferative disease (Immunodeficiency Polyendocrinopathy, Enteropathy, X-linked syndrome, IPEX) that emphasizes the importance of Treg cells in maintaining peripheral tolerance, preventing autoimmune diseases, and limiting chronic inflammatory diseases.⁵¹ For these reasons, Foxp3 has been proposed as master regulator of Treg cells.

Acetylation has been reported to be crucial for Foxp3 regulation. Ectopically expressed histone aminoacetyl transferase (HAT) p300, as well as treatment with HDACi, led to Foxp3 acetylation and stabilization, thus increasing its protein levels and function.⁵² In addition, acetylation influences Foxp3 interactions with other partners to form transcriptional regulatory complexes.⁵³

Foxp3 interacts with HDAC6, 7, and 9, and SIRT1, and it is also likely that multiple HDACs work together to regulate Foxp3 expression.⁵⁴ Published data indicate that HDAC6 has a nuclear function, and it has been implicated in Foxp3 deacetylation in Tregs.^{9a} In addition, de Zoeten et al. showed that Treg cells in mice lacking HDAC6 express more Foxp3 mRNA than wild-type mice and have increased suppressor activity.¹⁰

In order to test the capability of our HDAC6 selective inhibitors to induce Foxp3 acetylation, we transiently transfected the HEK293 cell line with pCMV6-hFoxp3-Myc-FLAG vector (and pCMV6-Myc-FLAG as control vector). After transfection, cells were treated with compound **13**

at 500 nM for 6 h. Recombinant Foxp3 was immunoprecipitated with an anti-FLAG antibody, and its acetylation state was determined by WB using specific anti acetyl-lysine antibody. As shown in Figure 10A, treatment with compound **13** induced clear acetylation of ectopically-expressed Foxp3 protein.

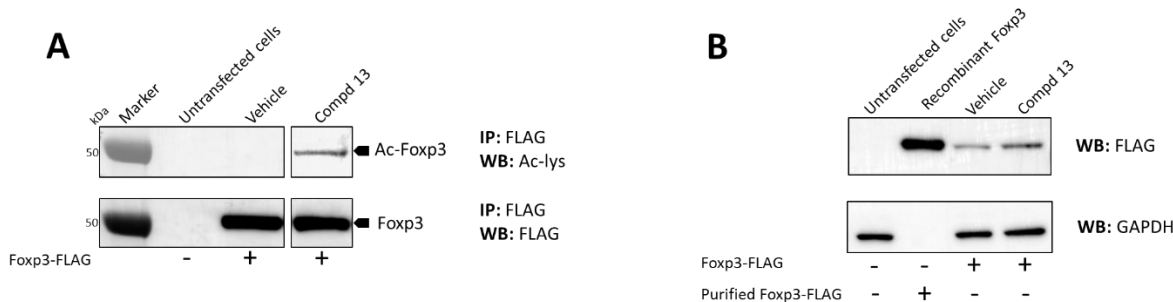


Figure 10. Compound **13** induces Foxp3 hyperacetylation. A), Anti-FLAG® immunoprecipitation from whole cell lysates. Immunoprecipitated materials were separated by sodium dodecyl sulfate polyacrylamide gel electrophoresis (SDS-PAGE) and further analyzed by western blotting (WB) with antibodies against acetyl-lysine (Ac-lys) and FLAG® as indicated. B) WB analysis from equal amounts (according to glyceraldehyde 3-phosphate dehydrogenase [GAPDH] signals) of whole lysates from human embryonic kidney (HEK) 293 cells treated with vehicle control and compound **13** for 6 h. ‘Foxp3-FLAG’ – represents untransfected cells used as the negative control. A purified Foxp3-FLAG protein was used as the positive control.

After establishing that HDAC6 inhibition, exemplified by the use of compound **13**, can induce Foxp3 acetylation, we wondered whether this inhibitor could enhance the suppressive function of Tregs in a well-established *in vitro* assay using Tregs and effector T cells (Teffs) isolated from the spleen of C57BL/6 mice.^{14b} Compound **13** was able to increase more than 3-fold the Treg-

associated suppressor activity compared to untreated cells (see Figure 11A). Furthermore, this increase was obtained over a wide range of Teff:Treg ratios as shown in Figure 11B. At the concentrations used (1 μ M), the direct activity on Teffs was <5% (well below the limit set as per protocol; see experimental section). When used at a lower concentration of 500 nM, compound **13** increased Treg suppressor activity with a relative suppression >1.5 and a negligible direct activity on Teffs (<0.5%; data not shown). These data demonstrated that our HDAC6 inhibitors are able to modulate the function of Tregs at well-tolerated concentrations and point to their usefulness in the treatment of auto-immune diseases or organ transplants.

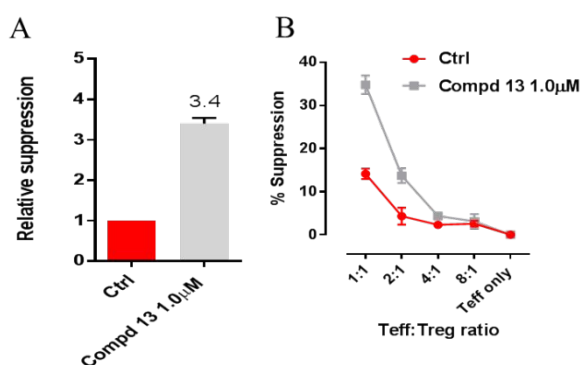
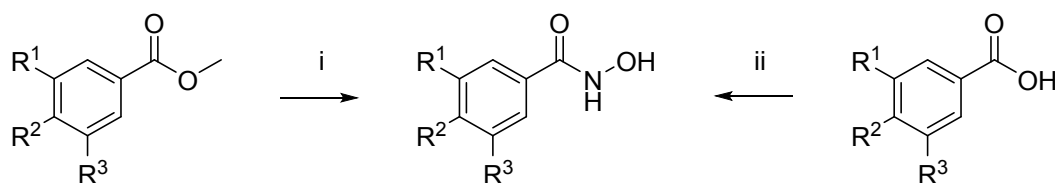


Figure 11. Compound **13** enhances Treg suppression function: A) Treg suppression function is expressed as relative suppression representing the area under the curve (AUC) ratio between compound **13**-treated samples and control (relative suppression=AUC compound/AUC control) or B) as suppression curve in which the % suppression is shown for each Teff:Treg ratio used. The graphs show the average values and the SD of two biological replicates.

CHEMISTRY. Most of the compounds described in the present paper were prepared via the synthesis of the corresponding methyl ester key intermediates, which were readily converted to

the final hydroxamic acids by hydroxylaminolysis upon treatment with a large excess of aqueous hydroxylamine and sodium hydroxide in methanol, being the strong alkaline conditions necessary for the conversion⁵⁵. In some cases, the final hydroxamic acids were obtained from the corresponding carboxylic acids and hydroxylamine hydrochloride under standard coupling conditions with 1-[bis(dimethylamino)methylene]-1H-1,2,3-triazolo[4,5-b]pyridinium 3-oxide hexafluorophosphate (HATU) and *N*-ethyl-*N*-(propan-2-yl)propan-2-amine (DIPEA) (Scheme 1).

Scheme 1. Synthesis of Hydroxamic Acid Derivatives^a



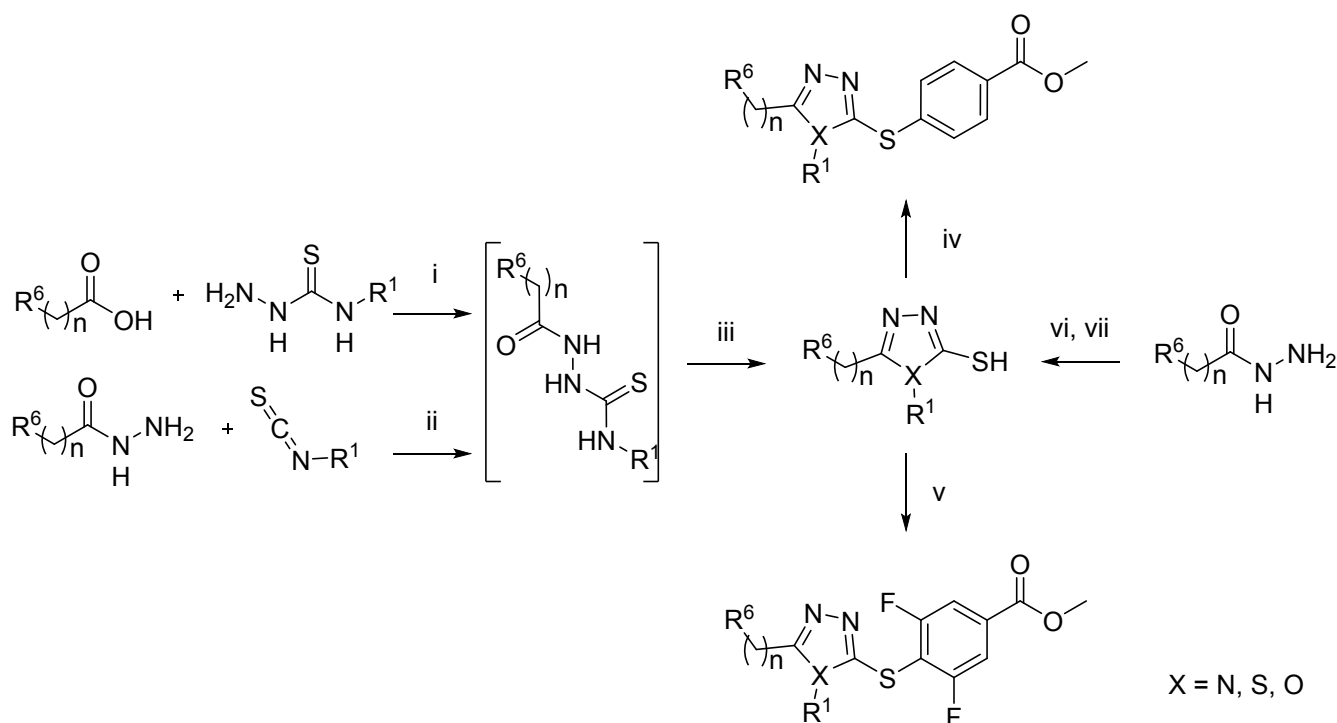
^a Reagents and conditions: (i) hydroxylamine (NH₂OH) 50% aq, 1M sodium hydroxide (NaOH), methanol (MeOH), 0°C → room temperature (rt).; (ii) HATU, DIPEA, NH₂OH•HCl, dimethylformamide (DMF), 0°C → rt

Methyl ester key intermediates have been synthesized in different ways according to the nature of the heterocyclic core scaffold.

Compounds bearing a 1,2,4-triazole thiol scaffold were synthesized starting either from the corresponding commercially available carboxylic acids, by activation with T3P (2,4,6-tripropyl-1,3,5,2,4,6-trioxatriphosphorinane-2,4,6-trioxide) and condensation with *N*-substituted hydrazine carbothioamide in the presence of DIPEA in DMF,⁵⁶ or from hydrazides, which were treated with *N*-substituted isothiocyanate in refluxing ethanol (Scheme 2).⁵⁷ Cyclization of the linear intermediates was achieved in aqueous basic conditions under heating to obtain 1,2,4-triazole-3-

thiols, which, by mean of nucleophilic aromatic substitution, were coupled with the corresponding aryl halide in the presence of potassium carbonate (K_2CO_3) to obtain key methyl ester intermediates. The reaction of 1,2,4-triazole-3-thiols with methyl 4-iodo-benzoate requires Cu(I)/L-proline catalysis and higher temperatures,⁵⁸ while the reaction with methyl 3,4,5-trifluoro-benzoate does not require any catalysis and occurs under mild conditions (55°C).⁵⁹ The same conditions were used for the synthesis of 1,3,4-oxadiazole-2-thiol- and 1,3,4-thiadiazole-2-thiol-derivatives by coupling reaction between the same aryl halides and the corresponding thiols. Non-commercially available 1,3,4-thiadiazole-2-thiols were obtained by treating different hydrazides with CS_2 under basic conditions (Scheme 2).

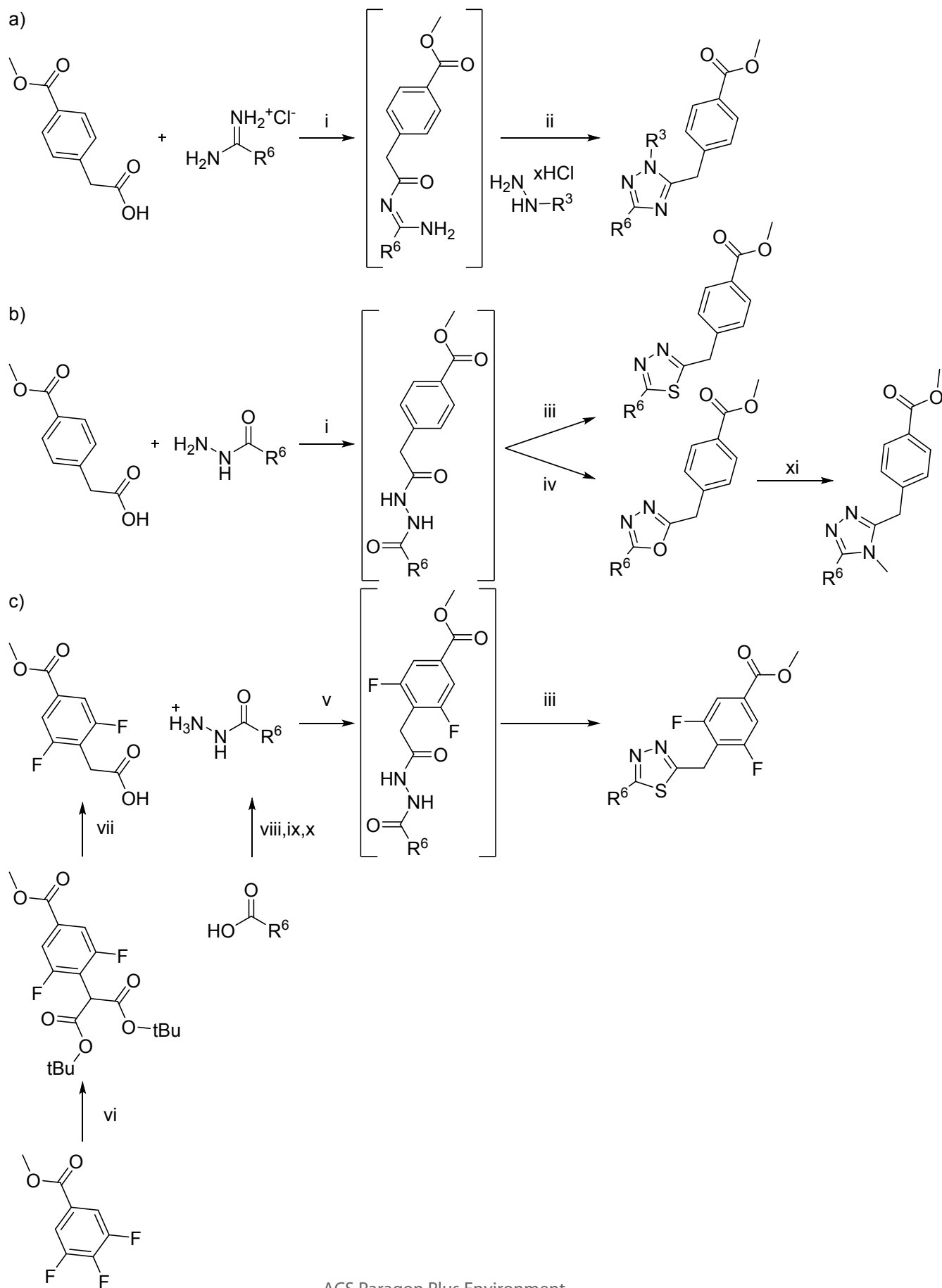
Scheme 2. Synthesis of compounds bearing a 1,2,4-triazole-3-thiol, 1,3,4-thiadiazole-2-thiol and 1,3,4-oxadiazole-2-thiol scaffold^a



^aReagents and Conditions: (i) T3P, DIPEA, DMF, 0°C → rt, 2 h; (ii) EtOH, reflux; (iii) 2M NaOH, 70°C, 16h; (iv) methyl 4-iodo-benzoate, K₂CO₃, CuI 5%, L-proline 10%, 120°C, DMF, 16 h; (v) methyl 3,4,5-trifluoro-benzoate, K₂CO₃, DMF, 55°C, 16h; (vi) CS₂, KOH, EtOH, 0°C, 1 h; (vii) H₂SO₄, acetone, 0°C, 1h.

Compounds containing a 1,2,4-triazole-2-methylene core scaffold were prepared as described in Scheme 3a starting from 2-(4-(methoxycarbonyl)phenyl)acetic acid via a reaction with a substituted amidine in the presence of HATU and DIPEA in dimethylformamide (DMF). The intermediate thus obtained was treated one-pot with hydrazine hydrate and an excess of acetic acid to yield the desired cyclic product. By treating the intermediate with a suitably substituted hydrazine, it was possible to obtain 1,3,5-substituted-1,2,4-triazole derivatives.⁶⁰

Scheme 3. Synthesis of compounds bearing 1,2,4-triazole (a and b), 1,3,4-oxadiazole (b) and 1,3,4-thiadiazole (b and c) scaffold^a



“Reagents and Conditions: (i) HATU, DIPEA, DMF, 2 h, rt; (ii) AcOH, 80°C, 16 h; (iii) Lawesson’s reagent, toluene, 120°C, 15 min; (iv) Burgess’ reagent, toluene, reflux; (v) SOCl₂, reflux, 1 h; (vi) *t*Bu-malonate, NaH, anhydrous DMF, 3 h, rt; (vii) TFA, DCE, reflux, overnight; (viii) SOCl₂, DCM, reflux, 1 h; (ix) NH₂NHBoc, TEA, 0°C → rt, 30 min; (x) TFA/DCM 1:2; (xi) MeNH₂ 2M, THF.

Compounds with 1,3,4-thiadiazole and 1,3,4-oxadiazole scaffolds were also obtained by cyclization of an open intermediate, that was prepared by condensation of 2-(4-(methoxycarbonyl)phenyl)acetic acid with appropriate hydrazide via HATU and DIPEA activation. Hydrazides were either commercially available or easily prepared from the corresponding carboxylic acid (Scheme 3c). Lawesson’s reagent was used as cyclizing agent for 1,3,4-thiadiazole derivatives, while the same intermediate cyclized upon treatment with an excess of Burgess’ reagent in refluxing toluene or tetrahydrofuran (THF) to provide 1,3,4-oxadiazoles (Scheme 3b). As for 2-(2,6-difluoro-4-(methoxycarbonyl)phenyl)acetic acid, it is not commercially available and was synthesized by reacting methyl 3,4,5-trifluorobenzoate and di-*tert*-butyl malonate in presence of sodium hydride in anhydrous dimethylformamide (DMF). The resulting di-*tert*-butyl 2-(2,6-difluoro-4-(methoxycarbonyl)phenyl)malonate was then decarboxylated by treating with trifluoroacetic acid (TFA) under reflux (Scheme 3c).

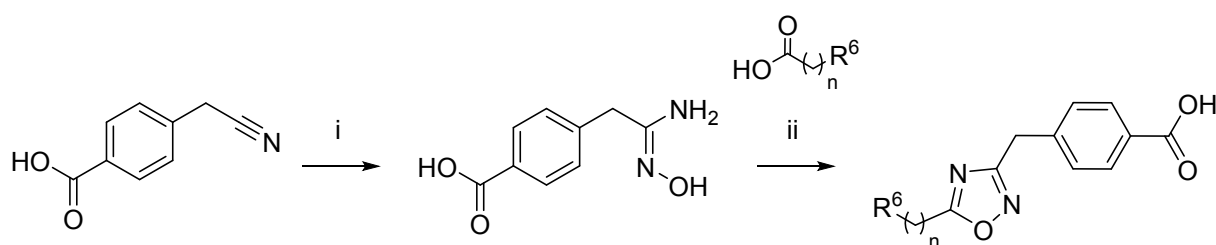
Due to the low reactivity of 2-(2,6-difluoro-4-(methoxycarbonyl)phenyl)acetic acid, it was necessary to activate it with thionyl chloride to achieve the condensation (Scheme 3c).

1,3,4-Oxadiazol derivatives were used as starting materials for the synthesis of compounds bearing the 4-methyl-4*H*-1,2,4-triazole core. The conversion was obtained by heating the oxadiazole in THF in presence of MeNH₂, as described in Scheme 3b.

1,2,4-Oxadiazole bearing compounds were synthesized starting from 4-(cyanomethyl)benzoic acid by treatment with hydroxylamine hydrochloride in the presence of an excess of potassium hydroxide in refluxing ethanol. The resulting 4-(2-amino-2-(hydroxyimino)ethyl)benzoic acid

was then reacted with the respective carboxylic acid, which was previously activated with HATU in the presence of DIPEA, to give a linear intermediate. Cyclization to 1,2,3-oxadiazole was achieved upon heating at 100°C in the presence of molecular sieves or cyclizing agents such as carbonyldiimidazole (Scheme 4).

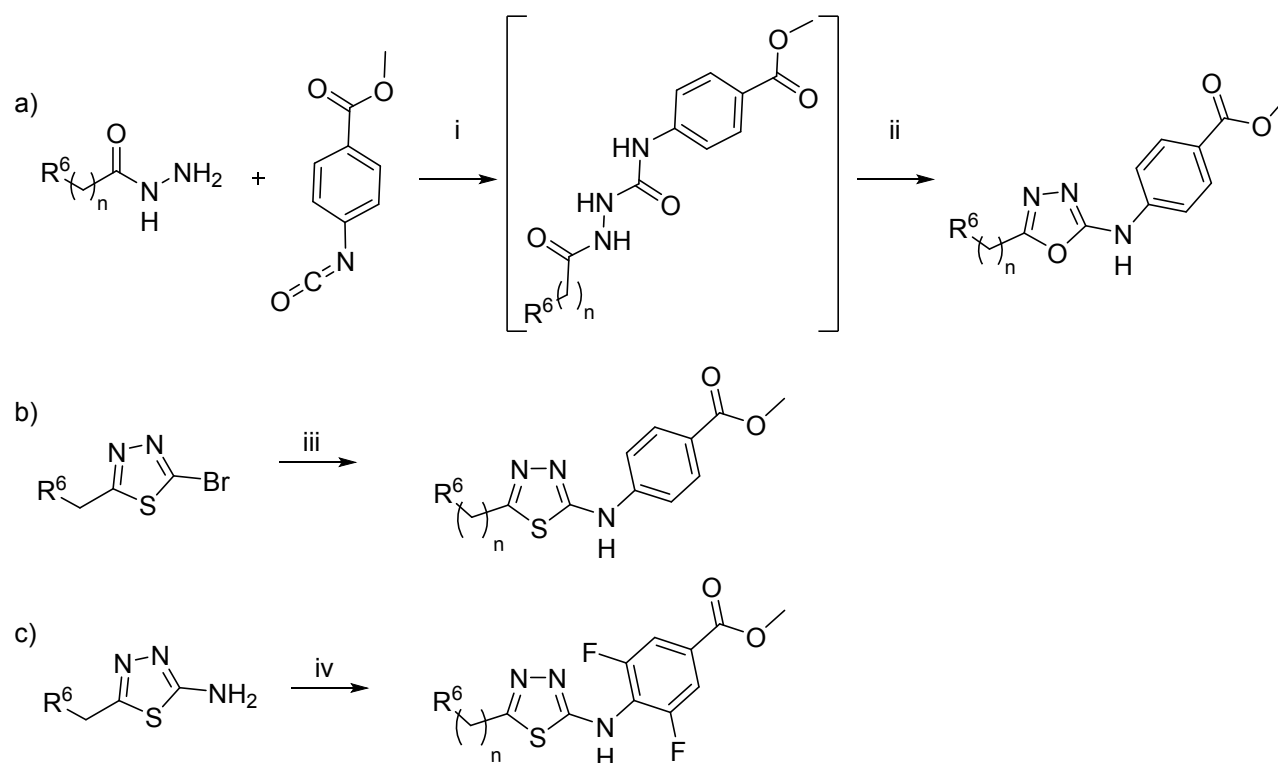
Scheme 4. Synthesis of compounds bearing a 1,2,4-Oxadiazole scaffold^a



^aReagents and Conditions: (i) $\text{NH}_2\text{OH}\cdot\text{HCl}$, NaOH , EtOH , reflux; (ii) a. HATU, DIPEA, DMF; b. carbonyldiimidazole, 100°C.

Compounds displaying a 2-amino-1,3,4-oxadiazole moiety were obtained by combining an acyl hydrazide with methyl 4-isocyanatobenzoate in THF at room temperature and refluxing the forming intermediate in the presence of an excess of Burgess' reagent (Scheme 5a).⁶¹

Scheme 5. Synthesis of compounds bearing a 2-amino-1,3,4-oxadiazole and 2-amino-1,3,4-thiadiazole scaffold^a

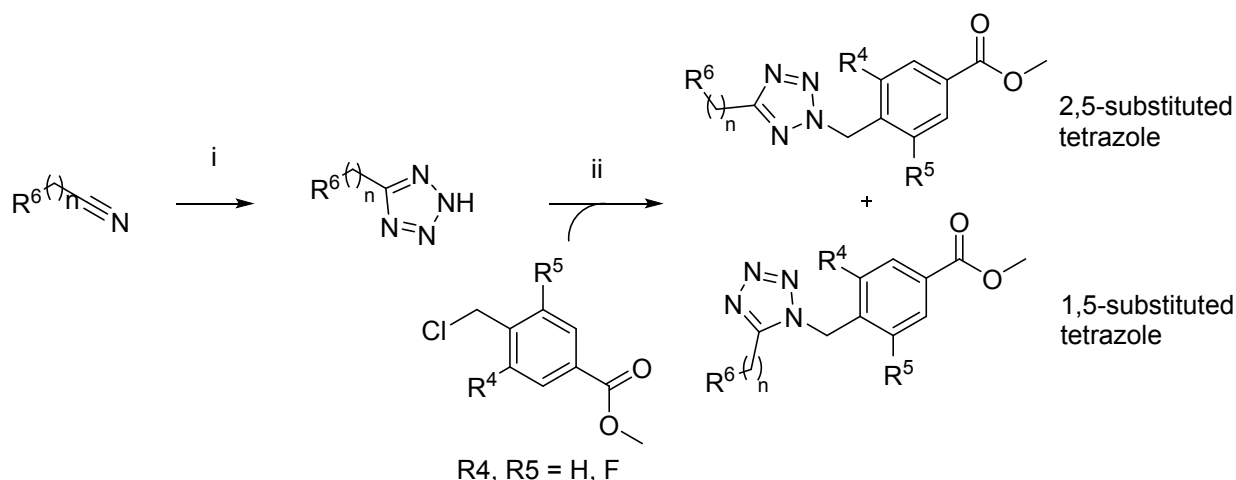


^aReagents and Conditions: (i) THF, 3 h, rt; (ii) Burgess' reagent, THF, reflux; (iii) methyl 4-aminobenzoate, NaH; (iv) methyl 3,4,5-trifluorobenzoate, K₂CO₃, tetrabutylammonium iodide (TBAI).

2-Amino-1,3,4-thiadiazole derivatives were obtained by nucleophilic substitution, which can be performed reacting 2-bromo-1,3,4-thiadiazoles with methyl 4-aminobenzoate or 2-amino-1,3,4-thiadiazoles with methyl 3,4,5-trifluorobenzoate (Scheme 5, b and c).

Compounds characterized by a tetrazole moiety were obtained by reaction of a *N*-H-tetrazole with methyl 4-(chloromethyl)benzoate or methyl 4-(chloromethyl)-3,5-difluorobenzoate in the presence of K₂CO₃ in acetonitrile (ACN) under heating (Scheme 6).⁶²

Scheme 6. Synthesis of compounds bearing a tetrazole scaffold^a



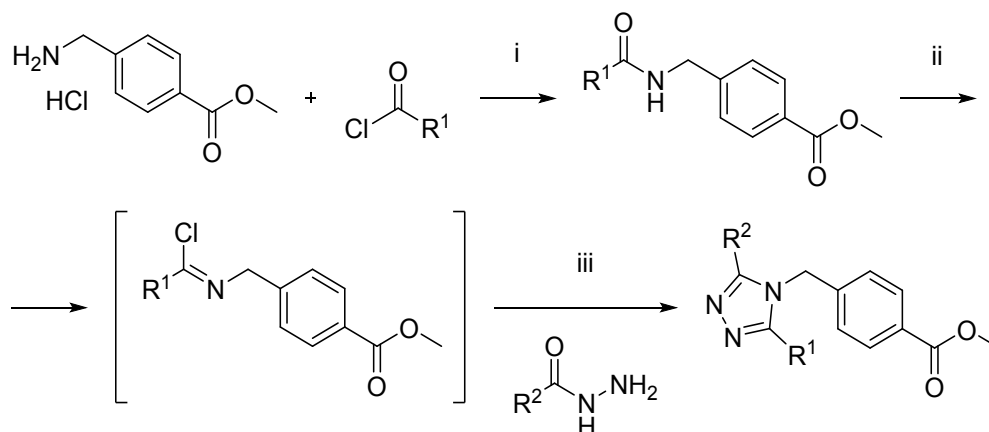
^aReagents and Conditions: (i) NaN₃, NH₄Cl, DMF, 100°C, 16 h; (ii) K₂CO₃, ACN, 100°C, 16

h.

Some *N*-H-tetrazoles were commercially available, while others were prepared by treating the respective nitrile with sodium azide and ammonium chloride in DMF under heating.

Regioselectivity depends on the tetrazole substrate with the 2,5-disubstituted product 2-10-fold favoured relative to the 1,5-disubstituted product. Regio-isomers could be identified by nuclear magnetic resonance (NMR) and easily separated by chromatography on silica gel.

Scheme 7. Synthesis of compounds bearing a 3,4,5-trisubstituted 1,2,4-triazole scaffold^a



“Reagents and Conditions: (i) TEA, DCM, rt, 18h; (ii) SOCl₂, reflux, 16 h; (iii) toluene, reflux, 16 h.

Compounds bearing a 3,4,5-trisubstituted 1,2,4-triazole as a scaffold were prepared starting from methyl p-aminomethylbenzoate hydrochloride and the corresponding acylchloride in presence of triethylamine. The resulting amide was refluxed in thionyl chloride to form an intermediate imidoyl chloride, which gave the desired product upon reaction with the corresponding hydrazide and subsequent cyclization in refluxing toluene (Scheme 7).⁶³

CONCLUSIONS

Selective HDAC6 inhibitors with improved safety and tolerability open the way for exploration of the multiple facets of this enzyme’s biology and its involvement in different diseases using a pharmacological agent. Several inhibitor chemotypes with exquisite selectivity for HDAC6 have been reported by different groups over the past decade. Indeed, for no other HDAC subtype has the same extent of inhibitor selectivity been chemically feasible thus far. While selectivity is a necessary prerequisite, the drug-like properties of HDAC6 selective inhibitors are equally important, but these are largely suboptimal for most of the described molecules.

In this study, we report on the development of a new class of HDAC6 inhibitors (see Table 10) that are very potent and selective over Class I HDACs *in vitro* and *in vivo*. Representatives of this chemical series are very well tolerated in mice, are metabolically stable, orally bioavailable, and present acceptable pharmacokinetics in the mouse. *In vitro*, these molecules are able to modulate the function of Tregs at well-tolerated concentrations, thus indicating them as useful compounds for the development of drugs for treatment of autoimmune diseases or organ

transplants. We envisage that these new inhibitors will also be useful as pharmacological tools to explore the therapeutic benefits of HDAC6 inhibition in several additional pathologies.

EXPERIMENTAL SECTION

GENERAL INFORMATION. All solvents and chemicals were used as purchased without any further purification. ¹H-NMR spectra were recorded on a Bruker Avance III spectrometer (400 MHz), and chemical shifts are reported in δ units (ppm) relative to TMS. MS experiments were carried out using an ABSciex 3200 QTRAP spectrometer or a Waters QDA mass spectrometer. Reactions were monitored by Agilent 1100 HPLC system with acetonitrile (ACN) and water spiked with 0.1% TFA as mobile phase or by Shimadzu UPLC LCMS-2020. Flash chromatographic purifications were performed using the automated Reveleris X2 system from Grace and prepacked cartridges, filled up with silica gel or reversed phase solid phase according to the case. Semipreparative RP-HPLC purifications were performed on a Waters system or on a Shimadzu UFLC 20 for preparative HPLC, LC-20AP. Purity of final compounds were determined by HPLC. For compounds intended to undergo preliminary screening, the purity was >85%. For compounds intended for in-depth studies, the purity was >95% (HPLC area %). The instrument used was Agilent 1100. Column was a Waters Xterra® RP18, 3.5 μ m particle size (150 x 2.1 mm); eluent A, water with 0.1% TFA; eluent B, CAN with 0.1% TFA; flow rate 0.2 ml/min, gradient from 0 to 100% B in 40 minutes; detection at 230 nm and column temperature of 40°C. In some cases column Phenomenex Jupiter® C18 (250 x 4.6 mm) was used, with flow rate of 1 ml/min, gradient from 5 to 85% of eluent B and column temperature of 25°C.

Some compounds described in this work were prepared by straightforward conversion of the commercially available carboxylic acid into hydroxamic acid.

General procedure (A) for the conversion of carboxylic acid into hydroxamic acid. To a solution of the acid (1 equiv) in DMF, 1-[bis(dimethylamino)methylene]-1H-1,2,3-triazolo[4,5-b]pyridinium 3-oxide hexafluorophosphate (HATU) (1.3 equiv) and *N,N*-diisopropylethylamine (DIPEA) (1.3 equiv) were added. The reaction mixture was stirred at room temperature (rt) for 15 min. A solution of NH_2OH hydrochloride (5 equiv) and DIPEA (5 equiv) in DMF was then added to the reaction mixture. After 1 h at rt, the mixture was poured into water. A white solid formed was collected by filtration and rinsed with water.

General procedure (B) for the conversion of methyl ester intermediate into hydroxamic acid (Scheme 1). The ester was suspended in methanol, and the reaction mixture obtained was cooled to 0°C in an ice bath and magnetically stirred. After hydroxylamine (50%, aqueous solution, 40 equiv) addition, a 1M sodium hydroxide (10 equiv) aqueous solution was added dropwise. The ice bath was then removed, allowing the solution to reach rt. Conversion of the starting product into hydroxamic acid was confirmed by HPLC (around 1 h). The methanolic portion was removed by evaporation under reduced pressure, and the reaction was subsequently quenched by adding 1M hydrochloric acid aqueous solution and ethyl acetate (EtOAc). Phases were separated, and the aqueous layer was re-extracted with additional EtOAc (3x). The organic phases were combined and washed with a saturated sodium bicarbonate solution (2x) and brine (2x), dried over sodium sulfate, filtered, and concentrated to dryness to yield a pure product.

***N*-Hydroxybenzamide (1)** was purchased from Enamine Ltd and used without any modification nor purification.

4-Aminobenzohydroxamic acid hydrochloride (2). The title compound was synthesized from commercially available ethyl 4-aminobenzoate according to general procedure B (7.9 mmol, 16%). ^1H NMR (400 MHz, DMSO) δ 7.77 (d, J = 8.6 Hz, 1H), 7.24 (d, J = 8.6 Hz, 1H). ^{13}C NMR (101

MHz, DMSO) δ 163.7 (s, 1C), 138.9 (s, 1C), 129.2 (s, 1C), 128.5 (s, 2C), 120.7 (s, 2C). $[M-H]^+ = 153.40$.

4-Acetamido-*N*-hydroxybenzamide (3). The title compound was synthesized from commercially available 4-acetamidobenzoic acid according to general procedure A (2.99 mmol, 18%). 1H NMR (400 MHz, DMSO) δ 11.09 (s, 1H), 10.16 (s, 1H), 8.95 (s, 1H), 7.70 (d, $J = 8.8$ Hz, 1H), 7.63 (d, $J = 8.8$ Hz, 1H), 2.07 (s, 3H). ^{13}C NMR (101 MHz, DMSO) δ 168.8 (s, 1C), 164.1 (s, 1C), 141.9 (s, 1C), 127.7 (s, 2C), 127.1 (s, 1C), 118.3 (s, 2C), 24.2 (s, 1C). $[M-H]^+ = 195.50$.

4-Aminomethyl-*N*-hydroxy-benzamide (4). The title compound was synthesized from commercially available 4-((((9H-fluoren-9-yl)methoxy)carbonyl)amino)methyl)benzoic acid according to general procedure A (0.17 mmol, 22.1% over two steps). 1H NMR (400 MHz, DMSO) δ 7.70 (d, $J = 8.2$ Hz, 2H), 7.40 (d, $J = 8.1$ Hz, 2H), 3.76 (s, 2H). ^{13}C NMR (101 MHz, DMSO) δ 164.2 (s, 1C), 147.2 (s, 1C), 130.9 (s, 1C), 127.0 (s, 2C), 126.8 (s, 2C), 42.8 (s, 1C). $[M-H]^+ = 293.1$

***N*-Hydroxy-4-(5-methyl-4H-1,2,4-triazol-3-yl)benzamide (5).** The title compound was synthesized from commercially available 4-(5-methyl-4H-1,2,4-triazol-3-yl)benzoic acid according to general procedure A (0.024 mmol, 4.5%). 1H NMR (400 MHz, DMSO) δ 11.27 (s, 1H), 9.07 (s, 1H), 8.39 (s, 1H), 8.04 (d, $J = 8.6$ Hz, 2H), 7.83 (d, $J = 8.5$ Hz, 2H), 2.41 (s, 3H).

^{13}C NMR (101 MHz, DMSO) δ 164.0 (s, 1C), 159.2 (s, 1C), 154.8 (s, 1C), 133.4 (s, 1C), 133.0 (s, 1C), 127.4 (s, 2C), 125.6 (s, 2C), 12.0 (s, 1C). $[M-H]^+ = 167.00$.

4-((4H-1,2,4-Triazol-3-yl)methyl)-*N*-hydroxybenzamide (6). The title compound was synthesized from commercially available 4-((4H-1,2,4-triazol-3-yl)methyl)benzoic acid according to general procedure A (0.063 mmol, 11%). 1H NMR (400 MHz, DMSO) δ 11.16 (s,

1H), 9.16 (s, 2H), 8.36 (s, 1H), 7.69 (d, $J = 7.8$ Hz, 2H), 7.34 (d, $J = 7.8$ Hz, 2H), 4.13 (s, 2H). ^{13}C NMR (101 MHz, DMSO) δ 164.1 (s, 1C), 158.4 (q, $^2J_{\text{C-F}} = 36.2$ Hz, 1C, CO TFA), 157.5 (s, 1C), 146.7 (s, 1C), 140.7 (s, 1C), 131.2 (s, 1C), 128.7 (s, 2C), 127.1 (s, 2C), 115.8 (q, $^1J_{\text{C-F}} = 291.6$ Hz, 1C, TFA), 32.3 (s, 1C). $[\text{M-H}]^+ = 219.18$.

General procedure (C) for the synthesis of compounds with 1,2,4-triazole scaffold - *N*-hydroxy-4-((5-phenyl-4H-1,2,4-triazol-3-yl)methyl)benzamide (7a). The synthesis of **7a** is representative for general procedure C (Scheme 3a). In a round-bottom flask 2-(4-(methoxycarbonyl)phenyl)acetic acid (0.5 mmol, 1 equiv), benzimidamide hydrochloride (0.89 mmol, 1.78 equiv) and HATU (0.55 mmol, 1.1 equiv) were suspended in DMF (2 mL). DIPEA (1.5 mmol, 3 equiv) was added, and the reaction mixture was stirred at rt. The complete conversion of the starting materials into the intermediate compound was observed after 3 h. Hydrazine hydrochloride (0.92 mmol, 1.84 equiv) and acetic acid (5 mmol, 10 equiv) were added, and the reaction mixture was heated to 80°C and stirred overnight. When the conversion of the intermediate compound into the triazolic product was complete, the reaction mixture was allowed to reach rt, and it was then diluted with EtOAc and washed with NaHCO_3 saturated solution and brine. The organic layer was dried over Na_2SO_4 , filtered, and evaporated to dryness. The crude material was purified by flash chromatography (silica cartridge, *n*-hexane/EtOAc). The obtained methyl ester was converted into hydroxamic acid according to general procedure B (0.136 mmol, 27% over 2 steps). ^1H NMR (400 MHz, DMSO) δ 11.44 (br s, 1H), 9.04 (br s, 1H), 7.98 (d, $J = 6.8$ Hz, 2H), 7.71 (d, $J = 8.2$ Hz, 2H), 7.41-7.50 (m, 3H), 7.39 (d, $J = 8.2$ Hz, 2H), 4.16 (s, 2H). ^{13}C NMR (101 MHz, DMSO) δ 164.1 (s, 1C), 140.9 (s, 2C), 131.2 (s, 1C), 129.3 (s, 2C), 128.9 (s, 2C), 128.7 (s, 2C), 127.2 (s, 2C), 125.9 (s, 2C), 32.6 (s, 1C). $[\text{M-H}]^+ = 293.1$.

***N*-Hydroxy-4-((5-phenyl-1,3,4-oxadiazol-2-yl)methyl)benzamide (7b) (Scheme 3b).** A solution of Boc-hydrazine (3.6 mmol, 1 equiv) in ACN (5 mL) and NaHCO₃ (3.6 mmol, 1 equiv) were added to a solution of benzoyl chloride (3.6 mmol, 1 equiv) in ACN (5 mL). After 3 h at rt, the solvent was evaporated under an air flow. The residue was treated with TFA for 3 h. The acid was removed under an air stream, the residue was taken up with EtOAc, and washed with a 2.5% NaHCO₃ solution. The combined organic layers were dried over Na₂SO₄, filtered, and evaporated to dryness. The resulting hydrazide was dissolved in tetrahydrofuran (THF), and the solution was added to 2- (4-(methoxycarbonyl)phenyl)acetic acid (1.3 equiv), previously activated with HATU (1.3 equiv) and DIPEA (2.6 equiv) in THF. After 3 h at rt, complete conversion of the starting reagents into the desired open intermediate was observed. Solvent was removed by evaporation under an air stream. The residue was taken up in water, and the precipitate was filtered on a sintered septum. The product was suspended in dry toluene (5 mL), Burgess' reagent (1.72 equiv) was added, and the mixture was heated under reflux. After 1 h, complete conversion of the starting compound into the cyclized product was observed. Solvent was removed by evaporation under reduced pressure. The residue was taken up with dichloromethane (DCM) and washed with 1N HCl and water. The organic phase was dried on Na₂SO₄, filtered, and evaporated to dryness. The resulting methyl ester was converted into hydroxamic acid following general procedure B (0.53 mmol, 14.2% over four steps). ¹H NMR (400 MHz, DMSO) δ 8.79 (s, 2H), 7.97 (dd, *J* = 8.1, 1.7 Hz, 2H), 7.76 (d, *J* = 8.2 Hz, 2H), 7.61 (m, 3H), 7.48 (d, *J* = 8.2 Hz, 2H), 4.44 (s, 2H). ¹³C NMR (101 MHz, DMSO) δ 165.3 (s, 1C), 164.4 (s, 1C), 163.9 (s, 1C), 137.6 (s, 1C), 132.0 (s, 1C), 131.9 (s, 1C), 129.5 (s, 2C), 129.1 (s, 2C), 127.4 (s, 2C), 126.5 (s, 2C), 123.4 (s, 1C), 30.7 (s, 1C). [M+H]⁺ = 296.04.

General procedure (D) for the synthesis of compounds with tetrazole scaffold - *N*-hydroxy-4-((5-phenyl-2H-tetrazol-2-yl)methyl)benzamide (7c). The synthesis of **7c** is representative for general procedure D (Scheme 6). Sodium azide (2.2 equiv) and ammonium chloride (2.2 equiv) were added to a solution of benzonitrile (1 equiv) in DMF at rt. The suspension was heated at 120°C and stirred overnight. After complete conversion of the starting material, the mixture was cooled to 0°C in an ice bath, diluted with 10 mL of water, and acidified with 1N HCl aqueous solution. The resulting precipitate was collected by filtration and washed twice with water before drying under reduced pressure. The resulting tetrazole was added to a reaction vessel charged with potassium carbonate (742 mg, 1 equiv) and 5 mL of ACN under magnetic stirring at rt. A solution of methyl 4-chloromethylbenzoate (1.1 equiv) in 5 mL of ACN was added. The mixture was heated at 100°C and stirred overnight. The complete conversion of starting material into the two regio-isomeric products (1,5-disubstituted and 2,5-disubstituted tetrazoles) was checked by liquid chromatography-mass spectroscopy (LC-MS). Insoluble material was removed by filtration, and the filtrate was evaporated under reduced pressure. The two regio-isomers were isolated by column chromatography on silica gel (toluene : EtOAc). The obtained methyl ester was converted into hydroxamic acid following general procedure B. ¹H NMR (400 MHz, DMSO) δ 9.72 (br s, 1H), 8.02-8.09 (m, 2H), 7.78 (d, *J* = 8.1 Hz, 2H), 7.51-7.60 (m, 3H), 7.47 (d, *J* = 8.1 Hz, 2H), 6.07 (s, 2H). ¹³C NMR (101 MHz, DMSO) δ 164.6 (s, 1C), 163.6 (s, 1C), 136.9 (s, 1C), 133.3 (s, 1C), 130.7 (s, 1C), 129.4 (s, 2C), 128.4 (s, 2C), 127.5 (s, 2C), 126.8 (s, 1C), 126.5 (s, 2C), 55.8 (s, 1C). [M-H]⁺ = 296.50.

4-((5-Benzyl-2H-tetrazol-2-yl)methyl)-*N*-hydroxybenzamide (7d). The title compound was synthesized from commercially available 5-benzyl-2H-tetrazole according to general procedure D (0.3 mmol, 30.7% over two steps, HPLC purity 88% - used only for preliminary screening).

¹H NMR (400 MHz, DMSO) δ 11.23 (s, 1H), 9.07 (s, 1H), 7.75 (d, *J* = 8.4 Hz, 2H), 7.40 (d, *J* = 8.4 Hz, 2H), 7.21-7.34 (m, 5H), 5.95 (s, 2H), 4.23 (s, 2H). ¹³C NMR (101 MHz, DMSO) δ 165.5 (s, 1C), 137.1 (s, 1C), 137.0 (s, 1C), 133.1 (s, 1C), 129.9 (s, 1C), 128.8 (s, 2C), 128.6 (s, 2C), 128.4 (s, 2C), 127.5 (s, 1C), 126.8 (s, 2C), 55.4 (s, 1C), 30.9 (s, 1C). [M+H]⁺ = 310.18

***N*-Hydroxy-4-((5-phenyl-1,2,4-oxadiazol-3-yl)methyl)benzamide (7e) (Scheme 4).** A mixture of the methyl 4-(cyanomethyl)benzoate (11 mmol, 1 equiv), NH₂OH hydrochloride (22 mmol, 2 equiv) and NaHCO₃ (22 mmol, 2 equiv) in 40 mL of methanol was refluxed overnight. After filtration and concentration, the crude product thus obtained was purified by column chromatography (10% of EtOAc in DCM). The purified methyl (Z)-4-(2-amino-2-(hydroxyimino)ethyl)benzoate (1.44 mmol, 1 equiv) was then dissolved in 2 mL of anhydrous DMF. DIPEA (4.32 mmol, 3 equiv) and benzoyl chloride (1.73 mmol, 1.2 equiv) were added and the reaction mixture was stirred overnight at rt. The reaction was quenched with water and extracted with EtOAc. Column chromatography purification (neat DCM) yielded the pure ester intermediate, which was converted into hydroxamic acid according to general procedure B. ¹H NMR (400 MHz, DMSO) δ 11.18 (br s, 1H), 9.01 (br s, 1H), 8.09 (d, *J* = 7.8 Hz, 2H), 7.67-7.76 (m, 3H), 7.63 (t, *J* = 7.6 Hz, 2H), 7.44 (d, *J* = 8.0 Hz, 2H), 4.25 (s, 2H). ¹³C NMR (101 MHz, DMSO) δ 175.3 (s, 1C), 169.8 (s, 1C), 164.0 (s, 1C), 139.0 (s, 1C), 133.4 (s, 1C), 131.6 (s, 1C), 129.6 (s, 2C), 129.1 (s, 2C), 127.9 (s, 2C), 127.3 (s, 2C), 123.4 (s, 1C), 31.3 (s, 1C). [M+H]⁺ = 296.5.

***N*-Hydroxy-4-((5-phenyl-1,3,4-thiadiazol-2-yl)methyl)benzamide (7f) (Scheme 3b).** HATU (2.21 mmol, 1.3 equiv) was added to a solution of 2-(4-(methoxycarbonyl)phenyl)acetic acid (1.7 mmol, 1 equiv) and DIPEA (4.42 mmol, 2.6 equiv) in 20 mL of anhydrous THF. After 1 h benzoylhydrazine (2.21 mmol, 1.3 equiv) was added, and the reaction mixture was stirred

overnight at rt. The solvent was evaporated, and the residue was treated with water, filtered, and then dried. The resulting linear intermediate (0.88 mmol, 1 equiv) was taken up with toluene (5 mL), and Lawesson's reagent (0.86 mmol, 0.98 equiv) was added to the mixture. The vessel was sealed, and the mixture was stirred at 120°C for 15 min. Full conversion into the cyclic product was observed by ultraperformance liquid chromatographic (UPLC) monitoring. The solvent was evaporated, and the residue was purified by column chromatography first using EtOAc in hexane (gradient 20% to 100%) followed by 5% MeOH in DCM. The resulting methyl ester was converted into hydroxamic acid according to general procedure B. ¹H NMR (400 MHz, DMSO) δ 11.21 (s, 1H), 9.03 (s, 1H), 7.93 (dd, *J* = 2.0, 7.5 Hz, 2H), 7.76 (d, *J* = 8.2 Hz, 2H), 7.5-7.57 (m, 3H), 7.47 (d, *J* = 8.2 Hz, 2H), 4.58 (s, 2H). ¹³C NMR (101 MHz, DMSO) δ 169.1 (s, 1C), 168.6 (s, 1C), 164.0 (s, 1C), 140.7 (s, 1C), 131.8 (s, 1C), 131.3 (s, 1C), 129.7 (s, 1C), 129.5 (s, 2C), 129.0 (s, 2C), 127.7 (s, 2C), 127.5 (s, 2C), 35.0 (s, 1C). [M+H]⁺ = 312.12.

***N*-Hydroxy-4-((5-phenyl-1H-tetrazol-1-yl)methyl)benzamide (7g).** The title compound was synthesized from commercially available 5-phenyl-1H-tetrazole according to general procedure D (0.3 mmol, 15.2% over two steps). ¹H NMR (400 MHz, DMSO) δ 10.86 (br s, 1H), 9.50 (br s, 1H), 7.74 (d, *J* = 7.1 Hz, 2H), 7.70 (d, *J* = 7.9 Hz, 2H), 7.66-7.52 (m, 3H), 7.18 (d, *J* = 7.8 Hz, 2H), 5.85 (s, 2H). ¹³C NMR (101 MHz, DMSO) δ 163.5 (s, 1C), 154.3 (s, 1C), 137.4 (s, 1C), 132.9 (s, 1C), 131.4 (s, 1C), 129.3 (s, 1C), 128.8 (s, 1C), 127.5 (s, 1C), 127.4 (s, 1C), 123.56 (s, 1C), 50.7 (s, 1C). [M-H]⁺ = 294.0

***N*-Hydroxy-4-(5-phenyl-[1,3,4]oxadiazol-2-yl)-benzamide (8).** The title compound was synthesized from commercially available 4-(5-phenyl-1,3,4-oxadiazol-2-yl)benzoic acid according to general procedure A (0.035 mmol, 13%). ¹H NMR (400 MHz, DMSO) δ 11.46 (br

s, 1H), 9.22 (br s, 1H), 8.22 (d, $J = 8.4$ Hz, 2H), 8.16 (dd, $J = 1.8, 7.7$ Hz, 2H), 8.00 (d, $J = 8.4$ Hz, 2H), 7.61-7.70 (m, 3H). ^{13}C NMR (101 MHz, DMSO) δ 164.4 (s, 1C), 163.6 (s, 1C), 163.2 (s, 1C), 135.8 (s, 1C), 132.3 (s, 1C), 129.5 (s, 2C), 128.0 (s, 1C), 126.9 (s, 2C), 126.8 (s, 2C), 125.6 (s, 1C), 123.3 (s, 2C). $[\text{M}-\text{H}]^+ = 282.50$.

***N*-Hydroxy-4-((4-methyl-5-phenyl-4H-1,2,4-triazol-3-yl)methyl)benzamide (9) (Scheme 3b).** Acetic acid (0.3 mL) was added dropwise to a solution of crude methyl 4-((5-phenyl-1,3,4-oxadiazol-2-yl)methyl)benzoate (1.29 mmol, 1 equiv) in 2M solution of MeNH₂ in THF (15 mL). The reaction vessel was sealed, and the reaction mixture was stirred at 150°C overnight. After cooling, the solvent was evaporated, and the residue was treated with water and extracted with EtOAc. The organic phase was dried and evaporated yielding an orange oil which was converted into hydroxamic acid following general procedure B. ^1H NMR (400 MHz, DMSO) δ 11.19 (br s, 1H), 9.08 (br s, 1H), 7.74 (d, $J = 8.2$ Hz, 2H), 7.69 (m, 2H), 7.54 (m, 3H), 7.37 (d, $J = 8.2$ Hz, 2H), 4.29 (s, 2H), 3.55 (s, 3H). ^{13}C NMR (101 MHz, DMSO) δ 164.0 (s, 1C), 154.3 (s, 1C), 154.0 (s, 1C), 139.6 (s, 1C), 131.4 (s, 1C), 129.8 (s, 1C), 128.9 (s, 2C), 128.8 (s, 2C), 128.6 (s, 2C), 127.6 (s, 1C), 127.3 (s, 2C), 31.3 (s, 1C), 30.4 (s, 1C). $[\text{M}+\text{H}]^+ = 309.1$.

***N*-Hydroxy-4-((5-phenyl-1,3,4-oxadiazol-2-yl)thio)benzamide (10a) (Scheme 2).** A mixture of 5-phenyl-1,3,4-oxadiazole-2-thiol (4.1 mmol, 1 equiv), 4-iodobenzoic acid (4.92 mmol, 1.2 equiv), L-proline (0.4 mmol, 0.1equiv) and K₂CO₃ (16.4 mmol, 4 equiv) in 20 mL of anhydrous DMF was degassed and CuI (0.2 mmol, 0.05 equiv) was added. The reaction vessel was sealed, and the mixture was stirred at 120°C for 48 h. After complete conversion of the starting thiol, the reaction mixture was poured into 150 mL of water and filtered through a pad of Celite. The filtrate was acidified with HCl. The resulting precipitate was filtered and rinsed successively with water. The obtained acid was converted into hydroxamic acid following general procedure

1
2
3 A. The reaction mixture was diluted with water and extracted with EtOAc. After evaporation, a
4 very viscous orange oil was obtained. Trituration with ACN (~15min sonication) led to the
5 formation of a precipitate which was collected by filtration, rinsed with acetonitrile and ether,
6 and then dried (0.24 mmol, 20% over two steps). ¹H NMR (400 MHz, DMSO) δ 11.35 (s, 1H),
7 9.15 (br s, 1H), 7.92-7.98 (m, 2H), 7.84 (d, *J* = 8.5 Hz, 2H), 7.75 (d, *J* = 8.5 Hz, 2H), 7.56-7.67
8 (m, 3H). ¹³C NMR (101 MHz, DMSO) δ 166.2 (s, 1C), 163.3 (s, 1C), 161.3 (s, 1C), 133.6 (s,
9 1C), 132.4 (s, 2C), 131.9 (s, 2C), 131.0 (s, 1C), 129.6 (s, 2C), 128.3 (s, 1C), 126.7 (s, 2C), 123.0
10 (s, 1C). [M+H]⁺ = 314.3.

11
12 ***N*-Hydroxy-4-((5-phenyl-1,3,4-thiadiazol-2-yl)thio)benzamide (10b) (Scheme 2).** KOH
13 (26.47 mmol, 1.1 equiv) was dissolved in anhydrous ethanol. Benzohydrazide (24.06 mmol, 1
14 equiv) was added and the reaction mixture was cooled to 0–5°C. CS₂ (27.67 mmol, 1.15 equiv)
15 was added dropwise and the reaction mixture was stirred at 0–5°C for 1 h. The resulting
16 precipitate was collected, rinsed with cold acetone, and dried. The resulting intermediate was
17 added in small portions to 25 mL of sulfuric acid previously cooled to 0–5°C. After 1 h, the
18 reaction mixture was poured into ice water, and the resulting precipitate was collected by
19 filtration, rinsed with water, dried, and dissolved in dry DMF. 4-iodobenzoic acid (4.92 mmol,
20 1.2 equiv), L-proline (0.4 mmol, 0.1equiv) and K₂CO₃ (16.4 mmol, 4 equiv) were added to the
21 solution and degassed. Finally, CuI (0.2 mmol, 0.05 equiv) was added. The reaction vessel was
22 sealed, and the reaction mixture was stirred at 120°C for 48 h. After complete conversion of the
23 starting thiol, the reaction mixture was poured into water and filtered through a pad of Celite.
24 The filtrate was acidified with HCl. The resulting precipitate was filtered and rinsed successively
25 with water, acetonitrile, and ether. The resulting acid was converted into hydroxamic acid
26 according to general procedure A. The reaction mixture was diluted with water and extracted
27
28
29
30
31
32
33
34
35
36
37
38
39
40
41
42
43
44
45
46
47
48
49
50
51
52
53
54
55
56
57
58
59
60

with EtOAc. After evaporation, a very viscous oil was obtained. Trituration with acetonitrile (~15 min sonication) led to formation of a precipitate, which was collected by filtration, rinsed with ACN and ether, and dried. ¹H NMR (400 MHz, DMSO) δ 11.37 (br s, 1H), 9.18 (br s, 1H), 7.99 – 7.71 (m, 6H), 7.63 – 7.44 (m, 3H). ¹³C NMR (101 MHz, DMSO) δ 169.6 (s, 1C), 165.2 (s, 1C), 163.1 (s, 1C), 134.0 (s, 1C), 133.9 (s, 1C), 132.8 (s, 2C), 131.7 (s, 2C), 129.6 (s, 2C), 129.2 (s, 1C), 128.6 (s, 1C), 127.7 (s, 2C). [M+H]⁺= 330.3.

***N*-Hydroxy-4-((5-phenyl-1,3,4-thiadiazol-2-yl)amino)benzamide (11a) (Scheme 5b).**

Methyl 4-aminobenzoate (0.46 mmol, 1.1 equiv) was dissolved in 5 mL of anhydrous DMF, and NaH (1.5 equiv) was added. The reaction mixture was stirred for 1 h at rt. 2-bromo-5-phenyl-1,3,4-thiadiazole (0.41 mmol, 1 equiv) was added. The resulting solution was stirred at 80°C overnight, quenched with water, and extracted with EtOAc. The crude product was purified by column chromatography using EtOAc/hexane mixture as eluent (gradient 0% to 90%). The resulting methyl ester was converted into hydroxamic acid following general procedure B (0.01 mmol, 2.2% over two steps). ¹H NMR (400 MHz, DMSO) δ 11.14 (s, 1H), 10.87 (s, 1H), 8.97 (s, 1H), 7.85-7.95 (m, 2H), 7.81 (d, *J* = 8.6 Hz, 2H), 7.74 (d, *J* = 8.5 Hz, 2H), 7.48-7.59 (m, 3H). ¹³C NMR (101 MHz, DMSO) δ 164.1 (s, 1C), 163.7 (s, 1C), 158.5 (s, 1C), 142.9 (s, 1C), 130.5 (s, 1C), 130.3 (s, 1C), 129.4 (s, 2C), 128.3 (s, 2C), 127.0 (s, 2C), 126.0 (s, 1C), 116.8 (s, 2C). [M+H]⁺= 313.08.

***N*-Hydroxy-4-((5-phenyl-1,3,4-oxadiazol-2-yl)amino)benzamide (11b) (Scheme 5a).**

Benzohydrazide (1 equiv) and methyl 4-isocyanobenzoate (1 equiv) were mixed in THF (5 mL) at rt. The resulting solution was stirred for 3 h. The intermediate formation was monitored by HPLC and LC-MS. The solvent was removed by evaporation under reduced pressure. The residue was taken up with toluene, and the mixture was heated to reflux temperature. Burgess'

reagent (2.5 equiv) was added in small portions until the intermediate was completely converted into the cyclic product. The mixture was cooled to rt and washed with water twice. The organic phase was dried, filtered, and evaporated to dryness. The crude product was purified by crystallization from DCM. The methyl ester obtained was converted into hydroxamic acid according to general procedure B (0.089 mmol, 14.8% over two steps, HPLC purity 87% - used only for preliminary screening). ¹H NMR (400 MHz, DMSO) δ 11.14 (s, 1H), 11.09 (s, 1H), 8.95 (s, 1H), 7.92 (br d, *J* = 3.6 Hz, 2H), 7.80 (d, *J* = 8.4 Hz, 2H), 7.68 (d, *J* = 8.4 Hz, 2H), 7.60 (m, 3H). ¹³C NMR (101 MHz, DMSO) δ 164.1 (s, 1C), 158.1 (s, 1C), 141.3 (s, 1C), 131.2 (s, 1C), 129.5 (s, 2C), 128.2 (s, 2C), 126.0 (s, 1C), 125.7 (s, 2C), 123.8 (s, 1C), 116.5 (s, 2C). [M+H]⁺ = 297.09.

General procedure (E) for the synthesis of compounds with 1,2,4-triazole-3-thiol scaffold - *N*-hydroxy-4-((4-methyl-5-(thiophen-2-yl)-4H-1,2,4-triazol-3-yl)thio)benzamide (13). The synthesis of **13** is representative for general procedure E (Scheme 2). 2-thiophene-2-carboxylic acid (1 equiv) and 4-methyl-3-thiosemicarbazide (1.1 equiv) were suspended in 2 mL of DMF. The temperature was lowered to 0°C in an ice bath, and T3P (propylphosphonic anhydride, 50% DMF solution, 1.5 equiv) and DIPEA (1.78 equiv) were slowly added while stirring. The ice bath was removed, and the mixture was allowed to react at rt for 16 h. The complete conversion of the starting material was confirmed by HPLC. 2 mL EtOAc, 2 mL of water, and 2 mL of 4M NaOH aqueous solution were added to the mixture. Phases were separated, and the organic layer was re-extracted with 4M NaOH aqueous solution. The combined aqueous phases were stirred for 16 h at 70°C. Conversion of the linear intermediate into the desired cyclized product was confirmed by LC-MS. The reaction mixture's pH was adjusted to 5 by dropwise addition of concentrated HCl under stirring. A precipitate formed, which was then collected by filtration. 4-

methyl-5-(thiophen-2-yl)-4H-1,2,4-triazole-3-thiol obtained (1.08 equiv) was dissolved in dry DMF, and methyl 4-iodobenzoate (1 equiv), L-proline (0.2 equiv) and K_2CO_3 (3 equiv) were added. The mixture was degassed and CuI (0.1 equiv) was added. The reaction vessel was sealed, and the reaction mixture was stirred at 120°C overnight. The reaction mixture was diluted with 3 mL of water, the resulting precipitate was collected, rinsed with water, and dried in air. The resulting methyl ester was converted into hydroxamic acid according to general procedure B (2.4 mmol, 24.4% over two steps). 1H NMR (400 MHz, DMSO) δ 11.23 (br s, 1H), 9.08 (br s, 1H), 7.84 (dd, J = 1.1, 5.1 Hz, 1H), 7.73 (ddd, J = 2.0, 2.0, 8.9 Hz, 2H), 7.70-7.72 (m, 1H), 7.33 (ddd, J = 2.0, 2.0, 8.9 Hz, 2H), 7.28 (dd, J = 3.7, 5.1 Hz, 1H), 3.77 (s, 3H). ^{13}C NMR (101 MHz, DMSO) δ 163.5 (s, 1C), 151.6 (s, 1C), 147.1 (s, 1C), 136.2 (s, 1C), 131.6 (s, 1C), 129.4 (s, 1C), 128.4 (s, 1C), 128.3 (s, 1C), 128.2 (s, 2C), 128.1 (s, 1C), 127.7 (s, 2C), 32.5 (s, 1C). $[M+H]^+$ = 332.99.

4-(4,5-Diphenyl-4H-[1,2,4]triazol-3-ylsulfanyl)-N-hydroxy-benzamide (12). The title compound was synthesized from commercially available 4,5-diphenyl-4H-1,2,4-triazole-3-thiol, according to general procedure E (0.037 mmol, 3.7% over two steps). 1H NMR (400 MHz, DMSO) δ 11.24 (s, 1H), 9.06 (br s, 1H), 7.67 (d, J = 8.5 Hz, 2H), 7.5-7.3 (m, 10H), 7.28 (d, J = 8.5 Hz, 2H). ^{13}C NMR (101 MHz, DMSO) δ 163.3 (s, 1C), 155.6 (s, 1C), 148.0 (s, 1C), 135.7 (s, 1C), 134.0 (s, 1C), 131.7 (s, 1C), 130.1 (s, 1C), 130.1 (s, 1C), 129.7 (s, 2C), 128.65 (s, 2C), 128.56 (s, 2C), 128.3 (s, 2C), 128.0 (s, 2C), 127.9 (s, 2C), 126.6 (s, 1C). $[M+H]^+$ = 389.05.

4-((5-(1,5-Dimethyl-1H-pyrazol-3-yl)-4-methyl-4H-1,2,4-triazol-3-yl)thio)-N-hydroxybenzamide (14). The title compound was synthesized from commercially available 5-(1,5-dimethyl-1H-pyrazol-3-yl)-4-methyl-4H-1,2,4-triazole-3-thiol according to general procedure E (1.44 mmol, 30.2% over two steps). 1H NMR (400 MHz, DMSO) δ 11.20 (br s,

1H), 9.09 (br s, 1H), 7.72 (ddd, $J = 2.0, 2.0, 8.6$ Hz, 2H), 7.27 (ddd, $J = 2.0, 2.0, 8.6$ Hz, 2H), 6.64 (br q, $J = 0.6$ Hz, 1H), 3.83 (s, 3H), 3.82 (s, 3H), 2.33 (d, $J = 0.6$ Hz, 3H). ^{13}C NMR (101 MHz, DMSO) δ 163.4 (s, 1C), 151.0 (s, 1C), 146.5 (s, 1C), 140.3 (s, 1C), 138.4 (s, 1C), 136.2 (s, 1C), 131.7 (s, 1C), 128.2 (s, 2C), 127.5 (s, 2C), 105.5 (s, 1C), 36.6 (s, 1C), 32.6 (s, 1C), 10.7 (s, 1C). $[\text{M}+\text{H}]^+ = 344.98$.

4-((4-Amino-5-(3-(*N,N*-diethylsulfamoyl)phenyl)-4H-1,2,4-triazol-3-yl)amino)-*N*-hydroxybenzamide (15). The title compound was synthesized from commercially available 3-(4-amino-5-mercapto-4H-1,2,4-triazol-3-yl)-*N,N*-diethylbenzenesulfonamide according to general procedure E (0.277 mmol, 15.8% over two steps, HPLC purity 87% - used only for preliminary screening). ^1H NMR (400 MHz, DMSO) δ 10.75 (br s, 1H), 10.38 (br s, 1H) 8.54 (dd, $J = 1.7, 1.7$ Hz, 1H), 8.37 (ddd, $J = 1.6, 1.2, 7.7$ Hz, 1H), 7.94 (ddd, $J = 1.2, 1.7, 7.8$ Hz, 1H), 7.79 (d, $J = 7.6$ Hz, 1H), 7.76 (ddd, $J = 2.0, 1.8, 8.7$ Hz, 2H), 7.49 (ddd, $J = 2.1, 1.8, 8.7$ Hz, 2H), 6.36 (s, 2H), 3.22 (q, $J = 7.1$ Hz, 4H), 1.07 (t, $J = 7.1$ Hz, 6H). $[\text{M}+\text{H}]^+ = 463.12$.

***N*-Hydroxy-4-((1-(2-methoxyphenyl)-3-(thiophen-2-yl)-1H-1,2,4-triazol-5-yl)methyl)benzamide (16).** The title compound was synthesized from commercially available thiophene-2-carboximidamide hydrochloride and (2-methoxyphenyl)hydrazine hydrochloride according to general procedure C (0.044 mmol, 4.1% over three steps). ^1H NMR (400 MHz, DMSO) δ 11.15 (br s, 1H), 8.99 (br s, 1H), 7.64 (d, $J = 8.3$ Hz, 2H), 7.61 (m, 2H), 7.55 (dt, $J = 1.5, 7.8$ Hz, 1H), 7.43 (dd, $J = 1.5, 7.7$ Hz, 1H), 7.24 (d, $J = 8.3$ Hz, 1H), 7.12 (m, 4H), 4.03 (s, 2H), 3.68 (s, 3H). ^{13}C NMR (101 MHz, DMSO) δ 164.0 (s, 1C), 157.1 (s, 1C), 156.3 (s, 1C), 154.1 (s, 1C), 139.2 (s, 1C), 133.6 (s, 2C), 131.8 (s, 1C), 131.2 (s, 1C), 128.8 (s, 1C), 128.6 (s, 2C), 128.1 (s, 1C), 127.3 (s, 1C), 127.0 (s, 1C), 126.0 (s, 1C), 125.1 (s, 1C), 120.8 (s, 1C), 112.8 (s, 1C), 55.8 (s, 1C), 31.5 (s, 1C). $[\text{M}+\text{H}]^+ = 407.04$.

4-((1-Benzyl-3-(4-chlorophenyl)-1H-1,2,4-triazol-5-yl)methyl)-N-hydroxybenzamide (17).

The title compound was synthesized from commercially available amino(4-chlorophenyl)methaniminium chloride and benzylhydrazine dihydrochloride according to general procedure C (0.0074 mmol, 1% over three steps, HPLC purity 85% - used only for preliminary screening). ¹H NMR (400 MHz, DMSO) δ 11.17 (s, 1H), 9.01 (s, 1H), 7.96 (d, *J* = 8.7 Hz, 2H), 7.66 (d, *J* = 8.3 Hz, 2H), 7.50 (d, *J* = 8.7 Hz, 2H), 7.31 (m, 5H), 7.19 (dd, *J* = 1.8, 7.4 Hz, 2H), 5.49 (s, 2H), 4.34 (s, 2H). ¹³C NMR (101 MHz, DMSO) δ 164.0 (s, 1C), 159.2 (s, 1C), 155.4 (s, 1C), 139.5 (s, 1C), 136.1 (s, 2C), 133.7 (s, 2C), 131.4 (s, 1C), 129.8 (s, 1C), 128.9 (s, 2C), 128.8 (s, 2C), 128.7 (s, 2C), 127.9 (s, 1C), 127.6 (s, 2C), 127.5 (s, 1C), 127.2 (s, 1C), 51.4 (s, 1C), 30.9 (s, 1C). [M+H]⁺ = 419.01.

4-((5-Cyclopropyl-1-phenyl-1H-1,2,4-triazol-3-yl)thio)-N-hydroxybenzamide (18). The title compound was synthesized from commercially available 5-cyclopropyl-1-phenyl-1H-1,2,4-triazole-3-thiol according to general procedure E (0.45 mmol, 45.33% over two steps, HPLC purity 85% - used only for preliminary screening). ¹H NMR (400 MHz, DMSO) δ 11.29 (s, 2H), 9.09 (s, 1H), 7.71 (ddd, *J* = 2.0, 2.0, 8.7 Hz, 1H), 7.48-7.58 (m, 5H), 7.37 (ddd, *J* = 2.2, 2.2, 8.7 Hz, 2H), 2.05 (tt, *J* = 4.9, 8.4 Hz, 1H), 0.94-1.00 (m, 2H), 0.83-0.88 (m, 2H). ¹³C NMR (101 MHz, DMSO) δ 166.1 (s, 1C), 163.4 (s, 1C), 147.6 (s, 1C), 136.7 (s, 1C), 134.5 (s, 1C), 132.2 (s, 1C), 129.8 (s, 2C), 129.4 (s, 2C), 129.2 (s, 1C), 128.0 (s, 2C), 125.0 (s, 2C), 117.7 (s, 1C), 8.9 (s, 1C), 7.9 (s, 1C). [M+H]⁺ = 353.07.

N-Hydroxy-4-((4-methylthiazol-2-yl)amino)benzamide (19). The title compound was synthesized from commercially available 4-((4-methylthiazol-2-yl)amino)benzoic acid according to general procedure A (0.3 mmol, 63.8%, HPLC purity 93.2% - used only for preliminary screening). ¹H NMR (400 MHz, DMSO) δ 11.04 (br s, 1H), 10.42 (s, 1H), 7.71 (d, *J* = 8.8 Hz,

2H), 7.65 (d, $J = 8.8$ Hz, 2H), 6.53 (br q, $J = 1.0$ Hz, 1H), 2.25 (d, $J = 0.9$ Hz, 3H). ^{13}C NMR (101 MHz, DMSO) δ 164.2 (s, 1C), 162.7 (s, 1C), 158.5 (q, $^2J_{\text{C-F}} = 37.9$ Hz, 1C, TFA CO), 147.4 (s, 1C), 143.5 (s, 1C), 128.1 (s, 2C), 125.2 (s, 1C), 116.2 (s, 2C), 115.3 (q, $^1J_{\text{C-F}} = 290.0$ Hz, 1C, CF_3 TFA), 103.2 (s, 1C), 17.2 (s, 1C). $[\text{M}+\text{H}]^+ = 249.99$.

***N*-Hydroxy-4-((5-phenylthiazol-2-yl)thio)benzamide (20).** The title compound was synthesized from commercially available 5-phenylthiazole-2-thiol according to general procedure E (0.49 mmol, 33% over two steps). ^1H NMR (400 MHz, DMSO) δ 11.29 (br s, 1H), 9.17 (br s, 1H), 8.16 (s, 1H), 7.90-7.95 (m, 2H), 7.84 (ddd, $J = 1.8, 1.8, 8.4$ Hz, 2H), 7.72 (ddd, $J = 1.8, 1.8, 8.4$ Hz, 2H), 7.45 (ddt, $J = 1.3, 1.4, 7.2$ Hz, 2H), 7.37 (ddt, $J = 1.3, 6.8, 7.2$ Hz, 1H). ^{13}C NMR (101 MHz, DMSO) δ 163.3 (s, 1C), 162.5 (s, 1C), 155.3 (s, 1C), 135.0 (s, 1C), 133.6 (s, 1C), 133.5 (s, 1C), 132.2 (s, 2C), 129.0 (s, 2C), 128.5 (s, 1C), 128.5 (s, 1C), 126.1 (s, 2C), 117.0 (s, 1C). $[\text{M}+\text{H}]^+ = 286.95$.

4-((1H-Pyrazol-1-yl)methyl)-*N*-hydroxybenzamide (21). The title compound was synthesized from commercially available 4-((4-methylthiazol-2-yl)amino)benzoic acid according to general procedure A (0.6 mmol, 48,6%). ^1H NMR (400 MHz, DMSO) δ 11.19 (s, 1H), 9.04 (broad s, 1H), 7.86 (dd, $J = 0.5, 2.1$ Hz, 1H), 7.71 (d, $J = 8.3$ Hz, 2H), 7.48 (dd, $J = 0.5, 1.8$ Hz, 1H), 7.25 (d, $J = 8.3$ Hz, 2H), 6.30 (dd, $J = 1.8, 2.1$ Hz, 1H), 5.39 (s, 2H). ^{13}C NMR (101 MHz, DMSO) δ 164.4 (s, 1C), 141.3 (s, 1C), 139.6 (s, 1C), 132.5 (s, 1C), 130.8 (s, 1C), 127.8 (s, 2C), 127.5 (s, 1C), 106.0 (s, 2C), 54.7 (s, 1C). $[\text{M}+\text{H}]^+ = 218.2$.

***N*-Hydroxy-4-[5-(4-trifluoromethyl-phenyl)-tetrazol-2-ylmethyl]-benzamide (22).** The title compound was synthesized from commercially available 5-(4-(trifluoromethyl)phenyl)-2H-tetrazole according to general procedure D (0.056 mmol, 11.27% over two steps). ^1H NMR (400 MHz, DMSO) δ 11.00 (s, 1H), 9.08 (s, 1H), 8.26 (d, $J = 8.0$ Hz, 2H), 7.92 (d, $J = 8.0$ Hz, 2H),

7.78 (d, $J = 8.1$ Hz, 2H), 7.49 (d, $J = 8.1$ Hz, 2H), 6.10 (s, 2H). ^{13}C NMR (101 MHz, DMSO) δ 163.7 (s, 1C), 163.4 (s, 1C), 136.8 (s, 1C), 133.2 (s, 1C), 130.7 (q, $^2J_{\text{C-F}} = 32.1$ Hz, 1C), 130.6 (q, $^4J_{\text{C-F}} = 1.5$ Hz, 2C), 128.5 (s, 2C), 127.6 (s, 1C), 127.3 (s, 2C), 126.4 (q, $^3J_{\text{C-F}} = 3.7$ Hz, 2C), 124.0 (q, $^1J_{\text{C-F}} = 272.3$ Hz, 1C), 56.0 (s, 1C). $[\text{M-H}]^+ = 364.60$.

***N*-Hydroxy-4-((5-(4-(pentafluorosulfanyl)phenyl)-2H-tetrazol-2-yl)methyl)benzamide**

(23). The title compound was synthesized from commercially available 4-(pentafluorosulfaneyl)benzonitrile according to general procedure D (0.27 mmol, 65.8% over three steps, HPLC purity 92.2% - used only for preliminary screening). ^1H NMR (400 MHz, DMSO) δ 11.24 (br s, 1H), 9.14 (br s, 1H), 8.27 (d, $J = 9.0$ Hz, 2H), 8.11 (ddd, $J = 2.3, 2.2, 9.0$ Hz, 2H), 7.78 (ddd, $J = 1.7, 1.8, 8.4$ Hz, 2H), 7.50 (d, $J = 8.4$ Hz, 2H), 6.12 (s, 2H). ^{13}C NMR (101 MHz, DMSO) δ 163.6 (s, 1C), 162.9 (s, 1C), 154.0 (m, $^2J_{\text{C-F}} = 16.5$ Hz, 1C), 136.8 (s, 1C), 133.2 (s, 1C), 130.5 (s, 1C), 128.5 (s, 2C), 127.6 (s, 2C), 127.5 (s, 2C), 127.1 (m, $^3J_{\text{C-F}} = 4.6$ Hz, 2C), 56.0 (s, 1C). $[\text{M+H}]^+ = 421.94$.

***N*-Hydroxy-4-((5-(3-(pentafluorosulfanyl)phenyl)-2H-tetrazol-2-yl)methyl)benzamide**

(24). The title compound was synthesized from commercially available 3-(pentafluorosulfaneyl)benzonitrile according to general procedure D (0.26 mmol, 59% over three steps). ^1H NMR (400 MHz, DMSO) δ 11.25 (s, 1H), 9.08 (s, 1H), 8.41 (dd, $J = 1.7, 2.2$ Hz, 1H), 8.34 (d, $J = 7.9$ Hz, 1H), 8.13 (ddd, $J = 1.0, 2.2, 8.1$ Hz, 1H), 7.85 (dd, $J = 7.9, 8.0$ Hz, 1H), 7.78 (ddd, $J = 1.8, 1.8, 8.4$ Hz, 1H), 7.49 (d, $J = 8.4$ Hz, 2H), 6.12 (s, 1H). ^{13}C NMR (101 MHz, DMSO) δ 163.7 (s, 1C), 163.0 (s, 1C), 153.4 (m, $^2J_{\text{C-F}} = 16.0$ Hz, 1C), 136.8 (s, 1C), 133.2 (s, 1C), 131.1 (s, 1C), 130.4 (s, 1C), 128.4 (s, 2C), 128.1 (s, 1C), 127.9 (m, $^3J_{\text{C-F}} = 4.6$ Hz, 1C), 127.6 (s, 2C), 123.1 (m, $^3J_{\text{C-F}} = 4.4$ Hz, 1C), 56.0 (s, 1C). $[\text{M+H}]^+ = 421.94$.

3-(2-(4-(Hydroxycarbamoyl)benzyl)-2H-tetrazol-5-yl)benzoic acid (25). The title compound was synthesized from commercially available *tert*-butyl 3-cyanobenzoate according to general procedure D (0.068 mmol, 13.7 % over four steps). ¹H NMR (400 MHz, DMSO) δ 13.30 (br s, 1H), 11.24 (s, 1H), 9.07 (s, 1H), 8.60 (br s, 1H), 8.29 (d, *J* = 7.8 Hz, 1H), 8.10 (d, *J* = 7.8 Hz, 1H), 7.78 (d, *J* = 8.2 Hz, 2H), 7.70 (t, *J* = 7.8 Hz, 1H), 7.50 (d, *J* = 8.2 Hz, 2H), 6.10 (s, 2H). ¹³C NMR (101 MHz, DMSO) δ 166.8 (s, 1C), 163.9 (s, 1C), 136.9 (s, 1C), 133.2 (s, 1C), 132.1 (s, 1C), 131.3 (s, 1C), 130.5 (s, 1C), 129.9 (s, 1C), 128.5 (s, 2C), 127.6 (s, 2C), 127.2 (s, 1C), 127.1 (s, 1C), 55.9 (s, 1C). [M+H]⁺ = 340.4.

4-((5-(4-Aminophenyl)-2H-tetrazol-2-yl)methyl)-*N*-hydroxybenzamide 2,2,2-trifluoroacetate (26). The title compound was synthesized from commercially available 4-aminobenzonitrile according to general procedure D (0.15 mmol, 3.1% over five steps). ¹H NMR (400 MHz, DMSO) δ 11.25 (s, 1H), 7.77 (d, *J* = 8.4 Hz, 2H), 7.76 (d, *J* = 8.7 Hz, 2H), 7.45 (d, *J* = 8.4 Hz, 2H), 6.76 (d, *J* = 8.4 Hz, 2H), 5.99 (s, 2H), 5.43 (broad s, 3H). ¹³C NMR (101 MHz, DMSO) δ 165.1 (s, 1C), 163.8 (s, 1C), 158.4 (q, ²*J*_{C-F} = 35.9 Hz, TFA), 148.7 (s, 1C), 137.3 (s, 1C), 133.0 (s, 1C), 128.3 (s, 2C), 127.7 (s, 2C), 127.5 (s, 2C), 115.5 (s, 1C), 115.3 (s, 2C), 55.5 (s, 1C). [M+H]⁺ = 311.5.

4-((5-(4-(Aminomethyl)phenyl)-2H-tetrazol-2-yl)methyl)-*N*-hydroxybenzamide 2,2,2-trifluoroacetate (27). The title compound was synthesized from commercially available *tert*-butyl (4-cyanobenzyl)carbamate according to general procedure D (0.125 mmol, 11% over four steps). ¹H NMR (400 MHz, DMSO) δ 11.26 (s, 1H), 9.09 (br s, 1H), 8.27 (br s, 3H), 8.11 (ddd, *J* = 1.9, 1.9, 8.5 Hz, 2H), 7.78 (ddd, *J* = 1.9, 1.9, 8.5 Hz, 2H), 7.64 (d, *J* = 8.5 Hz, 2H), 7.49 (d, *J* = 8.5 Hz, 2H), 6.08 (s, 2H), 4.13 (br q, *J* = 5.3 Hz, 2H). ¹³C NMR (101 MHz, DMSO) δ 164.1 (s, 1C), 163.7 (s, 1C), 158.3 (q, ²*J*_{C-F} = 31.9 Hz, CO TFA), 137.0 (s, 1C), 136.6 (s, 2C), 133.1 (s,

1C), 129.8 (s, 2C), 128.5 (s, 2C), 127.6 (s, 1C), 126.9 (s, 1C), 126.7 (s, 2C), 117.0 (q, $^1J_{\text{C-F}} = 299.7$ Hz, 1C, TFA), 55.8 (s, 1C), 42.0 (s, 1C). $[\text{M}+\text{H}]^+ = 325.3$.

***N*-Hydroxy-4-(5-pyridin-2-yl-tetrazol-2-ylmethyl)-benzamide (28).** The title compound was synthesized from commercially available 2-cyanopyridine according to general procedure D (0.19 mmol, 16.2% over three steps). ^1H NMR (400 MHz, DMSO) δ 11.19 (s, 1H), 9.04 (br d, $J = 1.3$ Hz, 1H), 8.82 (ddd, $J = 1.0, 1.7, 4.8$ Hz, 1H), 8.29 (ddd, $J = 1.0, 1.1, 7.8$ Hz, 1H), 8.09 (ddd, $J = 1.7, 7.8, 7.8$ Hz, 1H), 7.70 (d, $J = 8.4$ Hz, 2H), 7.66 (ddd, $J = 1.1, 4.8, 7.7$ Hz, 1H), 7.36 (d, $J = 8.4$ Hz, 2H), 6.26 (s, 2H). ^{13}C NMR (101 MHz, DMSO) δ 163.8 (s, 1C), 151.8 (s, 1C), 149.9 (s, 1C), 143.9 (s, 1C), 138.4 (s, 2C), 138.3 (s, 1C), 132.7 (s, 1C), 127.9 (s, 2C), 127.4 (s, 1C), 126.2 (s, 1C), 124.4 (s, 1C), 51.8 (s, 1C). $[\text{M}+\text{H}]^+ = 297.03$.

***N*-Hydroxy-4-(5-pyrimidin-2-yl-tetrazol-2-ylmethyl)-benzamide (29).** The title compound was synthesized from commercially available pyrimidine-2-carbonitrile according to general procedure D (0.01 mmol, 0.5% over three steps). ^1H NMR (400 MHz, DMSO) δ 11.22 (br s, 1H), 9.09 (br s, 1H), 9.01 (d, $J = 4.9$ Hz, 2H), 7.78 (d, $J = 8.5$ Hz, 2H), 7.67 (t, $J = 4.9$ Hz, 1H), 7.50 (d, $J = 8.5$ Hz, 2H), 6.12 (s, 2H). ^{13}C NMR (101 MHz, DMSO) δ 163.8 (s, 1C), 163.7 (s, 1C), 158.3 (s, 2C), 155.6 (s, 1C), 136.8 (s, 1C), 133.2 (s, 1C), 128.6 (s, 2C), 127.6 (s, 2C), 122.4 (s, 1C), 56.0 (s, 1C). $[\text{M}-\text{H}]^+ = 298.50$.

***N*-Hydroxy-4-(5-quinolin-2-yl-tetrazol-2-ylmethyl)-benzamide (30).** The title compound was synthesized from commercially available quinoline-2-carbonitrile according to general procedure D (0.097 mmol, 6% over three steps). ^1H NMR (400 MHz, DMSO) δ 11.16 (s, 1H), 9.02 (s, 1H), 8.67 (d, $J = 8.6$ Hz, 1H), 8.38 (d, $J = 8.6$ Hz, 1H), 8.19 (d, $J = 8.5$ Hz, 1H), 8.12 (dd, $J = 8.2, 0.9$ Hz, 1H), 7.92 (ddd, $J = 1.4, 7.0, 8.4$ Hz, 1H), 7.77 (ddd, $J = 1.0, 7.0, 8.2$ Hz, 1H), 7.71 (d, $J = 8.4$ Hz, 2H), 7.48 (d, $J = 8.4$ Hz, 2H), 6.44 (s, 2H). ^{13}C NMR (101 MHz, DMSO) δ

1
2
3 163.8 (s, 1C), 151.7 (s, 1C), 146.7 (s, 1C), 144.1 (s, 1C), 138.6 (s, 1C), 138.5 (s, 1C), 132.6 (s,
4 1C), 131.1 (s, 1C), 129.3 (s, 1C), 128.7 (s, 1C), 128.3 (s, 2C), 128.1 (s, 1C), 127.9 (s, 2C), 127.4
5 (s, 1C), 120.7 (s, 1C), 52.2 (s, 1C). [M+H]⁺ = 347.02.

6
7
8
9
10 ***N*-Hydroxy-4-(5-isoquinolin-1-yl-tetrazol-2-ylmethyl)-benzamide (31).** The title compound
11 was synthesized from commercially available isoquinoline-1-carbonitrile according to general
12 procedure D (0.29 mmol, 18.2% over three steps). ¹H NMR (400 MHz, DMSO) δ 11.17 (br s,
13 1H), 9.03 (br s, 1H), 8.77 (d, *J* = 5.6 Hz, 1H), 8.62 (ddd, *J* = 8.4, 1.2, 1.3 Hz, 1H), 8.15 (m, 2H),
14 7.92 (ddd, *J* = 1.2, 6.9, 8.2 Hz, 1H), 7.82 (ddd, *J* = 1.3, 6.9, 8.4 Hz, 1H), 7.67 (d, *J* = 8.4 Hz, 2H),
15 7.35 (d, *J* = 8.4 Hz, 2H), 6.03 (s, 2H). ¹³C NMR (101 MHz, DMSO) δ 163.7 (s, 1C), 151.8 (s,
16 1C), 143.6 (s, 1C), 142.0 (s, 1C), 138.0 (s, 1C), 136.5 (s, 1C), 132.7 (s, 1C), 131.4 (s, 1C), 129.3
17 (s, 1C), 128.1 (s, 2C), 127.6 (s, 1C), 127.3 (s, 2C), 126.8 (s, 1C), 126.2 (s, 1C), 123.7 (s, 1C),
18 51.6 (s, 1C). [M+H]⁺ = 347.01.

19
20
21
22
23
24
25
26
27
28
29
30
31 ***N*-Hydroxy-4-(5-pyridin-2-ylmethyl-tetrazol-2-ylmethyl)-benzamide trifluoroacetate (32).**
32 The title compound was synthesized from commercially available 2-(pyridin-2-yl)acetonitrile
33 according to general procedure D (0.048 mmol, 2.5% over three steps). ¹H NMR (400 MHz,
34 DMSO) δ 11.24 (s, 1H), 9.06 (br s, 1H), 8.50 (d, *J* = 4.0 Hz, 1H), 7.81 (dt, *J* = 1.6, 7.3 Hz, 1H),
35 7.75 (d, *J* = 8.2 Hz, 2H), 7.41 (d, *J* = 8.2 Hz, 3H), 7.32 (dd, *J* = 7.3, 5.5 Hz, 1H), 5.96 (s, 2H),
36 4.42 (s, 2H). ¹³C NMR (101 MHz, DMSO) δ 164.3 (s, 1C), 156.3 (s, 1C), 148.8 (s, 1C), 137.7 (s,
37 1C), 137.1 (s, 1C), 133.1 (s, 1C), 128.4 (s, 2C), 127.5 (s, 1C), 123.7 (s, 1C), 122.4 (s, 2C), 55.4
38 (s, 1C), 33.5 (s, 1C). [M+H]⁺ = 311.03.

39
40
41
42
43
44
45
46
47
48
49 **3,5-Difluoro-*N*-hydroxy-4-(5-pyridin-2-yl-tetrazol-2-ylmethyl)-benzamide (33).**

50 The title compound was synthesized from commercially available 2-cyanopyridine and methyl
51 4-(chloromethyl)-3,5-difluorobenzoate according to general procedure D (0.20 mmol, 20.6%
52
53
54
55
56
57
58
59
60

over three steps). ^1H NMR (400 MHz, DMSO) δ 11.41 (s, 1H), 9.31 (s, 1H), 8.81 (ddd, $J = 0.9$, 1.7, 4.7 Hz, 1H), 8.28 (ddd, $J = 0.9$, 1.2, 7.9 Hz, 1H), 8.12 (dt, $J = 1.7$, 7.7 Hz, 1H), 7.68 (ddd, $J = 1.2$, 4.7, 7.7 Hz, 1H), 7.48 (d, $J = 8.5$ Hz, 2H), 6.35 (s, 2H). ^{13}C NMR (101 MHz, DMSO) δ 161.1 (s, 1C), 160.6 (dd, $^1J_{\text{F-C}} = 250.3$, $^3J_{\text{F-C}} = 7.8$, Hz, 2C), 151.9 (s, 1C), 149.7 (s, 1C), 142.0 (s, 1C), 138.4 (s, 1C), 136.1 (t, $^3J_{\text{F-C}} = 9.0$ Hz, 1C), 126.2 (s, 1C), 124.4 (s, 1C), 113.7 (t, $^2J_{\text{F-C}} = 18.9$ Hz, 1C), 110.4 (d, $^2J_{\text{F-C}} = 26.7$ Hz, 2C), 41.5 (t, $^3J_{\text{F-C}} = 2.9$ Hz, 1C). $[\text{M}+\text{H}]^+ = 333.02$.

3,5-Difluoro-*N*-hydroxy-4-(5-pyrimidin-2-yl-tetrazol-2-ylmethyl)-benzamide (34). The title compound was synthesized from commercially available pyrimidine-2-carbonitrile and methyl 4-(chloromethyl)-3,5-difluorobenzoate according to general procedure D (0.072 mmol, 5% over three steps). ^1H NMR (400 MHz, DMSO) δ 11.40 (br s, 1H), 9.32 br (s, 1H), 9.00 (d, $J = 4.9$ Hz, 2H), 7.66 (t, $J = 4.9$ Hz, 1H), 7.57 (d, $J = 8.2$ Hz, 2H), 6.16 (s, 3H). ^{13}C NMR (400 MHz, DMSO) δ 164.1 (s, 1C), 161.5 (s, 1C), 161.1 (dd, $^1J_{\text{C-F}} = 251.3$, $^3J_{\text{C-F}} = 7.2$ Hz, 2C), 158.7 (s, 2C), 155.8 (s, 1C), 137.2 (t, $^3J_{\text{C-F}} = 8.8$ Hz, 1C), 122.8 (s, 1C), 112.7 (t, $^2J_{\text{C-F}} = 18.7$ Hz, 1C), 111.0 (d, $^2J_{\text{C-F}} = 25.2$ Hz, 2C), 45.2 (t, $^3J_{\text{C-F}} = 3.3$ Hz, 1C). $[\text{M}+\text{H}]^+ = 333.96$.

4-((5-(4-Aminophenyl)-2H-tetrazol-2-yl)methyl)-3,5-difluoro-*N*-hydroxybenzamide 2,2,2-trifluoroacetate (35). The title compound was synthesized from commercially available 4-aminobenzonitrile and methyl 4-(chloromethyl)-3,5-difluorobenzoate according to general procedure D (0.33 mmol, 5.3% over five steps). ^1H NMR (400 MHz, DMSO) δ 11.47 (br s, 1H), 9.34 (br s, 1H), 7.71 (ddd, $J = 1.9$, 2.2, 8.6 Hz, 2H), 7.56 (d, $J = 8.2$ Hz, 2H), 6.72 (d, $J = 8.6$ Hz, 2H), 6.01 (s, 2H). ^{13}C NMR (101 MHz, DMSO) δ 165.0 (s, 1C), 161.1 (s, 1C), 160.7 (dd, $^1J_{\text{C-F}} = 251.0$, $^3J_{\text{C-F}} = 7.3$, Hz, 2C), 158.4 (q, $^2J_{\text{C-F}} = 36.0$ Hz, CO TFA), 148.2 (s, 1C), 136.5 (t, $^3J_{\text{C-F}} = 8.9$ Hz, 1C), 127.7 (s, 2C), 115.9 (q, $^1J_{\text{C-F}} = 292.2$ Hz, CF_3 TFA), 115.7 (s, 1C), 115.6 (s, 2C),

112.6 (t, $^2J_{\text{C-F}} = 19.3$ Hz, 1C), 110.6 (d, $^2J_{\text{C-F}} = 26.2$ Hz, 2C), 44.3 (t, $^3J_{\text{C-F}} = 2.9$ Hz, 1C).

[M+H] $^{+}$ = 347.5.

4-((5-(4-(Aminomethyl)phenyl)-2H-tetrazol-2-yl)methyl)-3,5-difluoro-N-hydroxybenzamide 2,2,2-trifluoroacetate (36). The title compound was synthesized from commercially available tert-butyl (4-cyanobenzyl)carbamate and methyl 4-(chloromethyl)-3,5-difluorobenzoate according to general procedure D (0.16 mmol, 18.8% over four steps, HPLC purity 92% - used only for preliminary screening). ^1H NMR (400 MHz, DMSO) δ 11.50 (s, 1H), 9.36 (s, 1H), 8.29 (br s, 3H), 8.08 (ddd, $J = 1.8, 1.8, 8.4$ Hz, 2H), 7.63 (d, $J = 8.4$ Hz, 2H), 7.58 (d, $J = 8.2$ Hz, 2H), 6.11 (s, 2H), 4.13 (br s, 2H). ^{13}C NMR (101 MHz, DMSO) δ 164.1 (s, 1C), 161.1 (s, 1C), 160.7 (dd, $^1J_{\text{C-F}} = 251.3$, $^3J_{\text{C-F}} = 7.3$ Hz, 2C), 158.3 (q, $^2J_{\text{C-F}} = 31.1$ Hz, CO TFA), 136.7 (s, 1C), 129.8 (s, 2C), 126.7 (s, 2C), 117.3 (q, $^1J_{\text{C-F}} = 299.7$ Hz, CF_3 TFA), 112.4 (t, $^3J_{\text{C-F}} = 19.5$ Hz, 1C), 110.6 (d, $^2J_{\text{C-F}} = 25.9$ Hz, 2C), 44.6 (t, $^3J_{\text{C-F}} = 4.0$ Hz, 1C), 42.0 (s, 1C). [M+H] $^{+}$ = 361.0.

3,5-Difluoro-N-hydroxy-4-(5-isoquinolin-1-yl-tetrazol-2-ylmethyl)-benzamide (37). The title compound was synthesized from commercially available isoquinoline-1-carbonitrile and methyl 4-(chloromethyl)-3,5-difluorobenzoate according to general procedure D (0.19 mmol, 21.3% over three steps, HPLC purity 93.6% - used only for preliminary screening). ^1H NMR (400 MHz, DMSO) δ 11.35 (br s, 1H), 9.32 (br s, 1H), 8.75 (d, $J = 5.6$ Hz, 1H), 8.51 (dd, $J = 1.0, 8.4$ Hz, 1H), 8.17 (m, 2H), 7.92 (ddd, $J = 1.0, 8.2, 7.1$ Hz, 1H), 7.81 (ddd, $J = 1.4, 8.4, 7.1$ Hz, 1H), 7.37 (d, $J = 8.4$ Hz, 2H), 6.13 (s, 2H). ^{13}C NMR (101 MHz, DMSO) δ 160.9 (s, 1C), 160.4 (dd, $^1J_{\text{F-C}} = 250.6$, $^3J_{\text{F-C}} = 7.5$ Hz, 2C), 151.7 (s, 1C), 143.6 (s, 1C), 141.9 (s, 1C), 136.4 (s, 1C), 136.0 (t, $^3J_{\text{F-C}} = 8.9$ Hz, 1C), 131.5 (s, 1C), 129.3 (s, 1C), 127.6 (s, 1C), 126.7 (s, 1C), 125.9 (s,

1
2
3 1C), 123.7 (s, 1C), 113.3 (t, $^2J_{\text{F-C}} = 18.8$ Hz, 1C), 110.3 (d, $^2J_{\text{F-C}} = 26.4$ Hz, 2C), 41.0 (t, $^3J_{\text{F-C}} =$
4
5 2.9 Hz, 1C). $[\text{M}+\text{H}]^+ = 382.97$.

7
8 **3,5-Difluoro-*N*-hydroxy-4-(5-quinolin-2-yl-tetrazol-2-ylmethyl)-benzamide (38).** The title
9
10 compound was synthesized from commercially available quinoline-2-carbonitrile and methyl 4-
11
12 (chloromethyl)-3,5-difluorobenzoate according to general procedure D (0.23 mmol, 24.7% over
13
14 three steps, HPLC purity 93.9% - used only for preliminary screening). ^1H NMR (400 MHz,
15
16 DMSO) δ 11.41 (br s, 2H), 9.35 (br s, 1H), 8.69 (d, $J = 8.6$ Hz, 1H), 8.38 (d, $J = 8.6$ Hz, 1H),
17
18 8.15 (ddd, $J = 1.1, 8.5, 8.6$ Hz, 1H), 7.92 (ddd, $J = 1.4, 6.9, 8.6$ Hz, 1H), 7.78 (ddd, $J = 1.1, 6.9,$
19
20 8.5 Hz, 1H), 7.49 (d, $J = 8.4$ Hz, 2H), 6.55 (s, 2H). ^{13}C NMR (101 MHz, DMSO) δ 161.0 (s, 1C),
21
22 160.5 (dd, $^1J_{\text{F-C}} = 250.2, ^3J_{\text{F-C}} = 7.5$ Hz, 2C), 151.8 (s, 1C), 146.7 (s, 1C), 144.2 (s, 1C), 138.5 (s,
23
24 1C), 135.9 (t, $^3J_{\text{F-C}} = 9.9$ Hz, 1C), 131.1 (s, 1C), 129.1 (s, 1C), 128.7 (s, 1C), 128.3 (s, 1C), 128.1
25
26 (s, 1C), 120.7 (s, 1C), 113.9 (t, $^2J_{\text{F-C}} = 18.9$ Hz, 1C), 110.4 (d, $^2J_{\text{F-C}} = 26.4$ Hz, 2C), 42.1 (s, 1C).
27
28 $[\text{M}+\text{H}]^+ = 382.98$.

30
31
32
33 **4-((5-(1,5-Dimethyl-1H-pyrazol-3-yl)-4-methyl-4H-1,2,4-triazol-3-yl)thio)-3,5-difluoro-*N*-**
34
35 **hydroxybenzamide (39).** The title compound was synthesized from commercially available 5-
36
37 (1,5-dimethyl-1H-pyrazol-3-yl)-4-methyl-4H-1,2,4-triazole-3-thiol according to general
38
39 procedure F (0.51 mmol, 51.2% over two steps). ^1H NMR (400 MHz, DMSO) δ 11.49 (s, 2H),
40
41 9.37 (s, 1H), 7.58 (d, $J = 7.9$ Hz, 1H), 6.58 (s, 1H), 3.94 (s, 3H), 3.83 (s, 3H), 2.32 (s, 3H). ^{13}C
42
43 NMR (101 MHz, DMSO) δ 161.3 (dd, $^1J_{\text{F-C}} = 249.1, ^3J_{\text{F-C}} = 4.6$ Hz, 2C), 160.9 (s, 1C), 150.3 (s,
44
45 1C), 146.6 (s, 1C), 140.3 (s, 1C), 138.3 (s, 1C), 136.4 (t, $^3J_{\text{F-C}} = 8.8$ Hz, 1C), 110.9 (d, $^2J_{\text{F-C}} =$
46
47 27.7 Hz, 2C), 110.2 (t, $^2J_{\text{F-C}} = 21.6$ Hz, 1C), 105.4 (s, 1C), 36.5 (s, 1C), 32.6 (s, 1C), 10.6 (s,
48
49 1C). $[\text{M}+\text{H}]^+ = 380.94$.

4-((5-(1,5-Dimethyl-1H-pyrazol-3-yl)-4-methyl-4H-1,2,4-triazol-3-yl)thio)-2,3,5,6-tetrafluoro-*N*-hydroxybenzamide (40). 5-(1,5-Dimethyl-1H-pyrazol-3-yl)-4-methyl-4H-1,2,4-triazole-3-thiol (1 equiv), methyl 2,3,4,5,6-pentafluorobenzoate (1 equiv) and K₂CO₃ (2.3 equiv) were suspended in 2 mL of DMF under an argon atmosphere. The resulting mixture was warmed up to 40°C and stirred overnight. The reaction mixture was diluted with 10 mL of EtOAc and 10 mL of water. Phases were separated, and the aqueous layer was re-extracted with additional EtOAc (3x). The organic phases were combined and washed with brine (2x), dried over Na₂SO₄, filtered, and concentrated. The resulting methyl ester was converted into hydroxamic acid following general procedure B (0.046 mmol, 4.5% over two steps, HPLC purity 91.5% - used only for preliminary screening). ¹H NMR (400 MHz, DMSO) δ 11.44 (s, 1H), 9.72 (s, 1H), 6.59 (d, *J* = 0.7 Hz, 1H), 3.97 (s, 3H), 3.83 (s, 3H), 2.32 (s, 3H). ¹³C NMR (101 MHz, DMSO) δ 153.7 (s, 1C), 150.5 (s, 1C), 146.0 (s, 1C), 145.9 (ddd, ¹*J*_{C-F} = 248.5, ²*J*_{C-F} = 15.9, ³*J*_{C-F} = 5.4 Hz, 2C), 143.1 (dd, ¹*J*_{C-F} = 246.5, ²*J*_{C-F} = 20.2 Hz, 2C), 140.3 (s, 1C), 138.2 (s, 1C), 116.5 (t, ²*J*_{C-F} = 21.6 Hz, 1C), 112.5 (t, ²*J*_{C-F} = 20.0 Hz, 1C), 105.4 (s, 1C), 36.6 (s, 1C), 32.7 (s, 1C), 10.6 (s, 1C). [M+H]⁺ = 416.9.

4-((5-(1,5-Dimethyl-1H-pyrazol-3-yl)-4-methyl-4H-1,2,4-triazol-3-yl)thio)-2-fluoro-*N*-hydroxybenzamide (41). 5-(1,5-Dimethyl-1H-pyrazol-3-yl)-4-methyl-4H-1,2,4-triazole-3-thiol (1. equiv) was dissolved in dry DMA. Ethyl 2,4-difluorobenzoate (1.2 equiv), L-proline (0.1 equiv), K₂CO₃ (1.1 equiv), and CuI (0.05 equiv) were added. The reaction vessel was sealed, and the reaction mixture was stirred at 150°C overnight. The reaction mixture was diluted with water, acidified with 1N HCl aqueous solution, and extracted with EtOAc. The organic phase was dried over Na₂SO₄, filtered, and concentrated. The crude product was purified by silica gel chromatography (Toluene/EtOAc 9:1). The methyl ester thus obtained was converted into

hydroxamic acid following general procedure B (0.26 mmol, 54% over two steps, HPLC purity 91.5% - used only for preliminary screening). ¹H NMR (400 MHz, DMSO) δ 10.00 (br s, 1H), 8.13 (dd, *J* = 1.6, 11.6 Hz, 1H), 7.98 (dd, *J* = 1.6, 8.4 Hz, 1H), 7.74 (dd, *J* = 8.4, 8.4 Hz, 1H), 6.69 (s, 1H), 3.88 (s, 3H), 3.87 (s, 3H), 2.34 (s, 3H). ¹³C NMR (101 MHz, DMSO) δ 166.8 (s, 1C), 160.7 (s, 1C), 158.5 (d, ¹*J*_{C-F} = 248.8 Hz, 1C), 145.8 (s, 1C), 140.8 (s, 1C), 139.8 (d, ³*J*_{C-F} = 10.5 Hz, 1C), 136.4 (s, 1C), 130.4 (d, ³*J*_{C-F} = 4.6 Hz, 1C), 122.6 (d, ²*J*_{C-F} = 15.5 Hz, 1C), 118.8 (d, ⁴*J*_{C-F} = 3.3 Hz, 1C), 110.8 (d, ²*J*_{C-F} = 28.1 Hz, 1C), 106.0 (s, 1C), 36.8 (s, 1C), 33.3 (s, 1C), 10.7 (s, 1C). [M+H]⁺ = 363.2.

***N*-Hydroxy-4-(5-thiophen-2-yl-tetrazol-1-ylmethyl)-benzamide (42).** The title compound was synthesized from commercially available 5-thiophen-2-yl-2H-tetrazole according to general procedure D (17.9 mmol, 13.7% over two steps). ¹H NMR (400 MHz, DMSO) δ 11.19 (br s, 1H), 9.08 (br s, 1H), 7.95 (dd, *J* = 1.1, 5.1 Hz, 1H), 7.70-7.76 (m, 3H), 7.27 (dd, *J* = 3.8, 5.1 Hz, 1H), 7.24 (d, *J* = 8.4 Hz, 2H), 6.00 (s, 2H). ¹³C NMR (101 MHz, DMSO) δ 163.8 (s, 1C), 149.5 (s, 1C), 137.3 (s, 1C), 132.8 (s, 1C), 131.8 (s, 2C), 130.6 (s, 2C), 128.9 (s, 1C), 127.6 (s, 1C), 127.2 (s, 1C), 123.5 (s, 1C), 50.7 (s, 1C). [M+H]⁺ = 301.92.

3,5-Difluoro-*N*-hydroxy-4-((4-methyl-5-(thiophen-2-yl)-4H-1,2,4-triazol-3-yl)thio)benzamide (43). The title compound was synthesized from commercially available 4-methyl-5-(thiophen-2-yl)-4H-1,2,4-triazole-3-thiol according to general procedure F (0.51 mmol, 51.2% over two steps). ¹H NMR (400 MHz, DMSO) δ 11.49 (br s, 1H), 9.40 (br s, 1H), 7.83 (d, *J* = 4.9 Hz, 1H), 7.69 (d, *J* = 3.6 Hz, 1H), 7.61 (d, *J* = 8.0 Hz, 2H), 7.27 (dd, *J* = 3.9, 4.8 Hz, 1H), 3.86 (s, 3H). ¹³C NMR (101 MHz, DMSO) δ 161.5 (dd, ¹*J*_{C-F} = 249.5, ³*J*_{C-F} = 4.1 Hz, 2C), 160.8 (t, ⁴*J*_{C-F} = 2.9 Hz, 1C, CO), 150.9 (s, 1C), 147.3 (s, 1C), 136.9 (t, ³*J*_{C-F} = 8.7 Hz, 1C),

129.4 (s, 1C), 128.4 (s, 1C), 128.3 (s, 1C), 127.79 (s, 1C), 110.9 (dd, $^2J_{\text{C-F}} = 25.2$, $^4J_{\text{C-F}} = 2.5$ Hz, 2C), 109.7 (t, $^2J_{\text{C-F}} = 20.64$ Hz, 1C), 32.5 (s, 1C). $[\text{M}+\text{H}]^+ = 368.91$.

3,5-Difluoro-4-(5-furan-2-yl-tetrazol-2-ylmethyl)-N-hydroxy-benzamide (44). The title compound was synthesized from commercially available furan-2-carbonitrile and methyl 4-(chloromethyl)-3,5-difluorobenzoate according to general procedure D (0.22 mmol, 35.3% over three steps). ^1H NMR (400 MHz, DMSO) δ 11.47 (s, 1H), 9.35 (s, 1H), 7.94 (dd, $J = 0.8$, 1.8 Hz, 1H), 7.57 (d, $J = 8.2$ Hz, 2H), 7.20 (dd, $J = 0.8$, 3.5 Hz, 1H), 6.72 (dd, $J = 1.8$, 3.5 Hz, 1H), 6.09 (s, 2H). ^{13}C NMR (101 MHz, DMSO) δ 161.1 (s, 1C), 160.7 (dd, $^1J_{\text{C-F}} = 251.1$, $^3J_{\text{C-F}} = 7.4$ Hz, 2C), 157.7 (s, 1C), 145.5 (s, 1C), 141.9 (s, 1C), 136.7 (t, $^3J_{\text{C-F}} = 9.1$ Hz, 1C), 112.3 (t, $^2J_{\text{C-F}} = 18.9$ Hz, 1C), 112.2 (s, 1C), 111.9 (s, 1C), 110.6 (d, $^2J_{\text{C-F}} = 26.4$ Hz, 2C), 44.6 (t, $^3J_{\text{C-F}} = 2.9$ Hz, 1C). $[\text{M}+\text{H}]^+ = 321.97$.

3,5-Difluoro-N-hydroxy-4-((5-(pyridin-4-yl)-1,3,4-thiadiazol-2-yl)methyl)benzamide (45) (**Scheme 3c**). *t*-Bu-malonate (2 equiv) was added dropwise to a suspension of NaH (1.5 equiv) in anhydrous DMF. After 5 min at rt, methyl 3,4,5-trifluorobenzoate (1 equiv) was added. The reaction mixture was stirred for 3 h at rt (formation of a white precipitate was observed), diluted with water, and extracted with EtOAc. After concentration, the residue was purified by column chromatography. The inseparable mixture of the desired product and *t*-Bu-malonate, which was obtained, was dissolved in 5 mL of SOCl_2 , refluxed for 1 h, and then concentrated. The obtained crude chloroanhydride was mixed with isonicotinohydrazide (2 equiv) in 10 mL of anhydrous DMF followed by addition of DIPEA (5 equiv). The reaction mixture was stirred overnight at rt, quenched with water, extracted with EtOAc, and concentrated. The residue was treated with DCM and filtered. The crude material was dissolved in toluene, and Lawesson's reagent (0.98 equiv) was added. The vessel was sealed and stirred at 120°C for 15 min. Full conversion of the

starting material was monitored by UPLC. The solvent was evaporated, and the residue was purified by column chromatography first using EtOAc/*n*-hexane (gradient 20% to 100%) followed by 5% MeOH in DCM. The resulting methyl ester was converted into hydroxamic acid following general procedure B (0.077 mmol, 1% over five steps). ¹H NMR (400 MHz, DMSO) δ 11.42 (br s, 1H), 9.30 (br s, 1H), 8.76 (d, *J* = 5.8 Hz, 2H), 7.91 (d, *J* = 5.8 Hz, 2H), 7.55 (d, *J* = 8.0 Hz, 2H), 4.66 (s, 2H). ¹³C NMR (101 MHz, DMSO) δ 168.0 (s, 1C), 166.8 (s, 1C), 161.4 (s, 1C), 160.4 (dd, ¹*J*_{C-F} = 248.1, ³*J*_{C-F} = 8.0, Hz, 2C), 151.0 (s, 2C), 136.4 (s, 1C), 134.9 (t, ³*J*_{C-F} = 9.2 Hz, 1C), 121.6 (s, 2C), 115.7 (t, ²*J*_{C-F} = 20.5 Hz, 1C), 110.4 (d, ²*J*_{C-F} = 26.8 Hz, 2C), 23.1 (t, ³*J*_{C-F} = 2.9 Hz, 1C). [M+H]⁺ = 349.11.

General procedure (F) for the synthesis of difluorobenzohydroxamate-derivatives with 1,2,4-triazole-3-thiol scaffold - 3,5-difluoro-*N*-hydroxy-4-((4-methyl-5-(4-(piperidin-1-ylmethyl)phenyl)-4H-1,2,4-triazol-3-yl)thio)benzamide (46). The synthesis of **46** is representative for general procedure F (Scheme 2). 4-(piperidin-1-ylmethyl)benzoic acid (1 equiv) and 4-methyl-3-thiosemicarbazide (1.1 equiv) were suspended in 2 mL of DMF, and the mixture was cooled to 0°C in an ice bath. T3P (50% DMF solution, 1.5 equiv) and diisopropylethylamine (1.78 equiv) were slowly added to the reaction mixture with constant stirring. The ice bath was removed, and the mixture was stirred at rt for 16 h. The complete conversion of the starting material was confirmed by HPLC. 2 mL EtOAc, 2 mL of water, and 2 mL of 4M NaOH aqueous solution were added to the reaction mixture. Phases were separated, and the organic layer was extracted with additional 4 M NaOH. Aqueous phases were combined and stirred over 16 h at 70°C. Conversion into the desired cyclized product was confirmed by LC-MS. The reaction mixture's pH was adjusted to 5 by dropwise addition of concentrated HCl with constant stirring. The volume was reduced by evaporation under reduced pressure. The

resulting 4-methyl-5-(4-(piperidin-1-ylmethyl)phenyl)-4H-1,2,4-triazole-3-thiol (1 equiv) was dissolved in DMF, and methyl 3,4,5-trifluorobenzoate (1 equiv) and potassium carbonate (2.3 equiv) were added. The resulting mixture was warmed to 40°C and stirred overnight. The reaction mixture was diluted with 10 mL of EtOAc and 10 mL of water. The phases were separated, and the aqueous layer was re-extracted with additional EtOAc (3x). The organic phases were combined and washed with brine (2x), dried over Na₂SO₄, filtered, and concentrated. The crude reaction was purified by flash chromatography (Grace Reveleris X2, hexane: ethyl acetate). The obtained methyl ester was converted into hydroxamic acid following general procedure B (0.033 mmol, 3.36% over three steps). ¹H NMR (400 MHz, DMSO) δ 11.51 (br s, 3H), 9.40 (br s, 1H), 7.67 (d, *J* = 8.3 Hz, 2H), 7.60 (d, *J* = 7.7 Hz, 2H), 7.47 (d, *J* = 8.3 Hz, 2H), 3.74 (s, 3H), 3.51 (s, 2H), 2.36 (m, 4H), 1.51 (td, *J* = 5.5, 11.0 Hz, 4H), 1.41 (br td, *J* = 5.5, 5.6 Hz, 2H). ¹³C NMR (101 MHz, DMSO) δ 161.6 (dd, ³*J*_{C-F} = 4.5, ²*J*_{C-F} = 249.1 Hz, 2C), 160.8 (s, 1C), 155.7 (s, 1C), 147.1 (s, 1C), 141.1 (t, ⁴*J*_{C-F} = 2.6 Hz, 1C), 136.7 (t, ³*J*_{C-F} = 9.5 Hz, 1C), 129.2 (s, 2C), 128.3 (s, 2C), 125.4 (s, 1C), 110.9 (d, ²*J*_{C-F} = 27.6 Hz, 2C), 109.7 (t, ²*J*_{C-F} = 21.6 Hz, 1C), 62.4 (s, 1C), 54.0 (s, 2C), 32.4 (s, 1C), 25.6 (s, 2C), 24.0 (s, 1C). [M+H]⁺ = 460.01.

3,5-Difluoro-4-((5-(3-fluoropyridin-2-yl)-4-methyl-4H-1,2,4-triazol-3-yl)thio)-*N*-hydroxybenzamide (47). The title compound was synthesized from commercially available 3-fluoropicolinic acid according to general procedure F (0.066 mmol, 3.3% over three steps). ¹H NMR (400 MHz, DMSO) δ 11.51 (s, 1H), 9.38 (s, 1H), 8.63 (ddd, *J* = 1.4, 1.4, 4.4 Hz, 1H), 8.01 (ddd, *J* = 1.4, 8.6, 10.2 Hz, 1H), 7.71 (td, *J* = 4.4, 8.6 Hz, 1H), 7.61 (d, *J* = 7.8 Hz, 1H), 3.84 (s, 1H). ¹³C NMR (101 MHz, DMSO) δ 161.5 (dd, ¹*J*_{C-F} = 249.5, ³*J*_{C-F} = 4.4 Hz, 2C), 161.0 (s, 1C), 157.7 (d, ¹*J*_{C-F} = 264.2 Hz, 1C), 150.1 (d, ³*J*_{C-F} = 7.6 Hz, 1C), 148.4 (s, 1C), 145.8 (d, ³*J*_{C-F} = 5.0 Hz, 1C), 136.8 (t, ³*J*_{C-F} = 8.8 Hz, 1C), 134.8 (d, ²*J*_{C-F} = 11.7 Hz, 1C), 127.1 (d, ⁴*J*_{C-F} = 4.6 Hz,

1C), 125.6 (d, $^2J_{C-F}$ = 18.7 Hz, 1C), 111.0 (d, $^2J_{C-F}$ = 25.4 Hz, 2C), 109.6 (t, $^2J_{C-F}$ = 21.6 Hz, 1C), 32.6 (s, 1C). $[M+H]^+$ = 382.1.

4-((5-(3-(Azepan-1-ylmethyl)phenyl)-4-methyl-4H-1,2,4-triazol-3-yl)thio)-3,5-difluoro-N-hydroxybenzamide (48). The title compound was synthesized from commercially available 3-(azepan-1-ylmethyl)benzoic acid according to general procedure F (0.133 mmol, 6.7% over three steps). 1H NMR (400 MHz, DMSO) δ 11.23 (br s, 1H), 9.64 (br s, 1H), 7.48-7.68 (m, 6H), 3.74 (s, 3H), 3.69 (s, 2H), 2.59 (m, 4H), 1.57 (m, 8H). ^{13}C NMR (101 MHz, DMSO) δ 161.6 (dd, $^1J_{C-F}$ = 249.0, $^3J_{C-F}$ = 4.4 Hz, 2C), 160.8 (s, 1C), 155.9 (s, 1C), 147.1 (s, 1C), 141.0 (s, 1C), 136.8 (t, $^3J_{C-F}$ = 8.8 Hz, 1C), 130.3 (s, 1C), 128.8 (s, 1C), 128.4 (s, 1C), 126.9 (s, 1C), 126.7 (s, 1C), 110.9 (dd, $^2J_{C-F}$ = 25.7, $^4J_{C-F}$ = 2.2 Hz, 2C), 109.6 (t, $^2J_{C-F}$ = 22.3 Hz, 1C), 61.5 (s, 1C), 55.1 (s, 2C), 32.4 (s, 1C), 28.0 (s, 2C), 26.6 (s, 2C). $[M+H]^+$ = 474.4.

3,5-Difluoro-N-hydroxy-4-((4-methyl-5-(pyridazin-3-yl)-4H-1,2,4-triazol-3-yl)thio)benzamide (49). The title compound was synthesized from commercially available pyridazine-3-carboxylic acid according to general procedure F (0.414 mmol, 20.5% over three steps). 1H NMR (400 MHz, DMSO) δ 9.94 (br s, 1H), 9.36 (dd, J = 1.6, 5.0 Hz, 1H), 8.34 (dd, J = 1.6, 8.6 Hz, 1H), 7.91 (dd, J = 5.0, 8.6 Hz, 1H), 7.55 (d, J = 8.3 Hz, 2H), 4.11 (s, 3H). ^{13}C NMR (101 MHz, DMSO) δ 161.5 (dd, $^1J_{C-F}$ = 248.6, $^3J_{C-F}$ = 4.3, Hz, 2C), 160.9 (s, 1C), 152.1 (s, 1C), 151.8 (s, 1C), 151.1 (s, 1C), 150.1 (s, 1C), 128.2 (s, 2C), 126.6 (s, 2C), 110.0 (dd, $^2J_{C-F}$ = 25.0, $^4J_{C-F}$ = 3.3, Hz, 2C), 33.8 (s, 1C). $[M+H]^+$ = 365.1.

Enzyme inhibitory activity assay. Recombinant human HDAC enzymes (HDAC1–10) were purchased from BPS (San Diego, CA). HDAC11 was purchased from Enzo Life Sciences (Farmingdale, NY). Activities of HDAC1, -2, -3, -6, -10, and -11 were assayed using the Fluor de Lys deacetylase substrate (Enzo Life Sciences). HDAC8 activity was assayed using Fluor de

Lys Green deacetylase substrate (Enzo Life Science). Nε-Trifluoroacetyl-L-lysine was used to assay activities of HDAC 4, 5, 7, and 9. Recombinant enzymes were preincubated with the compounds to be tested at 30°C in a volume of 25 uL in wells of a microtiter plate. After a brief incubation, 25uL of substrate was added, and the fluorescent signal was generated by the addition of 50 uL of developer (Fluor de Lys Developer - Enzo Life Science) containing 2 μM Trichostatin A (Sigma-Aldrich) to stop the enzyme activity. For each assay, the amount of enzyme, incubation times, assay buffer, and substrate concentrations were optimized. The positive control for enzyme activity consisted of enzyme plus substrate. The fluorescence signal was detected using a Victor multilabel plate reader (PerkinElmer Life Sciences).

***In vitro* α-tubulin and H3 histone acetylation.** *In vitro* α-tubulin and H3 histone acetylation were evaluated in the human 697 B-precursor acute lymphoblastic leukemia (ACC 42, DSMZ). The test molecules were prepared at 20X in Roswell Park Memorial Institute (RPMI) 1640 medium containing 10% fetal calf serum (FCS) and 0.01% DMSO, added to the cells (15 x 10⁶ cells in 30 ml) to obtain the final concentrations of 1000, 333, 111, and 37 nM, and incubated at 37°C, 5% CO₂ for 16 h. At the end of the incubation period, each sample was divided in two aliquots (1) tubulin/acetyl tubulin (5x10⁶ cells) and (2) H3 histone/acetyl H3 histone (10x10⁶ cells) determinations.

The sample for tubulin was centrifuged for 5 min at 180 x g and washed in 0.9% NaCl at 4°C. The resulting pellet was lysed at 4°C for 30 min with 150 μL of Complete Lysis-M (Roche, cat: 04719956051) containing protease and phosphatase inhibitors (Complete Easy Pack proteinase inhibitor cocktail tablets cat: 04693116001; Phostop easypack phosphatase inhibitor cocktails, cat: 01906837001- Roche) and then centrifuged for 10 min at 14,000 rpm (20,817x g). The total protein extract (0.150 μg) was diluted in 100 μL of phosphate buffered saline (PBS) and

immobilized in Maxisorp F96 NUNC-IMMUNO Plate (Nunc cat # 5442404) at rt overnight. Plates were washed twice with wash buffer (PBS + 0.05% tween 20) and saturated for 1 h at rt with 300 μ L PBS containing 10% FCS. After washing with buffer (PBS containing 0.05% Tween 20), the plates were incubated for 2 h at rt in the presence of anti-acetylated- α -tubulin antibody (Mouse Monoclonal Anti-acetylated-tubulin clone 6-11B-1, cat#T6793 Sigma, 100 μ L diluted 1:1000 in PBS containing 10% FCS) or with total anti- α -tubulin antibody (Mouse Monoclonal Anti- α -tubulin antibody, cat#T6074 Sigma, diluted 1:1000). After washing, 100 μ L per well of TMB substrate kit were added for 10 min at rt in the dark. The reaction was stopped by adding 50 μ L of 2N H₂SO₄. The plates were read at Multiskan Spectrum spectrophotometer at OD = 450nm. The degree of acetylation was calculated by dividing the absorbance obtained for the acetylated α -tubulin by the absorbance of total α -tubulin.

The histone fraction was obtained by acidic extraction of the second sample (10x10⁶ cells) as described by Kazuhiro.⁶⁴ The resulting pellet, which represents total histones, was re-suspended in 50 μ L distilled water. The protein content determination of both total and acetylated histone extracts was carried out using a colorimetric assay using a Bicinchoninic Acid (BCA) Protein Assay Kit (Pierce cat: 23227). The amounts of total and acetylated histone H3 were quantified by commercial ELISA assays (PathScan acetylated histone H3 Sandwich Elisa kit, cat#7232C and PathScan total histone H3 Sandwich Elisa Kit, cat#7253C, Cell Signaling).

Treg suppression assays with murine cells. The detailed procedure of this test was described by Akimova et al.^{14b}

Spleens from C57BL/6 mice were harvested, and a single cell suspension was obtained with the aid of a 70 μ m strainer. The cell suspension was treated with ammonium-chloride-potassium (ACK) buffer in order to lyse red blood cells. Treg, antigen presenting cells (APC), and Teff

cells were separated using the Treg isolation kit (Miltenyi Biotec) via initial negative selection and final positive selection processes. Purified Teff cells, from the final step of positive selection were labeled with carboxyfluorescein succinimidyl ester ([CFSE], Molecular Probes) and APCs, from first step of negative selection, were treated with mitomycin C (500 $\mu\text{g/mL}$, Sigma) and plated at 4×10^5 APC and 5×10^4 T cells/well in 96-well plates.

Purified Tregs were added to the wells in serial dilutions to achieve the following Treg/Teff ratios 1:1, 1:2, 1:4, and 1:8. Each well thus contained APC, Teff, and Treg cells. HDACi were added into the appropriate wells. T cell proliferation was induced with antibody against CD3 ϵ (1 $\mu\text{g/mL}$, Miltenyi) and co-stimulation from mitomycin-treated APC. After 72 h, cells were labeled with fluorescent mAb against CD4 PE/Cy (Biolegend) and analyzed by flow cytometry. CD4 $^{+}$ cell divisions were determined by CFSE dilution. In order to detect any cytotoxic effects or direct inhibition of T cell proliferation, the CFSE dilution in the absence of Treg and in the presence of the inhibitors was determined. Only assays in which this effect was $<10\%$ were considered for the quantification of Treg-mediated suppression.

In order to compare the effects of compounds on the suppressive capacity of Tregs, the first step was to standardize the percentage of cell proliferation by applying the min-max normalization using GraphPad 7. The resulting values were converted into a standardized suppression percentage = $100\% - \text{standardized proliferation}$ and plotted against the ratio of Teffs/Tregs. The area under the curve (AUC) of the generated graph was then calculated. Relative suppression was obtained as the ratio of AUC compound/AUC control. A ratio >1.25 was considered significant according to the literature.

Evaluation of the pharmacodynamic markers in the mouse. The evaluation of the pharmacodynamic markers (the amount of acetylated-tubulin and acetylated-histone H3) was

carried out on protein extracts of the spleens of mice treated intraperitoneally with the test molecules at the dose of 30 mg/Kg. The study was carried out with C57BL/6 female mice (from Charles River, Italy) that were randomized into 15 mice/group. Compounds were dissolved in water for injection (wfi)/PEG 400 (1:1) + 5% DMSO. Each compound was dissolved at a final concentration of 3 mg/mL, and each solution was administered at 10 mL/Kg of body weight, corresponding to the final doses of 30 mg/Kg.

At different time points (1, 4, and 24 h) following drug administration, five mice/group were anesthetized with isoflurane and then sacrificed. A sample of blood was drawn from the tail vein, and the spleen was removed, weighed, and immediately stored at -80°C . Protein extraction from spleen samples was carried out using NE-PER Nuclear and Cytoplasmic Extraction Reagents (Thermo Scientific Cod. 78835). Spleen samples (80–100 mg) from each animal were extracted according to the supplier's instructions. Both cytoplasmic and nuclear protein extracts were stored at -80°C until used for the ELISA acetylation assay. An aliquot of each sample was used to evaluate the protein content using the BCA Protein Assay Kit.

Cytosolic protein extracts were diluted at 20 $\mu\text{g/mL}$ with PBS, and 96-well plates were then coated with 100 μL extracts overnight at rt. After washing with 0.05% PBS + Tween 20, the plates were saturated with 10% FCS in PBS for 60 min at rt. After washing as described above, mouse anti-acetylated-tubulin antibody (Sigma Cat. T6793) diluted 1:1000 with PBS + 10% FCS or mouse anti- α -tubulin antibody (Sigma Cat. T6074) diluted 1:1000 with PBS + 10% FCS was added for 120 min at rt.

After washing, goat anti-mouse IgG2b-HRP antibody (Southern Biotech Cat. 1091-05) diluted 1:5000 in PBS + 10% FCS was added to acetylated-tubulin wells, whereas goat anti-mouse

1
2
3 IgG1-HRP (Southern Biotech Cat. 1070-05) diluted 1:5000 in PBS + 10% FCS was added to α -
4 tubulin wells.
5

6
7 After washing, horseradish peroxidase (HRP) substrate (TMB, 3,3',5,5'-tetramethylbenzidine)
8 solution was added. Color development was stopped with H₂SO₄, and absorbance at 450 nm was
9
10 measured by a plate spectrophotometer.
11
12

13
14 Total and acetylated-histone H3 content of spleen nuclear protein extracts were determined by
15 commercially available sandwich ELISA kits (Cell Signaling Technology, cat. 7253 and 7232)
16
17 using 2 μ g/well of nuclear protein extract according to the kit's protocol.
18
19

20
21 **Stability to Phase I metabolism in rat and human S9 liver fraction.** The stability to Phase I
22 metabolism resulting from hepatic enzymes was assessed for each compound after incubation
23
24 with rat and human S9 liver fraction. In brief, 55 μ L of S9 liver fraction (Corning) 20 mg
25
26 protein/mL were diluted with 275 μ L phosphate buffer 100 mM pH 7.4, containing 3.3 mM
27
28 MgCl₂, and ten aliquots of 30 μ L were dispensed in a polypropylene 96-well plate. To each well,
29
30 10 μ L of 5 μ M substrate solution prepared in phosphate buffer pH 7.4 containing MgCl₂ were
31
32 added. Cofactor NADPH (Calbiochem) was added as 10 μ L of 6.5 mM solution in phosphate
33
34 buffer pH 7.4. Final concentration of substrate was 1 μ M. After shaking, the plate was incubated
35
36 at 37°C in a thermostated bath. The reaction was stopped at 0, 10, 30, 60, and 90 min for two
37
38 samples/time point by adding 400 μ L ACN containing 0.1% formic acid and the internal
39
40 standard, 20 nM verapamil (Sigma-Aldrich). Samples were centrifuged prior to injection into the
41
42 LC-MS/MS system (Shimadzu Prominence HPLC, triple quadrupole API4000 Sciex). Samples
43
44 were analyzed using an Agilent Zorbax SB-C18 50x2.1 mm, 3.5 μ m column, with a mobile
45
46 phase gradient starting at 19% up to 55% ACN containing 0.1% formic acid in 7 min at a flow
47
48 rate of 0.2 mL/min. Detection was done in multiple reaction monitoring (MRM) mode using an
49
50
51
52
53
54
55
56
57
58
59
60

electrospray ionization (ESI) source in positive polarity. Substrate peak area normalized to the internal standard peak area was divided for peak area ratio at 0 min in order to obtain the remaining percentage at each time point. Diclofenac (Calbiochem) was used as a positive control. Stability in plasma was assessed by adding 7 μ L of 100 μ M solution of substrate in DMSO to 7 mL of rat or human plasma (Biopredic). The sample was dispensed in a 96-well plate in twelve aliquots incubated at 37°C in a thermostated bath. Reactions were stopped at 0, 0.25, 0.5, 1, 2, and 4 h of incubation for two samples/time point. Deflazacort (USP) was used as a positive control. Samples treatment, analysis, and calculation of results were the same as described for the liver S9 fraction stability assay.

Pharmacokinetic evaluation. Plasma levels and the main pharmacokinetic parameters were evaluated after single intravenous and oral administration doses to male CD-1 mice (Charles River Laboratories Italia, Calco, Italy) of about seven weeks in age. In the PK study 5 animals/sampling time were treated and 8 sampling times were evaluated within 6h after administration. All of the animal procedures and ethical revisions were performed according to the current Italian legislation (Legislative Decree March 4th, 2014 n. 26), enforcing the 2010/63/UE Directive on the protection of animals used for biomedical research. Compounds were dissolved in the vehicle, 5% DMSO, in PEG400/water (50/50) at a concentration of 1 mg/mL. Dose/body weight is reported in Table 13. Plasma samples (100 μ L) were deproteinized by addition of acetonitrile containing 1% formic acid, vortex mixed, and centrifuged. For each sample, an aliquot of the supernatant was collected and diluted with water, filtered with 0.45 μ m regenerated cellulose filters, and analyzed by LC-MS/MS (Shimadzu Prominence HPLC, triple quadrupole API4000 Sciex). Plasma levels of the test compounds were calculated using a calibration curve prepared in the range 0.5–200 ng/mL.

Maximum Tolerated Dose determination. All of the animal procedures and ethical revisions were performed according to the current Italian legislation (Dlgs. 116/1992 and Dlgs. 26/2014), enforcing the 2010/63/UE Directive on the protection of animals used for biomedical research.

The evaluation of the maximum tolerated dose (MTD) was carried out in 7-week old C57BL/6 female mice (from Charles River Italy) that were randomized into eight mice/group. Test molecules were dissolved in water for injection (wfi)/PEG 400 (1:1) + 5% DMSO in a volume sufficient for five treatments and were stored at rt. Each compound was dissolved at the final concentrations of 1, 3, and 5 mg/mL, and each solution was administered at 10 mL/Kg of body weight, corresponding to a final dose of 10, 30, and 50 mg/Kg.

Vehicles (wfi/PEG 400 (1:1) + 5% DMSO) and test molecules were administered intraperitoneally. Each animal was treated daily from Monday to Friday for two consecutive weeks for a total of 10 drug administrations. Body weight was measured every other day, and clinical signs were recorded daily starting from day 1. Blood samples (50–75 μ L) were withdrawn 60 min after drug administration from the tail vein of each animal on days 1, 3, 5, and 8, whereas on day 12, samples were withdrawn from the abdominal aorta. The samples were collected in ethylenediaminetetraacetic acid (EDTA) tubes, and hematological analysis (red and white blood cells [RBC and WBC, respectively], and platelets [PLTs]) was carried out using a cell counter (Beckman Coulter).

On day 12, mice were anesthetized with isoflurane and sacrificed 1 h after the last treatment. Liver, spleen, lungs, and kidneys were collected, weighed, and stored at -80°C until the analysis of pharmacodynamic markers (such as protein acetylation). Signs of abnormal internal organs, possibly related to the toxicity of the compounds, were recorded.

Overexpression and acetylation of Foxp3

The following antibodies were used for the assays: (1) mouse HRP-conjugated anti-acetyl-lysine (cytoskeleton); (2) mouse HRP-conjugated anti-Flag M2 (Sigma-Aldrich); and (3) rabbit HRP-conjugated anti-GAPDH (Cell Signaling Technology). Mouse anti-DDK (FLAG) antibody (Origene) was used to immunoprecipitate Foxp3 Myc-FLAG-tagged protein. pCMV6-hFoxp3-Myc-FLAG and pCMV6-Myc-FLAG vectors were purchased from Origene. 100 ng of a purified recombinant Foxp3-FLAG protein (Origene) were used as positive control.

Transient transfection of HEK 293 cells. HEK 293 cells were maintained in Dulbecco's modified Eagle medium (DMEM, Thermo Fischer Scientific) supplemented with 10% heat-inactivated FBS and 1% penicillin/streptomycin (Sigma-Aldrich) at 37°C and 5% CO₂. Cells (1*10⁶) were seeded in 10 cm dishes and incubated overnight. The day after cell seeding, HEK 293 cells were transfected using TurboFectin 8.0 transfection reagent (Origene) with a mixture of 10 µg DNA and 20 µL TurboFectin reagent following the manufacturer's instructions. Cells transfected with pCMV6-Myc-DDK or treated with only transfection reagent were used as negative controls. 26 hours after transfection, cells were treated with 500 nM compound 13 (ITF3791) or vehicle (0.0025% DMSO in medium). The treatment duration was 6 h at 37°C and 5% CO₂. After that time, cells were harvested, washed twice with PBS, and lysed.

Immunoprecipitation and Western Blot analysis. HEK 293 cells were lysed in cComplete™ Lysis-M buffer (Sigma-Aldrich) supplemented with protease inhibitor cocktail tablet (Sigma-Aldrich), PhosSTOP (phosphatase inhibitor cocktail, Sigma-Aldrich), and with 10 µM Givinostat and 25 µM PU139 (HAT inhibitor, AOBIOUS). Insoluble cell debris were spun down, and the proteins in the supernatant fraction were quantified with a BCA Protein Assay Kit (Thermo Fischer Scientific). Next, 1 mg of lysate was mixed with anti-FLAG antibody (Origene) and incubated overnight at 4 °C to form immune complexes. Immunoprecipitation was then

performed at 4°C for 2 hours utilizing Dynabeads™ Protein G (Thermo Fischer Scientific). Beads were washed 3X in lysis buffer, resuspended, and boiled in lauryl dodecyl sulfate sample buffer (Thermo Fischer Scientific) supplemented with reducing buffer (Thermo Fischer Scientific) in order to elute the immunoprecipitated Foxp3 protein. Samples were subjected to electrophoresis on Bolt™ 4-12% Bis-Tris Plus gels (Thermo Fischer Scientific) at a constant voltage of 200 V. Proteins were transferred onto nitrocellulose membranes using the iBlot Gel Transfer Device and iBlot Gel Transfer Stacks (Thermo Fischer Scientific). Membranes were blocked with 5% BSA (Sigma-Aldrich) or Blotting Membrane Blocker (Bio-Rad) in PBS 0.1% Tween-20 (according to the antibody used) for 1 h at rt and probed with the appropriate antibody. After washing, immunocomplexes were detected using the Amersham enhanced chemiluminescence (ECL) detection kit (GE Healthcare). The chemiluminescence signal was recorded using a ChemiDoc MP system (Bio-Rad).

Statistical analysis and reproducibility. Biological raw data analysis was done using GraphPad Prism 7. Pharmacokinetic parameters were calculated for the mean plasma concentration curve using the software Kinetica v. 5.1, with a non-compartmental method.

ASSOCIATED CONTENT

Supporting Information. Additional data are included in the SI. The following files are available free of charge:

Table S1 – *In vitro* determinations of specific HDAC6 inhibitory activity (data related to Figure 8), Table S2 and S3 - *In vivo* determinations of specific HDAC6 inhibitory activity (data related

to Figure 9), Table S4 - Enzymatic activity and selectivity of some six-membered heteroaromatic central scaffold compounds, Table S5 – Repeats of enzyme assay IC₅₀ determination and standard deviations, Table S6 and S7 – Repeats of cytotoxicity assay on PBMC and on 697 cell line and standard deviations, cell cytotoxicity assay protocol, homology model protocol, docking protocol, HPLC chromatograms of key compounds (PDF file).

Molecular Formula String Spreadsheet of all molecules discussed in the article, including all related biological data (CSV file).

Docking results: structures of host (h-CD2-HDAC6) and best docking pose of compound **42** (Structures are the basis of figure 4); structures of host (h-CD2-HDAC6) and best docking pose of compound **13** (Structures are the basis of figure 5); structures of host (h-CD2-HDAC6) and the two conformers of compound **42** detected in docking experiments (Structures are the basis of figure 6); structures of host (h-CD2-HDAC6) and best docking pose of compound **35** (Structures are the basis of figure 7); Homology Model (Best hypothesis of h-CD2-HDAC6 structure, built by homology modeling software Modeler, available in Discovery Studio suite); Bavarostat,_ACY-1083 and Compound **35**_aligned (PDB file).

AUTHOR INFORMATION

Corresponding Author

*Phone: +390264433097, Email: a.stevenazzi@italfarmaco.com

ORCID

Andrea Stevenazzi:	0000-0001-5451-4638
Barbara Vergani:	0000-0002-8648-0660
Giovanni Sandrone:	0000-0002-4622-7345
Mattia Marchini:	0000-0001-8467-7817
Gianfranco Pavich:	0000-0002-9233-4280
Chiara Ripamonti:	0000-0001-6621-8668
Edoardo Cellupica:	0000-0001-6745-8663
Elisabetta Galbiati:	0000-0002-4054-5908
Gianluca Caprini:	0000-0001-7318-6174
Giulia Porro:	0000-0003-2418-9154
Ilaria Rocchio:	0000-0002-8420-5833
Maria Lattanzio:	0000-0003-4181-2227
Paola Cordella:	0000-0002-4820-9087
Roberta Pomarico:	0000-0001-6516-029X
Raffaella Perego:	0000-0003-1506-0519
Gianluca Fossati:	0000-0002-0060-5822
Christian Steinkh�ler:	0000-0001-8341-9699

Author contributions

All authors have given approval to the final version of the manuscript. †B.V., G.S. and M.M. contributed equally to this work. G.F., C.S. and A.S. were responsible for the supervision and development of the project. B.V., G.S., M.M. and A.S. assembled the manuscript. B.V., M.M., I.R., G.Pa., M.L. and M.P. synthesized, purified, and characterized the compounds discussed in

1
2
3 this paper. G.S. was responsible for the molecular design. C.R., E.C., E.G., G.C., G.Po., M.S.,
4 P.C., P.Pa., P.Po. and R.Po. assayed the compounds. D.M. supervised the cell assays. F.L.
5 supervised the MTD and the pharmacodynamic experiments. R.Pe. supervised the PK and the
6 metabolic stability studies.
7
8
9
10
11
12
13
14
15

16 ACKNOWLEDGMENT

17
18
19 The authors thank Selvita S.A. (Krakow) for the help in the synthesis of the described
20 compounds.
21
22
23
24

25 The authors received funding from Regione Lombardia, Grant 231836, as part of the “European
26 Regional Development Fund (ERDF) of the Regional Operational Program (ROP) 2014-2020”.
27
28
29
30
31

32 ABBREVIATIONS

33
34
35 HDAC: histone deacetylase; HSP: heat shock protein; Tregs: regulatory T cells; HAT: histone
36 acetyl transferase; NAD: nicotinamide adenine dinucleotide; KDAC: lysine deacetylase; FDA:
37 Food and Drug Administration; CTCL: cutaneous T-cell lymphoma; MM: multiple myeloma;
38 Foxp3: forkhead box 3; GVHD: graft versus host disease; ZBG: zinc binding group; MMP:
39 matrix metalloproteinase; TACE: tumor necrosis factor- α converting enzyme; HBD: hydrogen
40 bond donor; DS: Discovery Studio; ROC: receiving operator curves; B-Pre-ALL: 697 B-
41 precursor acute lymphoblastic leukemia; ELISA: enzyme-linked immunosorbent assay; MTD:
42 maximum tolerated dose; WBC: white blood cell; PLTs platelets; AUC: area under the curve;
43 CYP3A4: cytochrome P450 3A4; HLM: human liver microsomes; IPEX: immunodysregulation
44 polyendocrinopathy enteropathy X-linked; SIRT1: sirtuine 1; SDS-PAGE: sodium dodecyl
45
46
47
48
49
50
51
52
53
54
55
56
57
58
59
60

sulfate polyacrylamide gel electrophoresis; WB: western blotting; Ac-lys: acetyl-lysine; GADPH: glyceraldehyde 3-phosphate dehydrogenase; Teffs: effector T cells; HATU: 1-[bis(dimethylamino)methylene]-1H-1,2,3-triazolo[4,5-b]pyridinium 3-oxide hexafluorophosphate; DIPEA: *N*-ethyl-*N*-(propan-2-yl)propan-2-amine; DMF: dimethylformamide; TFA: trifluoroacetic acid; DCE: 1,2-dichloroethane; DCM: dichloromethane; THF: tetrahydrofuran; TBAI: tetrabutylammonium iodide; ACN: acetonitrile; NMR: nuclear magnetic resonance; TMS: tetramethylsilane; MS: mass spectrometry; UPLC: ultra-performance liquid chromatography; RP-HPLC: reverse phase high pressure liquid chromatography; EtOAc: ethyl acetate; DMSO: dimethyl sulfoxide; T3P: propylphosphonic anhydride; MeOH: methanol; RPMI: Roswell Park Memorial Institute; FCS: fetal calf serum; PBS: phosphate buffered saline; OD: optical density; ACK: ammonium-chloride-potassium; APC: antigen presenting cell; CFSE: carboxyfluorescein succinimidyl ester; PEG: polyethylene glycol; BCA: Bicinchoninic Acid ; HRP: horseradish peroxidase; TMB: 3,3',5,5'-tetramethylbenzidine; NADPH: reduced nicotinamide adenine dinucleotide phosphate; MRM: multiple reaction monitoring; ESI: electrospray ionization; USP: United States Pharmacopeia; wfi: water for injection; PEG: polyethylene glycol; EDTA: ethylenediaminetetraacetic acid; RBC: red blood cell; DMEM: Dulbecco's modified Eagle medium; ECL: enhanced chemiluminescence; EC₅₀: half maximal effective concentration; IC₅₀: half maximal inhibition concentration; SD: standard deviation.

REFERENCES

1. Vaijayanthi, T.; Pandian, G. N.; Sugiyama, H., Chemical Control System of Epigenetics. *Chem. Rec.* **2018**, *18* (12), 1833-1853.

2. Yoshida, M.; Kudo, N.; Kosono, S.; Ito, A., Chemical and Structural Biology of Protein Lysine Deacetylases. *Proc. Jpn. Acad. Ser. B Phys. Biol. Sci.* **2017**, *93* (5), 297-321.
3. (a) Choudhary, C.; Kumar, C.; Gnäd, F.; Nielsen, M. L.; Rehman, M.; Walther, T. C.; Olsen, J. V.; Mann, M., Lysine Acetylation Targets Protein Complexes and Co-regulates Major Cellular Functions. *Science* **2009**, *325* (5942), 834-840; (b) Choudhary, C.; Weinert, B. T.; Nishida, Y.; Verdin, E.; Mann, M., The Growing Landscape of Lysine Acetylation Links Metabolism and Cell Signalling. *Nat. Rev. Mol. Cell Biol.* **2014**, *15* (8), 536; (c) Narita, T.; Weinert, B. T.; Choudhary, C., Functions and Mechanisms of Non-Histone Protein Acetylation. *Nat. Rev. Mol. Cell Biol.* **2018**, *1*.
4. Kouzarides, T., Acetylation: a Regulatory Modification to Rival Phosphorylation? *EMBO J.* **2000**, *19* (6), 1176-1179.
5. (a) De Vreese, R.; D'Hooghe, M., Synthesis and Applications of Benzohydroxamic Acid-Based Histone Deacetylase Inhibitors. *Eur. J. Med. Chem* **2017**, *135*, 174-195; (b) Rodrigues, D. A.; Thota, S.; Fraga, C. A. M., Beyond the Selective Inhibition of Histone Deacetylase 6. *Mini-Rev. Med. Chem.* **2016**, *2016* (16), 1175-1184.
6. Qin, H. T.; Li, H. Q.; Liu, F., Selective Histone Deacetylase Small Molecule Inhibitors: Recent Progress and Perspectives. *Expert Opin. Ther. Pat.* **2017**, *27* (5), 621-636.
7. Shah, R. R., Safety and Tolerability of Histone Deacetylase (HDAC) Inhibitors in Oncology. *Drug Safety* **2019**, *42* (2), 235-245.
8. (a) Kalin, J. H.; Bergman, J. A., Development and Therapeutic Implications of Selective Histone Deacetylase 6 Inhibitors. *J. Med. Chem.* **2013**, *56* (16), 6297-6313; (b) Ran, J.; Zhou, J.,

Targeted Inhibition of Histone Deacetylase 6 in Inflammatory Diseases. *Thoracic Cancer* **2019**, *10* (3), 405-412; (c) Prior, R.; Van Helleputte, L.; Klingl, Y. E.; Van Den Bosch, L., HDAC6 as a Potential Therapeutic Target for Peripheral Nerve Disorders. *Expert Opin. Ther. Tar.* **2018**, *22* (12), 993-1007; (d) Caumanns, J. J.; Wisman, G. B. A.; Berns, K.; van der Zee, A. G. J.; de Jong, S., ARID1A Mutant Ovarian Clear Cell Carcinoma: A Clear Target for Synthetic Lethal Strategies. *Biochim. Biophys. Acta Rev. Cancer* **2018**, *1870* (2), 176-184; (e) Moreno-Gonzalo, O.; Mayor Jr, F.; Sánchez-Madrid, F., HDAC6 at Crossroads of Infection and Innate Immunity. *Trends Immunol.* **2018**, *39* (8), 591-595.

9. (a) Beier, U. H.; Wang, L.; Han, R.; Akimova, T.; Liu, Y.; Hancock, W. W., Histone Deacetylases 6 and 9 and Sirtuin-1 Control Foxp3+ Regulatory T Cell Function Through Shared and Isoform-Specific Mechanisms. *Sci. Signal.* **2012**, *5* (229), ra45; (b) Mobley, R. J.; Raghu, D.; Duke, L. D.; Abell-Hart, K.; Zawistowski, J. S.; Lutz, K.; Gomez, S. M.; Roy, S.; Homayouni, R.; Johnson, G. L., MAP3K4 Controls the Chromatin Modifier HDAC6 During Trophoblast Stem Cell Epithelial-to-Mesenchymal Transition. *Cell Rep.* **2017**, *18* (10), 2387-2400.

10. de Zoeten, E. F.; Wang, L.; Butler, K. V.; Beier, U. H.; Akimova, T.; Sai, H.; Bradner, J. E.; Mazitschek, R.; Kozikowski, A. P.; Matthias, P., Histone Deacetylase 6 and Heat Shock Protein 90 Control the Functions of Foxp3+ T-Regulatory Cells. *Mol. Cell. Biol.* **2011**, *31* (10), 2066-2078.

11. (a) Kalin, J. H.; Butler, K. V.; Akimova, T.; Hancock, W. W.; Kozikowski, A. P., Second-Generation Histone Deacetylase 6 Inhibitors Enhance the Immunosuppressive Effects of Foxp3+ T-regulatory Cells. *J. Med. Chem.* **2012**, *55* (2), 639-651; (b) Segretti, M. C. F.; Vallerini, G. P.; Brochier, C.; Langley, B.; Wang, L.; Hancock, W. W.; Kozikowski, A. P., Thiol-Based Potent and

Selective HDAC6 Inhibitors Promote Tubulin Acetylation and T-Regulatory Cell Suppressive Function. *ACS Med. Chem. Lett.* **2015**, 6 (11), 1156-1161.

12. Wing, J. B.; Tanaka, A.; Sakaguchi, S., Human FOXP3+ Regulatory T Cell Heterogeneity and Function in Autoimmunity and Cancer. *Immunity* **2019**, 50 (2), 302-316.

13. (a) Wang, L.; De Zoeten, E. F.; Greene, M. I.; Hancock, W. W., Immunomodulatory Effects of Deacetylase Inhibitors: Therapeutic Targeting of FOXP3+ Regulatory T Cells. *Nat. Rev. Drug Discov.* **2009**, 8 (12), 969; (b) Göschl, L.; Scheinecker, C.; Bonelli, M., Treg Cells in Autoimmunity: from Identification to Treg-Based Therapies. In *Seminars in Immunopathology*, Springer: **2019**; Vol. 41, pp 301-314; (c) Mohr, A.; Atif, M.; Balderas, R.; Gorochoy, G.; Miyara, M., The Role of FOXP 3+ Regulatory T Cells in Human Autoimmune and Inflammatory Diseases. *Clin. Exp. Immunol.* **2019**.

14. (a) Ellis, J. D.; Neil, D. A. H.; Inston, N. G.; Jenkinson, E.; Drayson, M. T.; Hampson, P.; Shuttleworth, S. J.; Ready, A. R.; Cobbold, M., Inhibition of Histone Deacetylase 6 Reveals a Potent Immunosuppressant Effect in Models of Transplantation. *Transplantation* **2016**, 100 (8), 1667-1674; (b) Akimova, T.; Levine, M. H.; Beier, U. H.; Hancock, W. W., Standardization, Evaluation, and Area-Under-Curve Analysis of Human and Murine Treg Suppressive Function. In *Suppression and Regulation of Immune Responses*, Humana Press: New York, NY, **2016**; Vol. 1371, pp 43-78.

15. Wang, X. X.; Wan, R. Z.; Liu, Z. P., Recent Advances in the Discovery of Potent and Selective HDAC6 Inhibitors. *Eur. J. Med. Chem.* **2018**, 143, 1406-1418.

16. (a) Avelar, L. A. A.; Ruzic, D.; Djokovic, N.; Kurz, T.; Nikolic, K., Structure-Based Design of Selective Histone Deacetylase 6 Zinc Binding Groups. *J. Biomol. Struct. Dyn.* **2019**,

DOI:10.1080/07391102.2019.1652687; (b) Choi, M. A.; Park, S. Y.; Chae, H. Y.; Song, Y.; Sharma, C.; Seo, Y. H., Design, Synthesis and Biological Evaluation of a Series of CNS Penetrant HDAC Inhibitors Structurally Derived from Amyloid- β Probes. *Sci. Rep.* **2019**, 9 (1), 1-12; (c) Erdeljic, N.; Bussmann, K.; Schöler, A.; Hansen, F. K.; Gilmour, R., Fluorinated Analogues of the Histone Deacetylase Inhibitor Vorinostat (Zolinza): Validation of a Chiral Hybrid Bioisostere, BITE. *ACS Med. Chem. Lett.* **2019**; (d) Fleming, C. L.; Natoli, A.; Schreuders, J.; Devlin, M.; Yoganantharajah, P.; Gibert, Y.; Leslie, K. G.; New, E. J.; Ashton, T. D.; Pfeffer, F. M., Highly Fluorescent and HDAC6 Selective Scriptaid Analogues. *Eur. J. Med. Chem.* **2019**, 162, 321-333; (e) Hsieh, Y. L.; Tu, H. J.; Pan, S. L.; Liou, J. P.; Yang, C. R., Anti-metastatic Activity of MPT0G211, a Novel HDAC6 Inhibitor, in Human Breast Cancer Cells in Vitro and in Vivo. *BBA-Mol. Cell Res.* **2019**, 1866 (6), 992-1003; (f) Huang, F. I.; Wu, Y. W.; Sung, T. Y.; Liou, J. P.; Lin, M. H.; Pan, S. L.; Yang, C. R., MPT0G413, a Novel HDAC6-selective Inhibitor, and Bortezomib Synergistically Exert Anti-tumor Activity in Multiple Myeloma Cells. *Front. Oncol.* **2019**, 9, 249; (g) Kassab, S. E.; Mowafy, S.; Alserw, A. M.; Seliem, J. A.; El-Naggar, S. M.; Omar, N. N.; Awad, M. M., Structure-based Design Generated Novel Hydroxamic Acid Based Preferential HDAC6 Lead Inhibitor with On-target Cytotoxic Activity Against Primary Choroid Plexus Carcinoma. *J. Enzyme Inh. Med. Chem.* **2019**, 34 (1), 1062-1077; (h) Li, Y.; Wang, F.; Chen, X.; Wang, J.; Zhao, Y.; Li, Y.; He, B., Zinc-dependent Deacetylase (HDAC) Inhibitors with Different Zinc Binding Groups. *Curr. Top. Med. Chem.* **2019**, 19 (3), 223-241; (i) Liang, T.; Hou, X.; Zhou, Y.; Yang, X.; Fang, H., Design, Synthesis, and Biological Evaluation of 2, 4-Imidazolidinedione Derivatives as HDAC6 Isoform-Selective Inhibitors. *ACS Med. Chem. Lett.* **2019**, 10 (8), 1122-1127; (j) Nam, G.; Jung, J. M.; Park, H. J.; Baek, S. Y.; Baek, K. S.; yeon Mok, H.; Jung, Y. H., Structure-Activity Relationship Study of Thiazolyl-hydroxamate Derivatives as Selective Histone Deacetylase 6

Inhibitors. *Bioorg. Med. Chem.* **2019**, 27 (15), 3408-3420; (k) Ruzic, D.; Petkovic, M.; Agbaba, D.; Ganesan, A.; Nikolic, K., Combined Ligand and Fragment-based Drug Design of Selective Histone Deacetylase-6 Inhibitors. *Mol. Inform.* **2019**, 38 (5), 1800083; (l) Schmitt, F.; Gosch, L. C.; Dittmer, A.; Rothmund, M.; Mueller, T.; Schobert, R.; Biersack, B.; Volkamer, A.; Höpfner, M., Oxazole-Bridged Combretastatin A-4 Derivatives with Tethered Hydroxamic Acids: Structure–Activity Relations of New Inhibitors of HDAC and/or Tubulin Function. *Int. J. Mol. Sci.* **2019**, 20 (2), 383; (m) Shen, S.; Hadley, M.; Ustinova, K.; Pavlicek, J.; Knox, T.; Noonepalle, S.; Tavares, M. T.; Zimprich, C. A.; Zhang, G.; Robers, M. B.; Bařinka, C.; Kozikowski, A. P.; Villagra, A., Discovery of a New Isoxazole-3-hydroxamate-Based Histone Deacetylase 6 Inhibitor SS-208 with Antitumor Activity in Syngeneic Melanoma Mouse Models. *J. Med. Chem.* **2019**, 62 (18), 8557-8577; (n) Song, Y.; Lim, J.; Seo, Y. H., A Novel Class of Anthraquinone-based HDAC6 Inhibitors. *Eur. J. Med. Chem.* **2019**, 164, 263-272; (o) Tang, C.; Du, Y.; Liang, Q.; Cheng, Z.; Tian, J., A Selenium-containing Selective Histone Deacetylase 6 Inhibitor for Targeted in Vivo Breast Tumor Imaging and Therapy. *J. Mater. Chem. B* **2019**, 7, 3528-3536; (p) Yang, F.; Zhao, N.; Ge, D.; Chen, Y., Next-generation of Selective Histone Deacetylase Inhibitors. *RSC Advances* **2019**, 9 (34), 19571-19583; (q) Zhao, C.; Gao, J.; Zhang, L.; Su, L.; Yepeng, L., Novel HDAC6 Selective Inhibitors with 4-Aminopiperidine-1-carboxamide as the Core Structure Enhanced Growth Inhibitory Activity of Bortezomib in MCF-7 Cells. *Biosci. Trends* **2019**, 13 (1), 91-97.

17. Butler, K. V.; Kalin, J.; Brochier, C.; Vistoli, G.; Langley, B.; Kozikowski, A. P., Rational Design and Simple Chemistry Yield a Superior, Neuroprotective HDAC6 Inhibitor, Tubastatin A. *J. Am. Chem. Soc.* **2010**, 132 (31), 10842-10846.

18. Shen, S.; Benoy, V.; Bergman, J. A.; Kalin, J. H.; Frojuello, M.; Vistoli, G.; Haeck, W.; Van Den Bosch, L.; Kozikowski, A. P., Bicyclic-Capped Histone Deacetylase 6 Inhibitors with

Improved Activity in a Model of Axonal Charcot–Marie–Tooth Disease. *ACS Chem. Neurosci.* **2016**, 7 (2), 240-258.

19. Bergman, J. A.; Woan, K.; Perez-Villarroel, P.; Villagra, A.; Sotomayor, E. M.; Kozikowski, A. P., Selective Histone Deacetylase 6 Inhibitors Bearing Substituted Urea Linkers Inhibit Melanoma Cell Growth. *J. Med. Chem.* **2012**, 55 (22), 9891-9899.

20. Lee, J. H.; Mahendran, A.; Yao, Y.; Ngo, L.; Venta-Perez, G.; Choy, M. L.; Kim, N.; Ham, W. S.; Breslow, R.; Marks, P. A., Development of a Histone Deacetylase 6 Inhibitor and Its Biological Effects. *Proc. Natl. Acad. Sci.* **2013**, 110 (39), 15704-15709.

21. Jochems, J.; Boulden, J.; Lee, B. G.; Blendy, J. A.; Jarpe, M.; Mazitschek, R.; Van Duzer, J. H.; Jones, S.; Berton, O., Antidepressant-like Properties of Novel HDAC6-Selective Inhibitors with Improved Brain Bioavailability. *Neuropsychopharmacol.* **2014**, 39 (2), 389.

22. Santo, L.; Hideshima, T.; Kung, A. L.; Tseng, J.-C.; Tamang, D.; Yang, M.; Jarpe, M.; van Duzer, J. H.; Mazitschek, R.; Ogier, W. C., Preclinical Activity, Pharmacodynamic, and Pharmacokinetic Properties of a Selective HDAC6 Inhibitor, ACY-1215, in Combination with Bortezomib in Multiple Myeloma. *Blood* **2012**, 119 (11), 2579-2589.

23. Pinori, M.; Mazzaferro, R.; Mascagni, P. Alpha-Amino Acid Derivatives with Antiinflammatory Activity. WO2006003068, **2006**.

24. Wagner, F. F.; Olson, D. E.; Gale, J. P.; Kaya, T.; Weïwer, M.; Aidoud, N.; Thomas, M. r.; Davoine, E. L.; Lemercier, B. r. n. C.; Zhang, Y.-L., Potent and Selective Inhibition of Histone Deacetylase 6 (HDAC6) Does Not Require a Surface-Binding Motif. *J. Med. Chem.* **2013**, 56 (4), 1772-1776.

25. Puerta, D. T.; Lewis, J. A.; Cohen, S. M., New Beginnings for Matrix Metalloproteinase Inhibitors: Identification of High-Affinity Zinc-binding Groups. *J. Am. Chem. Soc.* **2004**, *126* (27), 8388-8389.
26. Beckett, R. P.; Davidson, A. H.; Drummond, A. H.; Huxley, P.; Whittaker, M., Recent Advances in Matrix Metalloproteinase Inhibitor Research. *Drug Discov. Today* **1996**, *1* (1), 16-26.
27. Holms, J.; Mast, K.; Marcotte, P.; Elmore, I.; Li, J.; Pease, L.; Glaser, K.; Morgan, D.; Michaelides, M., Discovery of Selective Hydroxamic Acid Inhibitors of Tumor Necrosis Factor- α Converting Enzyme. *Bioorg. Med. Chem. Lett.* **2001**, *11* (22), 2907-2910.
28. Lauffer, B. E. L.; Mintzer, R.; Fong, R.; Mukund, S.; Tam, C.; Zilberleyb, I.; Flicke, B.; Ritscher, A.; Fedorowicz, G.; Vallero, R., Histone Deacetylase (HDAC) Inhibitor Kinetic Rate Constants Correlate With Cellular Histone Acetylation but not Transcription and Cell Viability. *J. Biol. Chem.* **2013**, *288* (37), 26926-26943.
29. Porter, N. J.; Mahendran, A.; Breslow, R.; Christianson, D. W., Unusual Zinc-Binding Mode of HDAC6-Selective Hydroxamate Inhibitors. *Proc. Natl. Acad. Sci.* **2017**, *114* (51), 13459-13464.
30. Somoza, J. R.; Skene, R. J.; Katz, B. A.; Mol, C.; Ho, J. D.; Jennings, A. J.; Luong, C.; Arvai, A.; Buggy, J. J.; Chi, E., Structural Snapshots of Human HDAC8 Provide Insights into the Class I Histone Deacetylases. *Structure* **2004**, *12* (7), 1325-1334.
31. (a) Valverde, I. E.; Bauman, A.; Kluba, C. A.; Vomstein, S.; Walter, M. A.; Mindt, T. L., 1,2,3-Triazoles as Amide Bond Mimics: Triazole Scan Yields Protease-Resistant Peptidomimetics

for Tumor Targeting. *Angew. Chem. Int. Ed.* **2013**, 52 (34), 8957-8960; (b) Brown, M. L.; Aaron, W.; Austin, R. J.; Chong, A.; Huang, T.; Jiang, B.; Kaizerman, J. A.; Lee, G.; Lucas, B. S.; McMinn, D. L., Discovery of Amide Replacements That Improve Activity and Metabolic Stability of a Bis-amide Smoothened Antagonist Hit. *Bioorg. Med. Chem. Lett.* **2011**, 21 (18), 5206-5209.

32. (a) Meanwell, N. A., Synopsis of Some Recent Tactical Application of Bioisosteres in Drug Design. *J. Med. Chem.* **2011**, 54 (8), 2529-2591; (b) Bonandi, E.; Christodoulou, M. S.; Fumagalli, G.; Perdicchia, D.; Rastelli, G.; Passarella, D., The 1,2,3-Triazole Ring as a Bioisostere in Medicinal Chemistry. *Drug Discov. Today* **2017**, 22 (10), 1572-1581.

33. Hai, Y.; Christianson, D. W., Histone Deacetylase 6 Structure and Molecular Basis of Catalysis and Inhibition. *Nat. Chem. Biol.* **2016**, 12 (9), 741.

34. (a) Finnin, M. S.; Donigian, J. R.; Cohen, A.; Richon, V. M.; Rifkind, R. A.; Marks, P. A.; Breslow, R.; Pavletich, N. P., Structures of a Histone Deacetylase Homologue Bound to the TSA and SAHA Inhibitors. *Nature* **1999**, 401 (6749), 188; (b) Lauffer, B. E.; Mintzer, R.; Fong, R.; Mukund, S.; Tam, C.; Zilberleyb, I.; Flicke, B.; Ritscher, A.; Fedorowicz, G.; Vallero, R., Histone Deacetylase (HDAC) Inhibitor Kinetic Rate Constants Correlate With Cellular Histone Acetylation but not Transcription and Cell Viability. *J. Biol. Chem.* **2013**, 288 (37), 26926-26943.

35. Von Zelewsky, A., *Stereochemistry of Coordination Compounds*. John Wiley & Sons: 1996; Vol. 3.

36. Porter, N. J.; Christianson, D. W., Structure, Mechanism, and Inhibition of the Zinc-Dependent Histone Deacetylases. *Curr. Opin. Struct. Biol.* **2019**, 59, 9.

37. Porter, N. J.; Osko, J. D.; Diedrich, D.; Kurz, T.; Hooker, J. M.; Hansen, F. K.; Christianson, D. W., Histone Deacetylase 6-Selective Inhibitors and the Influence of Capping Groups on Hydroxamate-Zinc Denticity. *J. Med. Chem.* **2018**, *61* (17), 8054-8060.
38. Miyake, Y.; Keusch, J. J.; Wang, L.; Saito, M.; Hess, D.; Wang, X.; Melancon, B. J.; Helquist, P.; Gut, H.; Matthias, P., Structural Insights Into HDAC6 Tubulin Deacetylation and Its Selective Inhibition. *Nat. Chem. Biol.* **2016**, *12* (9), 748.
39. Vögerl, K.; Ong, N.; Senger, J.; Herp, D.; Schmidtkunz, K.; Marek, M.; Müller, M.; Bartel, K.; Shaik, T. B.; Porter, N. J.; Robaa, D.; Christianson, D. W.; Romier, C.; Sippl, W.; Jung, M.; Bracher, F., Synthesis and Biological Investigation of Phenothiazine-Based Benzhydroxamic Acids as Selective Histone Deacetylase 6 Inhibitors. *J. Med. Chem.* **2019**, *62* (3), 1138-1166.
40. Porter, N. J.; Wagner, F. F.; Christianson, D. W., Entropy as a Driver of Selectivity for Inhibitor Binding to Histone Deacetylase 6. *Biochemistry* **2018**, *57* (26), 3916-3924.
41. Mayo, S. L.; Olafson, B. D.; Goddard, W. A., DREIDING: a Generic Force Field for Molecular Simulations. *J. Phys. Chem.* **1990**, *94* (26), 8897-8909.
42. Zhang, Y.; Ying, J. B.; Hong, J. J.; Li, F. C.; Fu, T. T.; Yang, F. Y.; Zheng, G. X.; Yao, X. J.; Lou, Y.; Qiu, Y.; Xue, W. W.; Zhu, F., How Does Chirality Determine the Selective Inhibition of Histone Deacetylase 6? A Lesson from Trichostatin A Enantiomers Based on Molecular Dynamics. *ACS Chem. Neurosci.* **2019**, *10* (5), 2467-2480.
43. (a) Van Duzer, J. H.; Mazitschek, R.; Ogier, W.; Bradner, J. E.; Huang, G.; Xie, D.; Yu, N. Reverse Amide Compounds as Protein Deacetylase Inhibitors and Methods of Use Thereof. US 8394810 B2, **2013**; (b) Regna, N. L.; Vieson, M. D.; Luo, X. M.; Chafin, C. B.; Puthiyaveetil, A.

G.; Hammond, S. E.; Caudell, D. L.; Jarpe, M. B.; Reilly, C. M., Specific HDAC6 Inhibition by ACY-738 Reduces SLE Pathogenesis in NZB/W Mice. *Clin. Immunol.* **2016**, *162*, 58-73.

44. (a) Meanwell, N. A., Fluorine and Fluorinated Motifs in the Design and Application of Bioisosteres for Drug Design. *J. Med. Chem.* **2018**, *61* (14), 5822-5880; (b) Koller, A. N.; Božilović, J.; Engels, J. W.; Gohlke, H., Aromatic N Versus Aromatic F: Bioisosterism Discovered in RNA Base Pairing Interactions Leads to a Novel Class of Universal Base Analogs. *Nucleic Acids Res.* **2010**, *38* (9), 3133-3146.

45. Müller, K.; Faeh, C.; Diederich, F., Fluorine in Pharmaceuticals: Looking Beyond Intuition. *Science* **2007**, *317* (5846), 1881-1886.

46. Dunitz, J. D.; Taylor, R., Organic Fluorine Hardly Ever Accepts Hydrogen Bonds. *Chem. Eur. J.* **1997**, *3* (1), 89-98.

47. (a) Bettinger, H. F., How Good is Fluorine as a Hydrogen-Bond Acceptor in Fluorinated Single-Walled Carbon Nanotubes? *ChemPhysChem* **2005**, *6* (6), 1169-1174; (b) Politzer, P.; Murray, J. S.; Concha, M. C., Halogen Bonding and the Design of New Materials: Organic Bromides, Chlorides and Perhaps Even Fluorides as Donors. *J. Mol. Model.* **2007**, *13* (6-7), 643-650.

48. Zhou, P.; Zou, J.; Tian, F.; Shang, Z., Fluorine Bonding How Does It Work In Protein-Ligand Interactions? *J. Chem. Inf. Model.* **2009**, *49* (10), 2344-2355.

49. Vergani, B.; Caprini, G.; Fossati, G.; Lattanzio, M.; Marchini, M.; Pavich, G.; Pezzuto, M.; Ripamonti, C.; Sandrone, G.; Steinkuehler, C.; Stevenazzi, A. Preparation of Novel Benzohydroxamic Compounds as Selective HDAC6 Inhibitors. WO2018189340, **2018**.

50. (a) Sakaguchi, S.; Miyara, M.; Costantino, C. M.; Hafler, D. A., FOXP3+ Regulatory T Cells in the Human Immune System. *Nat. Rev. Immunol.* **2010**, *10* (7), 490; (b) Tao, R.; De Zoeten, E. F.; Özkaynak, E.; Chen, C.; Wang, L.; Porrett, P. M.; Li, B.; Turka, L. A.; Olson, E. N.; Greene, M. I., Deacetylase Inhibition Promotes the Generation and Function of Regulatory T Cells. *Nat. Med.* **2007**, *13* (11), 1299.
51. Vignali, D. A. A.; Collison, L. W.; Workman, C. J., How Regulatory T Cells Work. *Nat. Rev. Immunol.* **2008**, *8* (7), 523.
52. van Loosdregt, J.; Vercoulen, Y.; Guichelaar, T.; Gent, Y. Y. J.; Beekman, J. M.; van Beekum, O.; Brenkman, A. B.; Hijnen, D. J.; Mutis, T.; Kalkhoven, E., Regulation of Treg Functionality by Acetylation-Mediated Foxp3 Protein Stabilization. *Blood* **2010**, *115* (5), 965-974.
53. van Loosdregt, J.; Coffey, P. J., Post-translational Modification Networks Regulating FOXP3 Function. *Trends Immunol.* **2014**, *35* (8), 368-378.
54. Zhang, H.; Xiao, Y.; Zhu, Z.; Li, B.; Greene, M. I., Immune Regulation by Histone Deacetylases: a Focus on the Alteration of FOXP3 Activity. *Immunol. Cell Biol.* **2012**, *90* (1), 95-100.
55. Reddy, A. S.; Kumar, M. S.; Reddy, G. R., A Convenient Method for the Preparation of Hydroxamic Acids. *Tetrahedron Lett.* **2000**, *41* (33), 6285-6288.
56. Bacchi, S. Process for Preparing Heterocyclic Thiazole or Triazole Derivatives. US 2007/0232808 A1, **2007**.
57. (a) Yan, L.; Liang, J.; Yao, C.; Wu, P.; Zeng, X.; Cheng, K.; Yin, H., Pyrimidine Triazole Thioether Derivatives as Toll-Like Receptor 5 (TLR5)/Flagellin Complex Inhibitors.

ChemMedChem **2016**, *11* (8), 822-826; (b) Rezki, N.; Al-Yahyawi, A. M.; Bardaweel, S. K.; Al-Blewi, F. F.; Aouad, M. R., Synthesis of Novel 2,5-Disubstituted-1,3,4-Thiadiazoles Clubbed 1,2,4-Triazole, 1,3,4-Thiadiazole, 1,3,4-Oxadiazole and/or Schiff Base as Potential Antimicrobial and Antiproliferative Agents. *Molecules* **2015**, *20* (9), 16048-16067.

58. Niu, L. F.; Cai, Y.; Liang, C.; Hui, X. P.; Xu, P. F., Efficient Copper-Catalyzed C–S Cross-Coupling of Heterocyclic Thiols With Aryl Iodides. *Tetrahedron* **2011**, *67* (16), 2878-2881.

59. (a) Dudutienė, V.; Zubrienė, A.; Smirnov, A.; Gylytė, J.; Timm, D.; Manakova, E.; Gražulis, S.; Matulis, D., 4-Substituted-2,3,5,6-Tetrafluorobenzenesulfonamides as Inhibitors of Carbonic Anhydrases I, II, VII, XII, and XIII. *Bioorg. Med. Chem.* **2013**, *21* (7), 2093-2106; (b) Nagarathnam, D.; Dumas, J.; Hatoum-mokdad, H.; Boyer, S.; Wang, C.; Pluempfe, H.; Feurer, A.; Bennabi, S. Preparation of Pyrimidinamines as Rho-kinase Inhibitors for Inhibiting Tumor Growth, Treating Erectile Dysfunction, and Other Therapeutic Uses. WO 2003/062225 A1, **2003**.

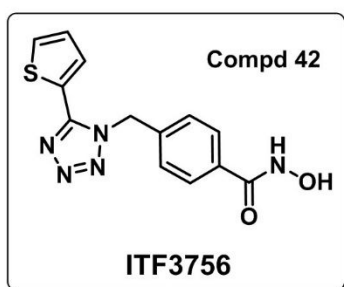
60. Castanedo, G. M.; Seng, P. S.; Blaquiére, N.; Trapp, S.; Staben, S. T., Rapid Synthesis of 1,3,5-Substituted-1,2,4-triazoles from Carboxylic Acids, Amidines, and Hydrazines. *J. Org. Chem.* **2011**, *76* (4), 1177-1179.

61. Dolman, S. J.; Gosselin, F.; O'Shea, P. D.; Davies, I. W., Superior Reactivity of Thiosemicarbazides in the Synthesis of 2-Amino-1,3,4-oxadiazoles. *J. Org. Chem.* **2006**, *71* (25), 9548-9551.

62. Karstens, W. F. J.; Van der Stelt, M.; Cals, J.; Azevedo, R. C. R. G.; Barr, K. J.; Zhang, H.; Beresis, R. T.; Zhang, D.; Duan, X. Preparation of Indazole Compounds as ROR γ T Inhibitors. WO 2012/06995 A1, **2012**.

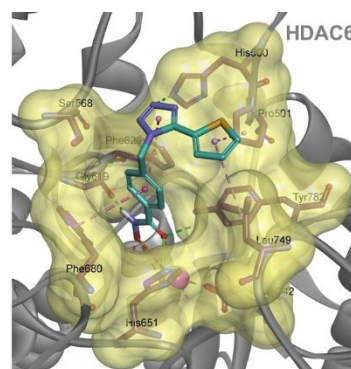
63. (a) Doemling, A.; Holak, T. Preparation of Benzylphenylpyrazolyindole Derivatives and Analogs for Use as p53-MDM2/p53-MDM4 Antagonists WO 2011/106650 A2, **2011**; (b) Begum, J.; Varga, G.; Docsa, T.; Gergely, P.; Hayes, J. M.; Juhász, L.; Somsák, L., Computationally Motivated Synthesis and Enzyme Kinetic Evaluation of N-(β -D-Glucopyranosyl)-1, 2, 4-triazolecarboxamides as Glycogen Phosphorylase Inhibitors. *MedChemComm* **2015**, 6 (1), 80-89; (c) Aster, S. D.; Graham, D. W.; Kharbanda, D.; Patel, G.; Ponpipom, M.; Santorelli, G. M.; Szymonifka, M. J.; Mundt, S. S.; Shah, K.; Springer, M. S., Bis-Aryl Triazoles as Selective Inhibitors of 11 β -Hydroxysteroid Dehydrogenase Type 1. *Bioorg. Med. Chem. Lett.* **2008**, 18 (9), 2799-2804.
64. Ito, K.; Lim, S.; Caramori, G.; Cosio, B.; Chung, K. F.; Adcock, I. M.; Barnes, P. J., A Molecular Mechanism of Action of Theophylline: Induction of Histone Deacetylase Activity to Decrease Inflammatory Gene Expression. *Proc. Natl. Acad. Sci.* **2002**, 99 (13), 8921-8926.

Table of Contents graphic



Enzyme activity
IC₅₀ HDAC6 **17 nM**
IC₅₀ HDAC1 **924 nM**
IC₅₀ HDAC2 **4017 nM**
IC₅₀ HDAC3 **865 nM**

In vitro stability
H plasma stb **91% @ 4hrs**
H S9 stb **100% @ 1.5hrs**
R plasma stb **62% @ 4hrs**
R S9 stb **82% @ 1.5hrs**



1
2
3
4
5
6
7
8
9
10
11
12
13
14
15
16
17
18
19
20
21
22
23
24
25
26
27
28
29
30
31
32
33
34
35
36
37
38
39
40
41
42
43
44
45
46
47
48
49
50
51
52
53
54
55
56
57
58
59
60